From the Department of Infectious Diseases and Microbiology

of the University of Lübeck

Director: Prof. Dr. med. Jan Rupp

CP-673451 inhibits the formation of neutrophil extracellular traps induced by PMA and immobilized immune complexes

Dissertation

for Fulfillment of

Requirements

for the Doctoral Degree

of the University of Lübeck

from the Department of Natural Sciences

Submitted by

Gigy Varghese

From Mahé, India

Lübeck 2017

First referee: Prof. Dr. Tamás Laskay

Second referee: Prof. Dr. Hauke Busch

Date of oral examination: 23.11.2017

Approved for printing: Lübeck, 28.11.2017

This work is dedicated to my beloved mother, Alice Varghese

Table of Contents

List of Abbreviations

Ab	Antibody
AUC	Area under the curve
BSA	Bovine serum albumin
CD	cluster of differentiation
CGD	Chronic granulomatous disease
DMSO	Dimethyl sulfoxide
DNA	Deoxyribonucleic acid
DNA	Deoxyribonucleic acid
DOX	Doxorubicin
DPI	diphenyleneiodonium
ELISA	Enzyme linked immuno sorbent assay
Erk1/2	Extracellular signal–regulated kinases 1/2
FCS	Fetal calf serum
FITC	Fluorescein isothiocyanate
FM	Fluorescent microscopy
fMLP	N-Formyl methionyl-leucyl-phenylalanine
HSA	Human serum albumin
IC	Immune complex
IFN-γ	Interferon gamma
iIC	Immobilized immune complexes
IL	Interleukin
IO	Ionomycin
LDH	Lactate dehydrogenase
LPS	Lipopolysaccharide
MAPK	Mitogen-activated protein kinases
MPO	Myeloperoxidase
NADPH	Nicotinamide adenine dinucleotide phosphate
NE	Neutrophil elastase
NETs	Neutrophil extracellular traps
NOX	NADPH oxidase
OD	Optical density

PBMCs	Peripheral blood mononuclear cells
PBS	Phosphate buffered saline
pDCs	Plasmacytoid dendritic cells
PDGF	Platelet derived growth factor
PDGFR	Platelet derived growth factor receptor
PE	Phycoerythrin
PHOX	Phagocytic oxidase.
PI	Propidium iodide
PI3K	Phosphatidylinositol-4,5-bisphosphate 3-kinase
PKC	Protein kinase C
PKCδ	Protein kinase C delta
PMA	Phorbol 12-myristate 13-acetate
PMB	Polymyxin B
RA	Rheumatoid arthritis
RIN	RNA integrity number
RNA	Ribonucleic acid
ROS	Reactive oxygen species
RT	Room temperature
SDS	Sodium dodecyl sulfate
SLE	Systemic lupus erythematosus
SOD	Superoxide dismutase
TCA	Trichloro acetic acid
TLR	Toll-like receptor
TNF	Tumor necrosis factor
VEGF	Vascular endothelial growth factor
VEGFR1/2	Vascular endothelial growth factor receptor-1/2

Summary

Neutrophils are essential cells of the innate antimicrobial defense. A recently identified anti-microbial function is the formation of Neutrophil Extracellular Traps (NETs) that are composed of decondensed chromatin and antimicrobial granular contents. NETs can capture and kill invading pathogens. However, the granule proteins on the NETs can also serve as auto-antigens leading to autoimmunity. NETs are released from neutrophils undergoing a unique kind of cell death the so called NETosis. The mechanisms involved in NETosis are poorly understood. In the present study, the signaling mechanisms involved in NETosis were investigated.

NETosis was induced with PMA and immobilized immune complexes (iIC) which both induce Reactive Oxygen Species (ROS) dependent NETosis. A library of 141 inhibitors of known signaling pathways was screened for molecules that inhibit the formation of NETs but do not inhibit ROS production to identify a NETosis inhibitor, downstream of ROS production. Through the screening, I identified a potent inhibitor of NETosis, CP-673451 which inhibited NETosis induced by PMA and iIC. CP-673451 was found to inhibit the formation of both PMA- and iIC-induced NETs in a dose dependent manner without inhibiting ROS release. CP-673451 treatment did not inhibit PMA induced phosphorylation of PKC, p38 MAPK, ERK1/2, and Akt. The iIC-induced phosphorylation of Src, p38 MAPK, PI3K, Akt, and ERK1/2 was also not affected by CP-673451. These findings suggest that CP-673451 exerts its inhibitory effect downstream of these pathways and ROS production. However, the inhibitor did not inhibit ROS-independent ionomycin-induced NETosis.

CP-673451 is known to target Platelet-derived growth factor receptor (PDGFR). However, my experimental results suggest that the inhibitory effect of CP-673451 on NETosis is independent of action on the known target, PDGFR. In addition, by using western blots, I could confirm the absence of PDGFR in human neutrophils. CP-673451 is not cytotoxic for neutrophils (up to 10μM) and do not inhibit basic neutrophil functions such as activation, migration, and phagocytosis. However, TNF-α mediated random migration was affected by the higher concentration of CP-673451 (above 1μM). Furthermore, the study revealed that CP-673451 activates certain neutrophil functions such as the upregulation of CD11b and shedding of CD62L. The activation was not inhibited by polymyxin treatment, confirming that the activation phenotype was not

due to LPS contamination. In support to the surface marker expression results, CP-673451 induced the phosphorylation of p38 MAPK, ERK1/2, and Akt in human neutrophils. Although, the study could not identify the molecular target of CP-673451 involved in NET-inhibition, the target of CP-673451 is apparently further downstream of p38 MAPK, ERK1/2, and Akt pathways. The results suggest that CP-673451 is activating the neutrophils through the same pathways which are involved in ROS production but downstream to ROS production it leads to NETosis inhibition through an unknown mechanism. The preliminary gene expression studies also indicated that CP-673451 is involved in inducing gene expression changes in neutrophils. However, their role in inhibition of NETosis needs to be further analyzed. Elucidating the molecular targets of CP-673451 in neutrophils could lead to the identification of novel signaling events involved in NET formation.

Zusammenfassung

Neutrophile Granulozyten sind essenzielle Zellen der angeborenen antimikrobiellen Abwehr. Eine kürzlich identifizierte antimikrobielle Funktion dieser Zellen ist die Ausbildung von extrazellulären Gebilden (NETs, engl. Neutrophil Extracellular Traps), welche aus dekondensiertem Chromatin und antimikrobiellen Granula bestehen. NETs können eindringende Pathogene fangen und töten. Allerdings können die granulären Proteine der NETs auch als Auto-Antigene dienen, welche zu Autoimmunität führen können. Um NETs freisetzen zu können, durchlaufen Neutrophile Granulozyten eine einzigartige Form des Zelltodes – der sogenannten NETosis. Die darin involvierten Mechanismen sind bis zum heutigen Zeitpunkt kaum nachvollzogen. In der vorliegenden Arbeit, sollen diese Mechanismen untersucht werden.

NETosis wurde durch PMA und immobilisierte Immunkomplexe ausgelöst, welche beide die Produktion von reaktiven Sauerstoffradikalen (ROS, engl. Reactive Oxigene Species) iniziieren. Ein Satz von 141 Inhibitoren bekannter Signalwege wurde auf Moleküle durchsucht, welche die Ausbildung von NETs, aber nicht die Produktion von ROS beeinträchtigen. Dies geschah, um einen Inhibitor zu identifizieren, welcher die Ausbildung von NETs jenseits der ROS-Produktion hemmt.

Tatsächlich konnte ich einen potenten Inhibitor der NETosis identifizieren: CP-673451, welcher die durch PMA und iIC induzierten NET Freisetzung dosierungsabhängig hemmt, ohne die Ausbildung von ROS zu vermindern. CP-673451 Behandlung verminderte nicht die PMA induzierte Phosphorilierung von PKC, p38 MAPK, ERK1/2 und Akt. Die iIC-induzierte Phosphorilierung von Src, p38 MAPK, PI3K, Akt und ERK1/2 war ebenfalls nicht durch CP-673451 beeinflusst. Diese Ergebnisse zeigen, dass CP-673451 seine inhibitorischen Effekte nach der obengenannten Signal wegen und der ROS-Produktion ausübt. Allerdings konnte dieser Inhibitor nicht die von ROS unabhängige Induktion von NETs durch Ionomycin verhindern.

Es ist bekannt, dass CP-673451 an den PDGF-Rezeptor (Platelet-derived growth factor receptor) bindet. In meinen Versuchen konnte ich allerdings zeigen, dass der inhibierende Effekt von CP-673451 auf die NETose von dem bekannten Bindungsprotein, dem PDGF-Rezeptor, unabhängig ist. Tatsächlich konnte ich die Abwesenheit dieses Bindungsproteins in Neutrophilen Granulozyten mit Hilfe von

Western Blots beweisen. CP-673451 ist in einer Konzentration bis 1µM nicht zytotoxisch für Neutrophile Granulozyten und inhibiert keine Grundfunktionen der Zelle, wie zum Beispiel die Möglichkeit der Aktivierung, Migration oder Phagozytose. Allerdings war die TNF-α vermittelte Migration beeinträchtigt ab einer Inhibitorkonzentration über 1µM. Außerdem zeigte meine Studie, dass CP-673451 bestimmte Funktionen der Neutrophilen aktiviert, wie beispielsweise die Hochregulation von CD11b auf der Zelloberfläche oder den Abbau von CD62L. Die Aktivierung konnte nicht durch Polymyxin inhibiert werden, was darauf schließen lässt, dass der aktivierte Phänotyp der Zelle nicht durch eine eventuelle LPS kontamination ausgelöst wurde.

Zusätzlich zur Veränderung der Zelloberflächenmarker konnte gezeigt werden, dass CP-673451 die Phosphorylierung von p38 MAP, ERK1/2, und Akt in humanen Neutrophilen induziert. Obwohl diese Studie nicht das molekulare Ziel von CP-673451 identifizieren konnte, welches in die NET-inhibition involviert ist, liegt der Angriftspunkt von CP-673451 vermutlich in der Signalkaskade nach p38 MAPK, ERK1/2 und Akt befinden. So kann davon ausgegangen werden, dass CP-673451 in den Reaktionswegen, welche zur ROS-Produktion führen, eine aktivierende Rolle einnimmt, jenseits der ROS Produktion allerdings für eine Inhibierung der NETose durch einen bisher nicht aufgeklärten Mechanismus sorgt. Ergebnise der vorangegangenen Genexpressionsanalyse zeigen auch, dass CP-673451 in der Veränderung der Genexpression von Neutrophilen beteiligt ist. Jedoch muss seine Rolle in der Inhibition von NETose weiter untersucht werden.

Die Zielproteine für CP-673451 in humanen Neutrophilen Granulozyten zu finden könnte dazu beitragen neue Signalwege zu identifizieren, welche in der NET Ausbildung eine entscheidende Rolle spielen.

Chapter 1. Introduction

1.1 Neutrophil granulocytes

Neutrophil granulocytes are the most abundant white blood cells in human circulation system (40% to 75%) [1]. They are formed from stem cells in the bone marrow and are short lived and replaced continuously throughout life [2]. Neutrophils are the first cells to be recruited to the area of infection and are part of innate immunity. They are well known for their anti-microbial functions like release of reactive oxygen species (ROS), phagocytosis, degranulation, cytokine release and the recently discovered formation neutrophil extracellular traps (NETs) containing anti-microbial proteins [2, 3].

1.2 Neutrophil activation and extravasation

The recruitment of neutrophils from circulation to the site of infection is a very critical in controlling infection. Bacterial-derived stimulants such as LPS, fMLP and the tissue resident leukocyte-derived pro-inflammatory cytokines tumor necrosis factor (TNF)-α, and interleukin (IL-)-1β can trigger endothelial cells to produce adhesion molecules on their surfaces such as P-selectin, E-selectin and ICAM [4, 5]. Neutrophils check the vessel walls and the circulating neutrophils can recognize stimulated endothelial cells. P-selectin glycoprotein ligand-1 (PSGL-1) and L-selectin expressed on the surface of neutrophils recognize the endothelial inflammatory signals [4, 6]. These molecules engage with P- and E- selectins of the endothelial cells which results in selectin mediated neutrophil tethering. It is followed by neutrophil rolling [7]. During rolling, neutrophils engage with stimulants which lead to clustering of β2 integrins on the surface of neutrophils leading to neutrophil activation. The β2 integrin family protein (LFA-1 and Mac-1) mediates arrest of rolling neutrophils and facilitates firm adhesion. The β2 integrins then engage with members of the ICAM-1 family and facilitate neutrophils to transmigrate to the target tissue [4, 8] **(Fig. 1)**.

Neutrophils recognize pathogens via various cell surface and intracellular receptors. Neutrophils also have numerous receptors that recognize host -derived proteins (such as IgG and complement) opsonizing the microbe. Pathogen-associated molecular patterns (PAMPs) such as LPS, peptidoglycan, and bacterial DNA are recognized by

neutrophil pattern-recognition receptors (PRRs). Many of these also engage with damage-associated molecular patterns (DAMPs) (e.g., mitochondrial DNA, released by necrotic cells). The PRRs C-type lectin receptors (e.g. Dectin-1), recognizes fungal β-glucan. Another group of PRRs is TLRs, which recognize lipids, carbohydrates, peptides, DNA, and single- and double-stranded RNA. At the RNA level, neutrophils express TLR1, −2, −4, −5, −6, −8, and −10 (and, after GM-CSF treatment, TLR9). Other PRRs include the cytosolic microbial sensors NOD1 and NOD2 (which recognize peptidoglycan-related molecules of gram-negative and gram-positive bacteria, respectively). The receptor recognition in turn activates neutrophils by intracellular signaling for various anti-microbial functions.

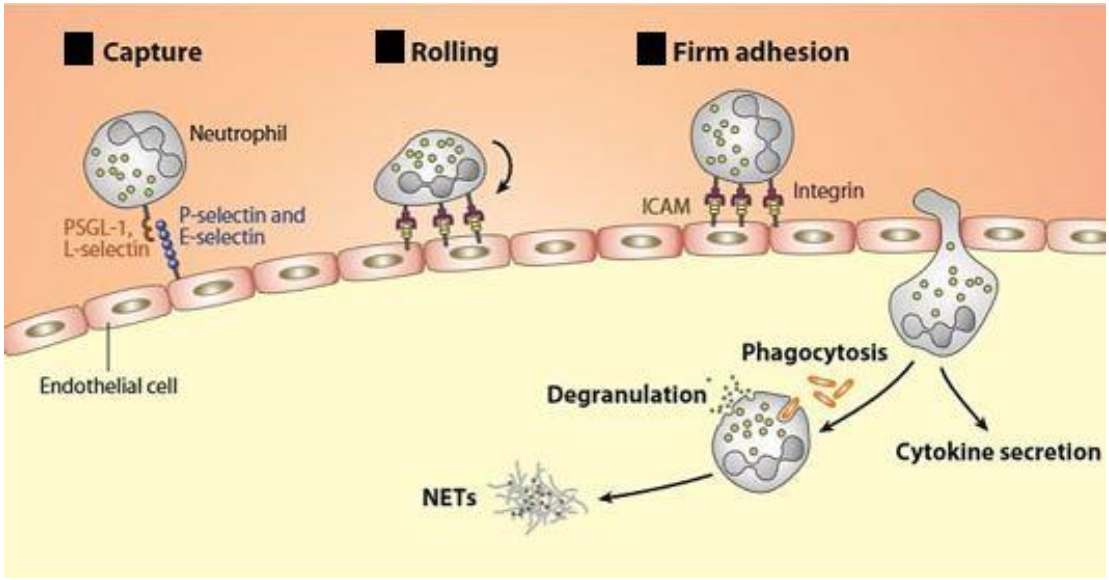

Figure 1. Extravasation of neutrophils and its anti-microbial functions. From [4].

1.3 Degranulation

Neutrophils are densely packed with secretory granules containing cytotoxic anti-microbial mediators. The secretion of cytotoxic mediators via exocytosis is referred to as degranulation. There are at least four types of granules: primary granules (azurophilic granules), secondary granules (specific granules), tertiary granules and secretory vesicles [9]. Azurophil granules are the main storage site of most toxic mediators like elastase, myeloperoxidase (MPO), cathepsins and defensins. The specific

granules and tertiary granules contain lactoferrin and metalloprotease-9 respectively [10, 11]. The stored proteinases and anti-microbial peptides in granules fuse with the phagosome during pathogen uptake. Granules fuse with plasma membrane causing the extracellular release of its contents. Generally, the release of secretory vesicles and tertiary vesicles occur during neutrophil activation and release of secondary and primary granules occur during phagosome leakage [9]. Neutrophils mainly contain cationic peptides which are released and these bind to the negatively charged surface components of pathogens resulting in membrane permeabilization and bind to intracellular targets results in disruption of the pathogen [9, 11, 12].

1.4 Phagocytosis

Neutrophils are capable of ingesting microorganisms, so they are called as phagocytes and the process of ingestion is called phagocytosis. Opsonization of microbes with immunoglobulins and complement factors enables efficient recognition of the antigens by the neutrophils [13]. The pathogen is engulfed into into a phagosome (phagocytic vesicle) [14]. Then the fusion of lysosome with the phagosome takes place, forming a phagolysosome. Concurrently, a strong oxidative burst is initiated in the phagosome by NADPH oxidase upon triggering of specific cell surface receptors, leading to the generation of highly toxic Reactive Oxygen Species (ROS). Together with the toxic hydrolytic granular contents, ROS play an important role in bacterial killing [13].

1.5 Cytokine production

As one of the first cell types to arrive at sites of infection, neutrophils secrete cytokines and chemokines that are critical in the inflammatory response and contribute to and regulate immune responses. The most abundantly produced cytokine in neutrophils is IL-8, which primarily serves to recruit other neutrophils [15, 16]. Similarly, neutrophils produce many pro- and anti- inflammatory cytokines. Neutrophil-derived proinflammatory IL-1β and TNF-α induce other cells to produce neutrophil chemo attractants. Neutrophils produce also several anti-inflammatory cytokines including TGF-β, IL-1ra etc [17, 18].

1.6 Reactive oxygen species (ROS) production

Reactive oxygen species (ROS) primarily produced via NADPH oxidase during activation which plays an important role in killing microorganisms by neutrophils [19]. The assembly of a functional NADPH oxidase (NOX) is formed by translocation of the cytosolic NADPH oxidase components p47phox, p67phox, and p40phox to the membrane, where gp91phox (NOX2), gp22phox, and the GTPase Rac2 (or Rac1) reside [9, 20, 21]. NADPH oxidase transfers an electron of the complex to the oxygen molecule in the phagosome or in the cytosol, generating superoxide anion (O_2^-) [20–23] and hydrogen peroxide (H_2O_2), which is formed by superoxide dismutase (SOD) activity [22, 23]. Most of the generated hydrogen peroxide is further processed by myeloperoxidase (MPO). MPO then catalyzes the formation of hypochlorous acid (HOCl) by oxidation of chloride ions, the primary oxidant bactericidal agent produced by neutrophils [19, 24] **(Fig. 2)**.

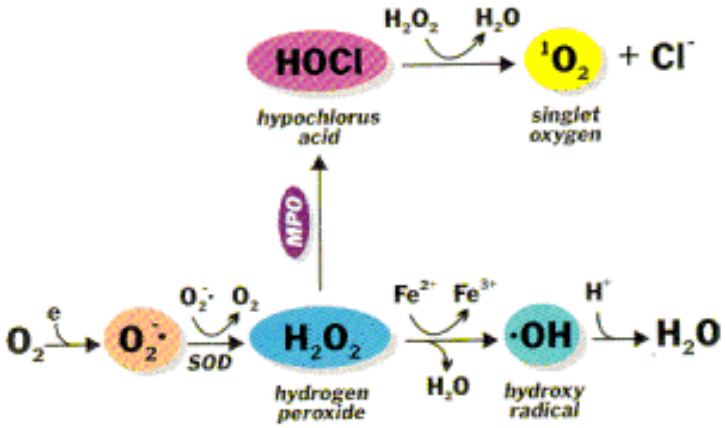

Figure 2. Generation of reactive oxygen species. From: rndsystems.com

Reactive oxygen species are highly toxic and play important role in neutrophil microbicidal activities [4]. Neutrophils of chronic granulomatous disease (CGD) patients, cannot form the reactive oxygen compounds (most importantly the superoxide radical) due to defective phagocyte NADPH oxidase and thus have the poor killing of ingested pathogens [25]. Diphenyleneiodonium (DPI) is commonly used agent to inhibit reactive oxygen species (ROS) production [26]. NADPH oxidase inhibition by DPI is mediated by targeting the flavin-containing subunit, withdrawing an electron from the oxidase and subsequently inhibiting superoxide formation [26-28].

1.7 Neutrophil extracellular trap formation (NETosis)

A novel antimicrobial mechanism of neutrophils has been described in 2004, upon activation the neutrophils release DNA and their granule contents, forming Neutrophil Extracellular Traps (NETs) [29]. It has been suggested that NETs are formed during active cell death, recently named NETosis. NETosis represents a form of cell death distinct from apoptosis and necrosis [30]. These extracellular chromatin structures, which contain histones and neutrophil granule proteins, can trap and kill a broad spectrum of microbes, including bacteria, fungi, protozoa, and viruses [31] **(Fig. 3)**.

There are two main NET release mechanisms proposed. The classical ROS-dependent NET-formation mechanism and the early/rapid ROS-independent mechanism [32, 33]. NETosis can be induced by various stimuli, most of them involve ROS production in neutrophils [34]. The oxidative burst triggers the dissociation and activation of neutrophil elastase (NE) from a membrane-associated complex called azurosome in a myeloperoxidase (MPO)-dependent process [35]. From the cytoplasm, NE translocates to the nucleus [36]. Furthermore, NE degrades histones, thereby promoting chromatin decondensation [37]. Histone deimination by peptidyl arginine deiminase 4 (PAD4) is a prominent post-translational modification in NETs that is induced by inflammatory stimuli [38-40]. In neutrophils, inhibition of PAD4 prevents citrullination of histone H3 and significantly reduces NET release induced by a calcium-ionophore or *Shigella flexneri* bacteria in differentiated HL60 cells [40]. Furthermore, PAD4 deficient mice failed to induce NETs [41] indicating citrullination is an important step in certain types of NETosis. The degradation and disassembly of the actin cytoskeleton take place towards the end of NETosis which may further facilitate the disruption of the cytoplasmic membrane, a requirement for NET release [35].

Since reactive oxygen species (ROS) and NET constituents can damage host tissue, it is important that these pathways are tightly regulated [42]. Recent studies suggest that many externalized NET components are potential autoantigens and can be involved in the generation of autoimmune responses [43]. Nevertheless, the mechanism of NET formation is not completely understood.

1.7.1 NETosis: a unique cell death

The term ETosis describes the process of cell death that leads to extracellular traps formation. When these ETs are produced by neutrophils, the term NETosis is used [44, 45]. In contrast to apoptosis or programmed necrosis, both the nuclear and granular membranes disintegrate during NETosis, but plasma membrane integrity is maintained [30]. No morphologic signs of apoptosis are observed, such as membrane blebbing, nuclear chromatin condensation or phosphatidylserine exposure before plasma membrane rupture [30]. Caspase activity is detected during apoptosis, but not during PMA-induced NETosis. Furthermore, inhibition of caspases did not affect PMA-induced NETosis [46]. The addition of necrostatin-1, an inhibitor of necroptosis also did not affect PMA-induced NETosis, indicating NETosis is different from necroptosis [46]. Moreover, stimuli that induce NETs did not promote the release of the cytosolic protein like lactate dehydrogenase (LDH), and activated cells excluded vital dyes for at least two hours after stimulation, ruling out necrosis as an associated phenomenon [29].

1.7.2 NET inducers

A large variety of microbes can induce NET formation. NET-inducing microbes include whole bacteria as well as cell surface components of both Gram-positive bacteria and Gram-negative bacteria. For example, LPS and bacteria-derived peptide formyl-Met-Leu-Phe (fMLP) stimulation leads to NET release [29, 38, 47]. NET inducing bacteria include, among others, *Staphylococcus aureus, Pseudomonas aeruginosa* [48-50]. Not only bacteria are capable of inducing NETs but also pathogenic fungi such as *Candida albicans* and *Aspergillus fumigatus* [51, 52]. NETs capturing HIV and promoting its elimination through MPO and α-defensin has been described, but the role of NETs in fighting viral infections remains unclear. Many parasites like *Leishmania amazonensis* and its surface lipophosphoglycan have been also reported to induce NETs. (46–48).

Various other stimulants have been also described to induce NETs such as phorbol myristate acetate (PMA), IL-8, interferons, as well as activated platelets [53]. The antigen-antibody complex forming immune complexes (ICs) can activate neutrophils and form NETs. Both the soluble and immobilized forms of immune complexes have been also known to induce NETosis [38, 54, 55].

1.7.3 Anti-microbial activity of NETs

Neutrophils can kill pathogens by both ROS -dependent and -independent mechanisms [42]. Neutrophils release granule proteins and anti-microbial enzymes, together with chromatin bind and kill bacteria and degrade virulence factors [29]. The extracellular DNA has rapid membrane-damaging antibacterial activity and exogenous or secreted microbial DNases protect bacteria against NET killing [50]. Many of the NET components was studied and proved to be necessary for the killing of microbes. Histones are the most abundant NET-bound proteins which possess direct membrane-acting anti-bacterial activity [56, 57]. Histones contribute in the killing of *Staphylococcus* and *Shigella* [29]. However, purified NET chromatin alone is not very efficient at killing *S. aureus*, and MPO present in NETs provides the bactericidal activity needed to kill this pathogen in the presence of hydrogen peroxide [58]. Cathepsin G, a granular serine protease, is required for the clearance of *Neisseria* by NETs [50]. Other NET components with antibacterial properties include LL-37, lactoferrin, neutrophil elastase, and proteinase-3 (PR3) [38]. Positively charged peptides and proteins such as defensins, LL-37, MPO and cationic proteases such as NE, cathepsin G, proteinase-3 can disrupt microbial membranes or inhibit microbial growth [59].

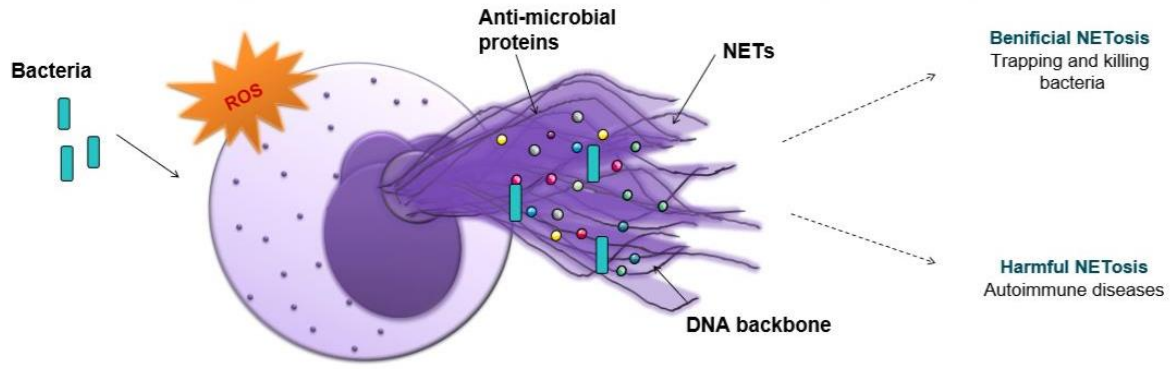

Figure 3. Neutrophil Extracellular Traps (NETs) ensnaring bacteria

1.7.4 NETosis associated- autoimmune diseases

Recently, several studies have linked NET formation with generation of autoimmune responses. This hypothesis is supported by the observation that initiation of

autoimmune responses often occurs following microbial infections [38]. Importantly, neutrophils from patients with various autoimmune diseases appear more prone to NETose. For example, neutrophils from rheumatoid arthritis (RA) patients exhibited increased spontaneous NET formation compared to healthy individuals [60]. NETs include the targets of most autoantibodies found in RA, systemic lupus erythematosus (SLE), and vasculitis [61, 62]. The clinical and biological overlaps observed between and RA, SLE, or SLE and vasculitis suggest that NETosis can be a major triggering event common to these disorders [63].

Many autoantibodies have so far been described in RA, but only anti-citrullinated protein antibodies (ACPA) are considered specific disease marker with sufficient specificity and sensitivity to be used as diagnostic tests of RA [64]. NETs contain histones which are converted from arginines to citrullines by peptidyl arginine deiminase IV (PAD4). The deiminated chromatin may function to capture bacterial pathogens. The complex of bacterial antigens and deiminated chromatin may be internalized by host phagocytes. The uptake and processing of deiminated chromatin together with bacterial adjuvants by phagocytes may induce the presentation of modified histone epitopes and co-stimulation, thus yielding a powerful stimulus to break tolerance. Autoantibodies against deiminated histones are prevalent in systemic lupus erythematosus (SLE) and patients with rheumatoid arthritis (RA). These observations clearly suggest that histone deamination can act as an autoantibody stimulant [65].

NETs containing antimicrobial proteins including DNA and LL37 combination are potent stimulus for plasmacytoid dendritic cells (pDCs) to synthesize type I IFNs [66]. Type I IFNs have antimicrobial roles but also have potent immunostimulatory effects in autoimmune diseases like SLE and psoriasis [38, 66, 67].

1.7.5 ROS-dependent NETosis

NETosis is classified into ROS-dependent and ROS-independent types. However, how ROS contribute to NETosis is not clear. Requirements for oxidant generation depend on the stimulus which induces NET formation [68]. The most frequently used compound to induce NETosis is PMA, a synthetic activator of the protein kinase C (PKC) family of

enzymes. PKC is directly responsible for activation of NADPH oxidase and ROS production [38]. Neutrophils from patients with chronic granulomatous disease (CGD), with non-functional NADPH-oxidase, failed to induce PMA-induced NET release [30, 69]. The requirement for ROS production was confirmed as NADPH oxidase inhibitor like diphenylene iodinium (DPI) and ROS-scavengers inhibited NETosis induced by PMA and *S.aureus* [30, 68, 70]. However, exogenous hydrogen peroxide, which is membrane permeable, could induce NETs, as hydrogen peroxide stimulates MPO downstream of NADPH oxidase. Superoxide itself is not essential, but the conversion of superoxide to hydrogen peroxide and to perchloric acid is essential for NET release. NETosis pathway in CGD neutrophils were rescued with the addition of exogenous peroxide [30, 68, 71].

Similarly, *Candida albicans* also induce ROS mediated NETosis in human neutrophils as well as in mouse neutrophils. Neutrophils from mice lacking functional NADPH oxidase (*gp91–/–)* mice, fail to produce ROS upon stimulation and could not make NETs [72, 73]. Immune complexes (ICs) can stimulate neutrophils to form NETs [74, 75]. Both soluble and immobilized immune complexes (iIC) are capable of inducing NETs [54, 55]. Pre-treatment with DPI had no effect on the soluble IC-induced NET formation, suggesting that ROS is not critical here [54]. However, ROS was found crucial for immobilized immune complex induced NET formation. The NADPH-oxidase inhibitor (DPI) and MPO inhibitor aminopyrine as well as ROS-scavengers were shown to abolish iIC-induced NETosis [55].

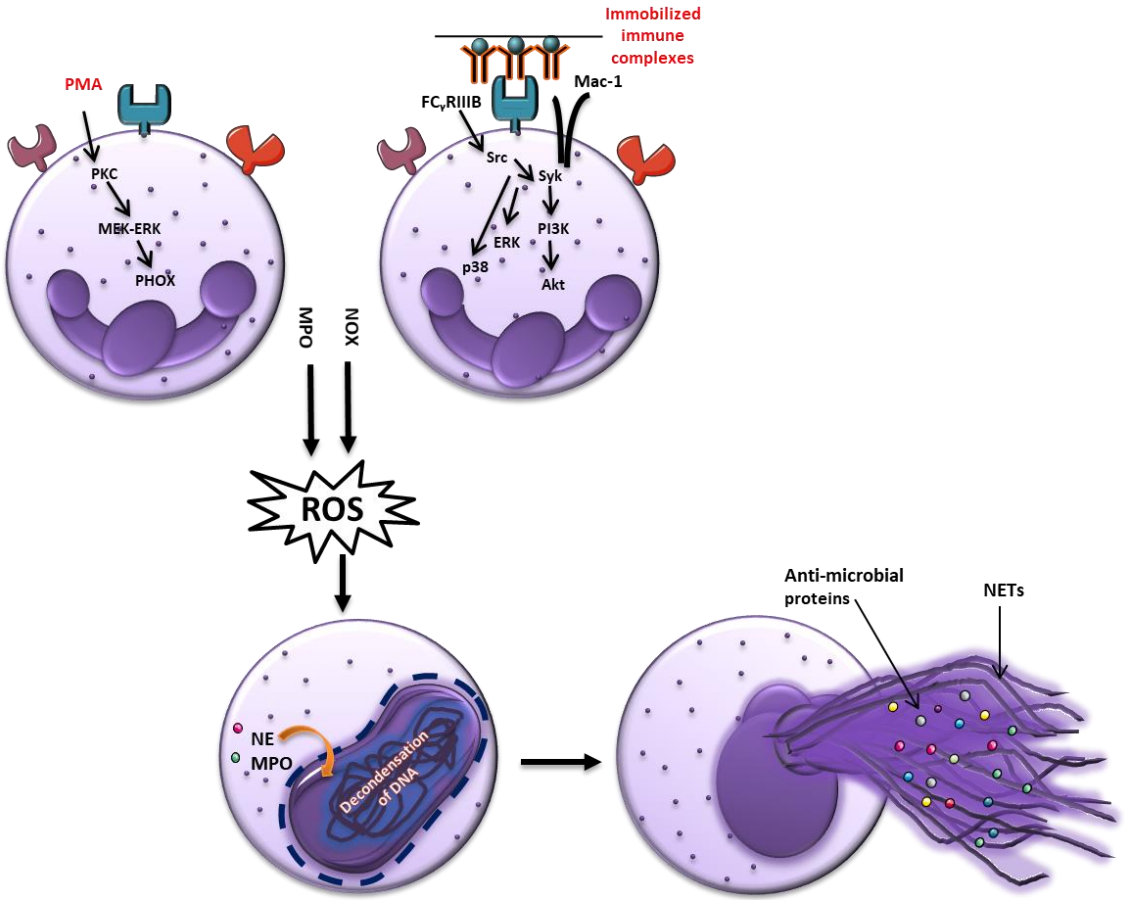

Figure 4. PMA- and immobilized Immune complex (iIC)- induced NETosis

1.7.5.1 Signaling mechanisms known in PMA-induced NETosis

NET formation induced by PMA is independent of transcription as well as of protein synthesis. This suggests that neutrophils contain all the factors required for NET formation when they emerge from the bone marrow as differentiated cells [76]. NETosis induced by PMA is PKC and NADPH oxidase (NOX) dependent. PMA stimulates conventional (α, βI, βII, γ) and novel (δ, ε, η, θ) PKC isoforms [77]. Conventional PKCs have a prominent role in NET formation. Furthermore, PKCβ is the major isoform crucial in NET formation [78]. NADPH subunit p47phox is phosphorylated to acquire a conformational rearrangement to expose the domains that are important for the NADPH oxidase function, and this phosphorylation is mediated by PKC [79]. Downstream of PKC and upstream of NADPH oxidase is Raf–MEK–ERK kinase pathway, which leads to NET signaling [80]. PMA-induced ROS mediated NETosis results in phosphorylation or activation of ERK1/2 and p38 MAPK pathway [81] **(Fig. 4)**.

However, conflicting evidence exists as to whether ERK is activated upstream or downstream of ROS production [80, 81]. Apparently, an additional contribution of ERK to this process may not be required as PKC can directly activate NADPH oxidase [82-85]. In addition, Syk is found to be involved in PMA dependent ROS and NET production, as Syk inhibition reduced the NET formation and almost abolished ROS production [55]. PMA-mediated phosphorylation of Akt has been shown, where Akt induces NETosis while suppressing apoptosis [86].

1.7.5.2 Signaling mechanisms known in iIC-induced NETosis

Immobilized immune complexes (iICs) stimulate the release of NETs in an NADPH-MPO associated and ROS-dependent manner. iICs are recognized by Fc_{γ}RIIIB and its signaling partner macrophage-1 Ag (Mac-1: CD11b/CD18). Mac-1 does not seem to play a role in iIC-induced ROS production as blocking of Mac-1 had no effect on MPO-dependent ROS and only slight inhibition of NADPH-oxidase (NOX) dependent super oxide production. iIC-induced ROS depends on both Fc_{γ}RIIA (CD32) and Fc_{γ}RIIIB (CD16). However, only Fc_{γ}RIIIB is sufficient for iIC-induced NET release.

Fc_{γ}RIIIB and Mac-1 downstream activates Src/Syk signaling, which activates neutrophils. Src/Syk further activates ERK1/2, PI3K/ Akt, and p38 MAPK pathways. Enhanced phosphorylation of, ERK1/2, PI3K/Akt and p38 MAPK is seen in iIC-stimulated neutrophils. The inhibitor studies on these intracellular molecules confirmed their importance. ERK1/2 inhibition almost abolished NET formation, whereas treatment with inhibitors of Akt and p38 MAPK partially inhibited iIC-induced NET formation. The activation of ERK1/2, PI3K/Akt or p38 MAPK results directly from Src family kinases/receptor activation and is not ROS mediated, as the ROS inhibition did not affect their phosphorylation [55] **(Fig. 4)**.

1.7.6 ROS-independent NETosis

NETosis can also occur in certain conditions through ROS-independent pathways [68, 87]. Generation of ROS did not complement the defect in NET formation by neonatal neutrophils, as it did in adult cells with inactivated NADPH oxidase, demonstrates that ROS is not sufficient for downstream signaling in neonate neutrophils [87]. NADPH

oxidase-independent NETosis that can be induced by stimuli including calcium ionophores [88]. Furthermore, a unique and very rapid way of NETosis in response to *S. aureus* showed that the first 5–60 min of NETosis is ROS-independent [89]. Nevertheless, the mechanisms for the NOX-independent pathway of NETosis are not well understood.

1.7.6.1 Signaling mechanisms known in Ionomycin-induced NETosis

Ionomycin, a natural Ca^{2+} Ionophore produced by the Gram-positive bacterium *Streptomyces conglobatus* can induce rapid NADPH oxidase (NOX)-independent NETosis [88, 90, 91]. Ionomycin acts as a motile Ca^{2+} carrier and enhances Ca^{2+} influx by direct stimulation of store-regulated cation entry across biological membranes [92]. In 2015 Douda et al. studied Ionomycin induced- NETosis. They showed that activation of the calcium-activated potassium channel of small conductance (SK channel) induces NOX-independent NETosis. In neutrophils with calcium influx, SK channels activate mitochondrial ROS production and activate potassium current. Mitochondrial ROS is needed for Ionomycin induced NOX-independent NETosis, but not for NOX-dependent NETosis. Furthermore, a large amount of mitochondrial ROS is being produced during NOX-independent NETosis, but not during NOX-dependent NETosis. In contrast to NOX-dependent NETosis, ERK is not substantially activated in NOX-independent NETosis, and inhibiting ERK does not inhibit NETosis. p38 and Akt are activated in both NOX-dependent and NOX-independent types of NETosis. However, the inhibition of p38 did not inhibit NOX-dependent NETosis [88]. PAD4 is a calcium-dependent enzyme, shown to be critical in Ionomycin-induced NETosis. Inhibition of PAD4 nearly abolishes Ionomycin induced NETs [40]. PAD4 mediates citrullination, which is the conversion of positively charged arginine side chains into polar but uncharged citrulline side chains, by deimination [93].

1.8 Platelet-derived growth factor receptors (PDGFRs)

Platelet-derived growth factor receptors (PDGFR) are cell surface tyrosine kinase receptors for members of the platelet-derived growth factor (PDGF) family [94]. The PDGF family consists of five members (i.e., disulfide-bonded dimers of homologous A-, B-, C-, and D-polypeptide chains, and the AB heterodimer) [95]. The PDGF-α receptor binds all PDGF chains except the D chain, whereas the β receptor binds PDGF-B and -D; thus, the different PDGF isoforms can induce αα-, αβ-, or ββ-receptor dimers [96]. PDGFR structure consists of Ig-like domains in their extracellular part, a single transmembrane domain, and an intracellular part consisting of a well-conserved juxtamembrane domain, a tyrosine kinase domain with a characteristic inserted sequence without homology with kinases, and a less well-conserved carboxy-terminal tail [96] **(Fig. 5)**. Gene knockout studies in mice indicated that PDGF and PDGF receptors have important roles to promote proliferation, migration, and differentiation of specific cell types during the embryonal development [97].

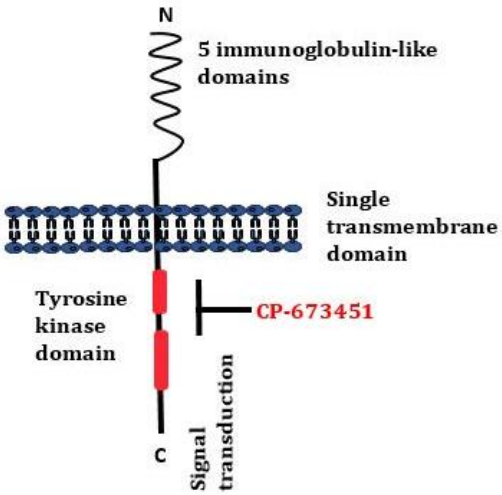

Figure 5. Structure of PDGFR

PDGF-A is expressed in most epithelial cells and PDGFR-α is expressed in most mesenchymal interstitial cells. The PFGF-A is important during organogenesis in stimulating cell proliferation. PDGF-B is expressed in most endothelial cells and is responsible for the proliferation of smooth muscle cells of the vessels and pericytes during angiogenesis [96, 97]. In 1982, Platelet-derived growth factor (PDGF) was shown to be chemotactic for monocytes and neutrophils [98]. On the contrary, in 1995 a study showed that neutrophils lack detectable mRNA for PDGF alpha-receptor and beta-receptors. This indicated that human neutrophils possibly do not possess functional PDGF receptors [99].

Dimerization is the key event in PDGF receptor activation as it allows for receptor autophosphorylation on tyrosine residues in the intracellular domain [100]. Autophosphorylation activates the receptor kinase and provides docking sites for

downstream signaling molecules [97, 101]. Both PDGFR-α and PDGFR-β engage several well-characterized signaling pathways like Ras-MAPK, PI3K, and PLC-γ which are involved in multiple cellular and developmental responses. PDGFRs connect to Ras-MAPK mainly through the adaptor proteins. Adapter proteins bind the activated PDGFR through its SH3 domains. Furthermore, Ras protein is activated, leading to downstream activation of Raf-1 and the MAPK cascade. MAPK signaling activates gene transcription, leading to stimulation of cell growth, differentiation, and migration [102, 103].

PDGFRs are mainly linked to certain cancers which are caused due to genetic aberrations leading to uncontrolled PDGF signaling in tumor cells. PDGFs are known also to help to recruit different types of stromal cells and promote angiogenesis. This process supports the invasion of metastatic cells [96, 97, 104]. To control overactivity of PDGF signaling various pharmacological antagonists have been developed. Several types of inhibitors are now available, including inhibitory antibodies against the receptors, and low molecular weight inhibitors of PDGF receptor kinases etc. [105]. The most efficient ways to block PDGFR signaling is to inhibit the PDGFR kinase activity. Kinase inhibitors act by binding at or near the ATP-binding pocket of the kinase domain. Several kinase inhibitors (example; CP-673451) have been developed that block PDGFRs **(Fig. 5)**, but the inhibitors available so far are not completely specific [97, 106-108].

1.9 CP-673451: inhibitor molecule targeting PDGFRs

CP-673451 is a pharmacological selective inhibitor of PDGFRα/β and PDGF-BB-stimulated autophosphorylation of PDGFR-beta with IC50 ranging from 1nM-10nM in cell-free assays. It exhibits >450-fold selectivity to PDGFRβ over other angiogenic receptors (e.g., vascular endothelial growth factor receptor 1 and 2 (VEGFR-1, VEGFR-2)) [106]. The chemical name of CP-673451 is 1-[2-[5-(2-Methoxyethoxy)-1H-benzimidazol-1-yl]-8-quinolinyl]-4-piperidinamine. Its molecular formula is $C_{24}H_{27}N_5O_2$ and it has a molecular weight of 417.52 **(Fig. 6)** [106].

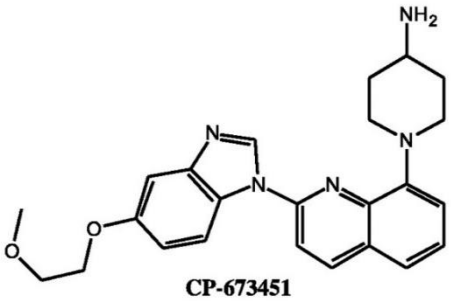

Figure 6. Molecular structure of CP-673451

CP-673451 has shown to have anti-angiogenic and anti-tumor activity. CP-673451 inhibits PDGFR-beta phosphorylation, selectively inhibits PDGF-BB-stimulated angiogenesis in vivo, and causes significant tumor growth inhibition in multiple human xenograft models [106]. Furthermore, CP-673451 inhibits the tumor growth in Colo205, LS174T, H460, and U87MG xenograft models. Inhibition of angiogenesis or tumor growth is correlated with plasma and tumor concentration and inhibition of phospho-PDGFR *in vivo*. U87MG human glioblastoma xenografts express PDGFR on the tumor cells; thus, inhibition could be due to a direct antitumor effect as well as an antiangiogenic effect. In kinase assays, CP-673451 does not show substantial potency against any other kinase tested, including, VEGFRs [106, 108-110].

Objectives of the Study

The process of neutrophil extracellular trap formation (NETosis) has been identified in 2004. Since then, several studies have been carried out to investigate the mechanisms involved in NET formation. These studies identified some molecular pathways involved in ROS-dependent NETosis which can be induced by PMA and iICs. However, the molecular pathways identified in ROS-dependent NETosis are upstream of ROS production. The signaling mechanism of NETosis downstream of ROS production is still not clear. Therefore, major objective of this study was to identify signaling mechanisms involved in NETosis downstream of ROS production.

As experimental approach, it was planned that an inhibitory library will be screened for substances which inhibit NETosis but do not inhibit ROS production. This approach might possibly give a specific inhibitor of NETosis which targets downstream to ROS production.

At the second stage of the study, the aim was to identify the target of the NETosis inhibitor to understand the mechanism of inhibition. The molecular target of the inhibitor was planned to confirm by other similar target inhibitors and the effect of the inhibitor on known pathways activated by PMA and iIC. It was hypothesized that the inhibitor which inhibits NETosis independent of ROS pathways could be used as a general inhibitor of NETosis. This was planned to be tested with the ROS-independent NETosis stimulus, Ionomycin.

The third aim of the study was to test whether the inhibitor affects basic neutrophil functions including activation, migration and phagocytosis. This could clarify if the pathway of NETosis is also involved in the regulation of other neutrophil functions. To check if the inhibitor results changes in gene expressions in neutrophils, a high-throughput RNA-seq approach to profile transcriptional responses was envisaged.

Chapter 2. Materials and Methods

2.1 Materials

2.1.2 Solutions, buffers and media

10 x Tris buffered saline (TBS):	200 mM Tris Ultra + 1.4 mM Sodium chloride, pH to 7.6.
1xRIPA buffer:	Dilute 1:10 ready-made 10xRIPA buffer in aqua dest with 1:10 ratio protease inhibitor (cOmplete mini)
4 x loading buffer:	0.16 M Tris Ultra pH 6.80 + 30 % glycerol + 2 % SDS + 0.71 M 2-β-mercaptoethanol + 0.002 % bromophenol blue.
Acetate buffer (Substrate buffer for migration assay);	6.8 g $CH_3COONa*3H_2O$ in 400ml aqua dest with HCl to adjust pH to 4 and with aqua dest up to 500 ml
Blocking buffer for immune complex formation:	TBS + 0.1 % Tween 20 + 1% BSA, filtered.
Blocking buffer for Western blot:	TBS + 0.1 % Tween 20 + 5% BSA.
Blotting buffer:	25 mM Tris Ultra + 192 mM glycine + 20% methanol.
CL-medium	RPMI 1640 medium special with 20 mM HEPES without NaHCO3, pH7.2, without phenol red
Complete medium:	RPMI 1640 medium + 200 mM L- glutamine + 20 mM HEPES + 10 % FCS + 100U/100µg/ml Penicillin/Streptomycin.
DMEM:	DMEM (41965-039) +10 % FCS +100 U/100 µg/ml Penicillin/ Streptomycin
Electrophoresis buffer (5x):	125 mM Tris Ultra + 0.960 M glycine + 0.5 % sodium dodecyl sulfate.
FACS buffer:	PBS + 1 % BSA + 0.01 % sodium azide + 1 % human serum.

Glycine buffer (Stop solution for migration assay):	15 g glycin in 400 aquadest, with NaOH to adjust the pH to 10.3 with aqua dest fill up to 500 ml
NET-medium:	CL-medium (RPMI 1640 medium special preparation from Biochrome #FZ 1235+ 20 mM HEPES w/o NaHCO3, pH7.2, w/o phenol red) + 0,5% HSA (Baxter) + 0,5 % Human serum albumin
TBS-Tween:	TBS + 0.1 % Tween 20

2.1.3 Laboratory supplies

Cell culture flask, 250 ml, 75 cm^2 with filter screw cap	Greiner bio-one, Frickenhausen
Cell culture plates (96, 24, 12, 6 well, flat bottom)	Greiner bio-one, Frickenhausen
Costar 3472 Corning®-Transwell® cell culture inserts 24 mm with 3 µm pore polycarbonate membrane insert	Costar- Corning, New York, USA
Eppendorf tubes (1.5; 2 ml (PP))	Biopure Eppendorf, Hamburg
Extra Thick Blot Filter Paper	Biorad, Munich
Microscope slides	Menzel, Braunschweig
Microtestplate + lid (96-well, V-bottom)	Sarstedt, Nümbrecht
Neubauer chambers	BRAND Gmbh + CO KG, Wertheim
Nitrocellulose (NC) membrane	Bio-Rad, Munich
Nunclon ELISA PLATES	Nunc, Langenselbold
Pipette 2, 5, 10, 25 ml	Greiner bio-one Frickenhausen
Pipette filter tips	Nerbe plus, Winsen
Plastic tubes (15 ml (PP), 50 ml (PP))	Sarstedt, Nümbrecht
Precast gels Any Kd	Bio-Rad, Munich
S-Monovette 9 ml, lithium-heparin	Sarstedt, Nümbrecht
Stericup® Filter Units	Merck Millipore, Billerica, Massachusetts, United States
Thermonox cover slides 13mm (174950)	Thermo Fisher Scientific, Waltham,

	MA, USA
Transfer pipette 3.5 ml	Sarstedt, Nümbrecht
U-tubes for flow cytometry	Sarstedt, Nümbrecht

2.1.4 Chemicals and reagents

2-β-Mercaptoethanol	Sigma-Aldrich, Steinheim
Acetone	Merck, Darmstadt
Annexin V FLUOS	Roche Diagnostics, Mannheim
Bovine serum albumin (BSA)	Sigma-Aldrich, Steinheim
Bromophenol blue dye	Serva, Heidelberg,
Calcium chloride	Sigma-Aldrich, Steinheim
CL-medium (RPMI 1640 medium special preparation #FZ 1235)	Biochrom, Berlin
cOmplete™, Mini Protease Inhibitor Cocktail	Roth, Karlsruhe
Coomassie	Thermo Fisher Scientific, Waltham, MA, USA
Crystal violet	Sigma-Aldrich, Steinheim
Diff-Quick® fixative solution	Medion Diagnostics, Duedingen, Switzerland
Diff-Quick® staining set	Medion Diagnostics, Duedingen, Switzerland
DMEM	Gibco, Karlsruhe
Dmso (Dimethyl sulfoxide)	Sigma-Aldrich, Steinheim
DPI (diphenyleneiodinium chloride)	Sigma-Aldrich, Steinheim
Fetal calf serum (FCS)	Sigma-Aldrich, Steinheim
Glycine	Sigma-Aldrich, Steinheim
HEPES	Biochrom, Berlin
Histopaque® 1077	Sigma-Aldrich, Steinheim
Histopaque® 1119	Sigma-Aldrich, Steinheim
Human serum albumin (HSA)	Apotheke
Immersions oil	Carl Zeiss, Jena
Immmobilion™ western	Millipore, MA, USA
Ionomycin calcium salt (I0634)	Sigma-Aldrich, Steinheim

Isopropanol	Roth, Karlsruhe
Latex beads (FluoSpheres® Polystyrene Microspheres, 1.0 µm)	Invitrogen, Eugene, OR, USA
L-Glutamine	Biochrom, Berlin
Lipopolysaccharide E. coli 0111: B4 (LPS)	Sigma-Aldrich, Steinheim
Luminol	Sigma-Aldrich, Steinheim
Methanol	Baker, Deventer, The Netherlands
N-Formylmethionyl-leucyl- phenylalanine (fMLP)	Sigma-Aldrich, Steinheim
PageRuler™ Unstained Protein Ladder	Thermo Fisher Scientific, Waltham, MA, USA
Paraformaldehyde	Sigma-Aldrich, Steinheim
PBS (1 x) sterile solution	Pharmacy of University of Lübeck, Lübeck
PBS (10 x) sterile solution	Gibco, Karlsruhe
PBS (20 x) sterile solution	Cell Signaling, Leiden, The Netherlands
Penicillin/streptomycin	Biochrom, Berlin
Percoll®	Sigma-Aldrich, Steinheim
PhoStop tablets	Roche Diagnostics, Mannheim
Pierce Prestained Protein MW Marker	Thermo Fisher Scientific, Waltham, MA, USA
PMA (phorbol 12-myristate 13-acetate)	Sigma-Aldrich, Steinheim
PMB (Polymyxin-B)	Biochrom, Berlin
Poly-L-Lysin	Sigma-Aldrich, Steinheim
ProLong™ Gold Antifade Mountant	Thermo Fisher Scientific, Waltham, MA, USA
Propidium iodide	Sigma-Aldrich, Steinheim
RIPA Buffer (10x)	Cell Signaling, Leiden, The Netherlands
RPMI 1640 medium	Sigma-Aldrich, Steinheim
Sodium azide	Merck, Darmstadt
Sodium chloride	Merck, Darmstadt
Sodium dodecylsulfate	Sigma-Aldrich, Steinheim

Staphylococcus aureus bioparticles®, Alexa Fluor 488 conjugate	Thermo Fisher Scientific, Waltham, MA, USA
SytoxGreen (nucleic acid stain)	Invitrogen, Eugene, OR, USA
TCA (Trichloro acetic acid)	Sigma-Aldrich, Steinheim
Tris Ultra	Roth, Karlsruhe
Triton X-100	Merck, Darmstadt
Trypan blue solution 0.4 %	Sigma-Aldrich, Steinheim
Trypsin-EDTA (0.25%)	Gibco, Karlsruhe
Tween -20	Sigma-Aldrich, Steinheim
β-Glucuronidase (G8420)	Sigma-Aldrich, Steinheim

2.1.5 Other selective inhibitors

Etoposide	Selleckchem (Houston, USA)
Flumequine	Selleckchem (Houston, USA)
Motesanib Diphosphate (AMG-706)	Selleckchem (Houston, USA)
Sunitinib	Selleckchem (Houston, USA)
Vandetanib (ZD6474)	Selleckchem (Houston, USA)

2.1.6 Ready to use kits

Immobilon Western HRP Substrate	Merck, Darmstadt
NextSeq 500/550 High Output Kit	Illumina, San Diego, California, USA
Pierce™ LDH Cytotoxicity Assay Kit	Thermo Fisher Scientific, Waltham, MA, USA
QIAamp RNA Blood Mini Kit	Qiagen, Hilden
RNase-Free DNase Set	Qiagen, Hilden

2.1.7 Antibodies

Goat anti-HSA- IgG	Cell Signaling, Leiden, The Netherlands
Goat anti-rabbit-HRP-linked	Cell Signaling, Leiden, The Netherlands
Horse anti-mouse-HRP-linked	Cell Signaling, Leiden, The Netherlands
Mouse anti-human CD11b-FITC	BioLegend, San Diego, CA, USA

Mouse anti-human IgG	New England Biolabs, USA
Rabbit anti-HSA -IgG	Sigma-Aldrich, Steinheim
Rabbit anti-human PDGFR	Cell Signaling, Leiden, The Netherlands
Rabbit anti-human phospho-Akt (Thr308)	Cell Signaling, Leiden, The Netherlands
Rabbit anti-human phospho-Erk1/2 (p44/42)	Cell Signaling, Leiden, The Netherlands
Rabbit anti-human phospho-p38 MAPK (Thr180/Tyr182)	Cell Signaling, Leiden, The Netherlands
Rabbit anti-human phospho-PI3	Cell Signaling, Leiden, The Netherlands
Rabbit anti-human phospho-PKC α/β	Cell Signaling, Leiden, The Netherlands
Rabbit anti-human phospho-PKC δ	Cell Signaling, Leiden, The Netherlands
Rabbit anti-human phospho-Serine	Merck, Darmstadt
Rabbit anti-human phospho-Src	Cell Signaling, Leiden, The Netherlands
Rabbit anti-human phospho-Threonine	Cell Signaling, Leiden, The Netherlands
Rabbit anti-human phospho-Threonine (Sepharose® bead conjugate)	Cell Signaling, Leiden, The Netherlands
Rabbit anti-human phospho-Tyrosin	Cell Signaling, Leiden, The Netherlands
Rabbit anti-human β-actin, HRP-linked	Cell Signaling, Leiden, The Netherlands

2.1.8 Cytokines

Recombinant human IFN-γ	R&D Systems, Wiesbaden-Nordenstadt
Recombinant human IL-8	R&D Systems, Wiesbaden-Nordenstadt
Recombinant human TNF-α	PeproTech, Rocky Hill, NJ, USA

2.1.9 Cell lines/cell line lysate

T129 lysate	Department of Neurosurgery, University of Lübeck
U87-MG	Department of Neurosurgery, University of Lübeck

2.1.10 Instruments

Analytical balance BP61S	Sartorius, Göttingen
Balance	Sartorius, Göttingen
Bioanalyzer	Agilent, Santa Clara, California, USA
Block thermostat HB	Peqlab, Erlangen
Carl Zeiss, Jena	Carl Zeiss, Jena
Centrifuge 5417R	Eppendorf, Hamburg
Centrifuge Biofuge fresco Kendro	Heraeus, Langenselbold
Centrifuge Megafuge 2.0R Kendro	Heraeus, Langenselbold
Centrifuge Microfuge R	Beckmann, Munich
Centrifuge Mikro 12-24	Hettich, Tuttlingen
Centrifuge Multifuge 3 and SR Kendro	Heraeus, Langenselbold
CO_2 Incubator IG 150	Jouan, Unterhaching
Cytocentrifuge Cytospin 3	Shandon, Frankfurt
Deep freezers, −20°C, −70°C	Liebherr, Ochsenhausen
Flow cytometer Canto II	Becton Dickinson, Heidelberg
Fusion Fxt chemiluminescence reader	Vilber Loumat, Eberhardzell
Incubator without CO_2	Agilent Technologies, Santa Clara, CA, USA
Infinite 200 Pro reader	Tecan, Crailsheim
Keyence Microscope	Osaka, Osaka Prefecture, Japan
Laminar flow workbench	Biohit, Cologne
Magnetic stirrer: Ikamag, Reo IKA	Labortechnik, Staufen
Microscope Axiocam HRc	Carl Zeiss, Jena
Microscope Axiostar plus	Carl Zeiss, Jena
Multichannel pipette	Eppendorf, Hamburg
NanoPhotometer Pearl®	Impeln, Munich
pH-meter Inolab	WTW GmbH, Weilheim
Pipette boy	Eppendorf, Hamburg
Ricoh HR-10m camera	Ricoh, Tokyo, Japan
Semi-dry protein transfer cell	Bio-Rad, Munich
Shaker Vibrofix VF1 Electronic	Janke & Kunkel IKA® Labortechnik, Staufen
Water bath	Köttermann, Uetze

2.1.11 Software

AxioVision release 4.8 software	Carl Zeiss, Jena
BD FACSDiva™ software 9	Becton Dickinson, Franklin Lakes, NJ, USA
Bioanalyzer 2100 Expert Software	Agilent, Santa Clara, California, USA
BioD1	Vilber Loumat, Eberhardzell
BZ II analyzer software	Keyence, NeuIsenburg
GraphPad Prism 5.0 and 6.0	La Jolla, CA USA
ImageJ software	NIH, Bethesda, USA
Tecan i-control 1.7 software	Tecan, Crailsheim

2.2 Methods

2.2.1 Neutrophil isolation from human blood

Peripheral blood was collected by venipuncture from healthy donors in lithium heparin-containing tubes. 12.5 ml Histopaque 1119 was layered in a 50-ml falcon tube and 12.5 ml of Histopaque 1077 was layered over it carefully. To the prepared bilayer gradient, 25ml blood was layered. The gradient was centrifuged for 5 min at 300 x g followed by 25 min at 800 x g. After centrifugation, the top layer containing plasma and the Histopaque 1077 layer rich in lymphocytes and monocytes were discarded and the last layer containing erythrocytes were discarded. The granulocyte rich layer of Histopaque 1119 layer was collected in 50 ml Falcon tube and washed with PBS for 10 min at 800 x g. The granulocytes were then resuspended in 2ml of complete medium and layered on the top of Percoll gradient. The Percolll gradient was prepared in a 15 ml tube by layering with densities 1.105 g/ml (85 %), 1.100 g/ml (80 %), 1.093 g/ml (75 %), 1.087 g/ml (70 %), and 1.081 g/ml (65 %) from the bottom to the top, respectively. The gradient column was centrifuged at 800 x g for 25 min. After centrifugation, the interphase between the 70 % and 85 % Percoll layers was collected and washed with PBS at 800 x g for 10 min and resuspended in complete medium. All the centrifugation steps were performed at room temperature. The cell preparations contained >99 % granulocytes. Neutrophil purity was >98 % as determined by morphological examination of cytocentrifuged slides stained with Diff Quick.

2.2.2 Culturing U87-MG Cell lines

U87-MG cells were continuously cultured in Dulbecco's Modified Eagle Medium (DMEM with FCS) at 37°C in humidified atmosphere containing 5 % CO_2 until they are confluent. Cells were exposed to trypsin/EDTA to detach the adherence at 37°C for 5 min and DMEM containing FCS was added to stop trypsinization. The medium was renewed every 2-3 days.

2.2.3 Cytospin and Diff-Quick staining

Neutrophils ($5x10^5$/ml in 100 µl complete medium) were cytocentrifuged at 400 x g for 5 min. The slides were air dried, fixed in Diff-Quick® fixative solution and,

subsequently, stained by Diff-Quick staining set according to the manufacturer's protocol.

2.2.4 Preparation of immobilized immune complexes

Immobilized immune complexes (iICs) were prepared by using human serum albumin (HSA) as antigen and anti–HSA IgG rabbit polyclonal antibody as described previously [111]. 100 µl of 20 mg/ml HSA in 50 mM bicarbonate buffer (pH 9.6) was coated overnight at 4˚C in 96 well Lumitrac 600 high-binding plates for chemiluminescence-based ROS detection and in Flurotrac 600 high-binding plates for fluorescence-based NET detection. The plates were then washed with 200 µl PBS containing 0.05% Tween 20 (wash buffer) and then blocked with 200 µl 1% biotin-free BSA in PBS (blocking buffer) for 1 h at room temperature (RT), following 1 h incubation with anti–HSA rabbit IgG (~10 mg/ml) diluted 1:400 in blocking buffer. The IC-coated wells were then washed twice with wash buffer and once with assay- medium. For fluorescence microscopic experiments, iICs were coated as described above by using 0.5 ml volume of reagents instead of 200 µl in an 24-well ibiTreat slides.

2.2.5 Detection of intra- and extracellular ROS

The intra- and extracellular ROS produced by neutrophils were measured by using luminol-based chemiluminescence assay [112, 113]. All chemiluminescent assays were performed in chemiluminescent medium (CL-medium). For the real-time-ROS-kinetics, neutrophils ($4x10^5$/ml cells/200 µl CL-medium) were added to the iIC-coated or to uncoated wells containing 0.1% dmso, medium for iIC-mediated ROS detection. For PMA mediated ROS production, $4x10^5$/ml cells/200 µl CL-medium was treated with PMA (20nM) or with 0.1% dmso or CL-medium. All the ROS detection assays were performed in Flurotrac 600 high-binding white plates. Different concentrations of inhibitors (10 µM, 3 µM, 1 µM, 0.3 µM, 0.1 µM) and 0.06 mM luminol were also added at the same time. In preliminary screening for inhibitors, a single concentration of 10 µM was used and cell suspension pre-treated for 30 min with 20nM DPI at 37°C was used as inhibition control. ROS-dependent chemiluminescence was analyzed using an Infinite 200 reader and Tecan i-control 1.7 software. ROS release was monitored for 1 h every

1-2 min at 37˚C. For statistical analysis, the area under the curve (AUC) of each sample was calculated.

2.2.6 SytoxGreen detection of NETs

The time kinetics of NET release was assessed by using the non-cell permeable DNA dye SytoxGreen [114-116]. For iIC-mediated ROS detection, neutrophils ($2x10^5$ cells/200 µl NET-medium) were added to the iIC-coated or to uncoated wells. For PMA mediated ROS production, $2x10^5$ cells/200 µl NET-medium were treated with PMA (20nM) or with 0.1% dmso or medium. In Ionomycin-induced NET assays, $2x10^5$ cells/200 µl in complete medium without FCS were tested with 7 µM, 5 µM, and 2.5 µM concentrations of Ionomycin for inducing NETosis. For the experiments with the inhibitor, 5 µM concentration of Ionomyin were used. For PMA and iIC NETs, NET-medium was used and for Ionomycin-induced NET formation, complete medium without FCS was used. All NET assays are performed in Flurotrac 600 high-binding black plates. Different concentrations of inhibitors (10 µM, 3 µM, 1 µM, 0.3 µM, 0.1 µM) and 5 µM SytoxGreen were also added to the wells at the same time. In preliminary screening for inhibitors, a single concentration of 10 µM was used and cell suspension pre-treated for 30 min with 20 nM DPI at 37°C was used as inhibition control. The NET-bound SytoxGreen fluorescence (excitation: 488 nm, emission: 510 nm) was analyzed for 4 h for PMA and 7 h for iIC with 5 min interval at 37°C by using Tecan infinite M200 Pro reader and Tecan i-control 1.7 Software. For statistical analysis, the area under the curve (AUC) was calculated.

2.2.7 Fluorescent microscopy for NETs

Fluorescent microscopy of NET formation/inhibition slides was prepared in 13 mm µ-slides. $5x10^5$ cells/500 µl NET medium were treated with different concentrations of CP-673451, Doxorubicin (10 µM, 3 µM, 1 µM, 0.3 µM, 0.1 µM), 0.1% dmso, DPI (20 nM) and NET-medium and incubated for 30 min at 37˚C. The cells were then added to iIC-coated µ-slides. For samples with PMA as stimulant the cells were added to Poly-L-Lysin coated µ-slides. The cells were then incubated for 4h and 7 h at 37˚C for PMA and iIC stimulated plates, respectively. Followed by fixation with 4% paraformaldehyde,

staining with SytoxGreen was carried out as described previously [117]. Samples were analyzed with Keyence BZ-9000E using the BZ II Analyzer Software.

2.2.8 Neutrophil activation assay

The surface marker expressions were analyzed by staining CD11b and CD62L markers on neutrophils. Upregulation of CD11b and shedding of CD62L was associated with neutrophils activation and this was monitored by flow cytometry. $5x10^5$ neutrophils in 200 µl complete medium were pre-incubated for 30 min at 37°C, 5% CO_2 with CP-673451 or with 0.1% dmso or with Polymyxin-B (PMB) (10 µg/ml), or with medium and stimulated with different stimulants; LPS (100 ng/ml), LPS (100 ng/ml) together with IFN_γ (200 U/ml), TNF-α (100 ng/ml), fMLP (1 µM) and with inhibitor CP-673451 (10 µM, 3 µM, 1 µM, 0.3 µM, 0.1 µM) for 4 h at 37°C. The cells were then stained with fluorescent-conjugated antibodies against CD11b and CD62L for 30 min at 4°C. The surface marker expression changes were analyzed using flow cytometer and analyzed by FACS Diva software **(Fig. 7)**. Percentage of the cells upregulating CD11b and shedding CD62L are considered as activated cells.

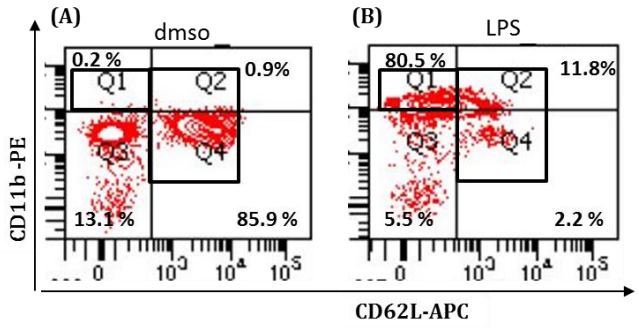

Figure. 7 Assessment of neutrophil activation using flow cytometry

Neutrophils were pre-treated with 0.1% dmso and stimulated with LPS (100ng/ml) **(B)** or left unstimulated **(A)** for 4 h at 37°C, 5% CO_2. The cells were then stained with fluorescent-conjugated antibodies against CD11b-PE and CD62L-APC for 30 min at 4°C. Percentage of the cells upregulating CD11b and shedding CD62L was assessed by flow cytometry and analyzed by FACS Diva software. Q1: cells upregulating CD11b and shedded CD62L. Q2+Q4: cells not upregulating CD11b and not-shedding CD62L. Q3: cells shedded CD62L, but not upregulating CD11b.

2.2.9 Neutrophil migration assay

The neutrophil migration assay was performed in 24 well trans well plates with a 3µm pore size (costar 3472). $6x10^5$ neutrophils in 100 µl complete medium were seeded in a 24 well plate and treated with different concentrations of the inhibitors (10 µM, 3 µM, 1 µM, 0.3 µM, 0.1 µM), or 0.1 % dmso, or medium. The cell suspension was incubated for 30 min at 37°C, followed by transferring into the upper filter of the trans well. Into the lower well of the trans well was added with 600µl of IL-8 (25 ng/ml), or TNF-α (50ng/ml) or medium. The cells were allowed to migrate for 1h at 37°C. The number of migrated cells was measured by using the beta-glucuronidase assay. The migrated cells in the lower well and $6x10^5$ untreated fresh neutrophils in 600 µl were lysed with 100 µl of 1 % Triton X-100 for 10 min. 100µl of the untreated fresh neutrophil lysates were transferred to a 96 well Nunc transparent plate and serially diluted to get the standard curve. For the beta-glucuronidase assay, 100µl and 600µl of substrate mix (containing 4-Nitrophenyl β-D-glucuronide) in acetate buffer to the 96 and 24 wells respectively and incubate overnight at 37°C. Next day, glycine buffer was added 100µl and 600µl to stop the reaction in both 96 and 24 well respectively. 300µl of the 24 well lysate was transferred to the 96 well plates and measured the absorbance at 405 nm and reference 620 nm. The migration indexes are calculated by normalizing the OD values of medium-treated neutrophils migrating in response to IL-8 or TNF-α as migration index of 1. The migration indices of inhibitor-treated neutrophils migrating in response to IL-8 or TNF-α are calculated from their OD values in relation to the index of 1.

2.2.10 Neutrophil phagocytosis assay

Neutrophils ($5x10^5$ cells/100 µl complete medium) were pre-incubated for 30 min with different concentrations of CP-673451 or 0.1% dmso or medium. Subsequently, Alexa-Fluor 488 conjugated non-viable *Staphylococcus aureus* bioparticles in (2:1 ratio; *S. aureus* to neutrophils) or FluoSphere carboxylate-modified latex microspheres with a diameter of 1 µm were added in 1 to 10 ratios to neutrophils. To certain samples stimulants LPS (100 ng/ml) and IFN_γ (200 U/ml) were also added, and incubated for further 30 min at 37°C with 5 % CO_2. Cells were washed in a v-bottom plate at 800 x g for 5 min to remove extracellular bacteria/beads. Trypan blue was added to quench the fluorescence of extracellular bacteria/beads sticking on the neutrophil surface. The

percentage of cells performed phagocytosis and the quantity of ingested bioparticles/beads were assessed by flow cytometry and analyzed by FACS Diva software **(Fig. 8)**.

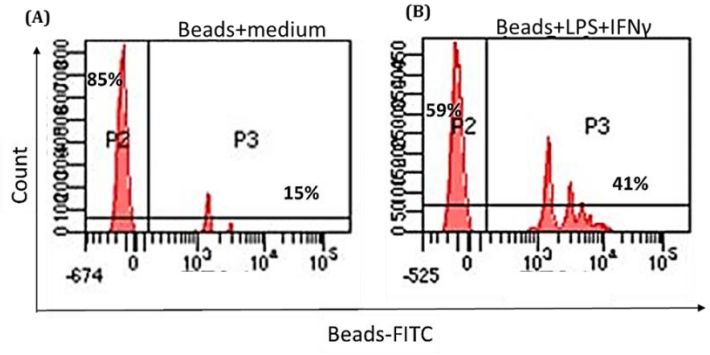

Figure. 8 Assessment of neutrophil phagocytosis using flow cytometry. Neutrophils were co-incubated with FITC-labelled-FluoSphere carboxylate-modified latex beads added in 1 to 10 ratio to neutrophils and stimulated with LPS (100ng/ml) and IFN_{γ} (200 U/ml) or left unstimulated in complete medium for 30 min at 37°C, 5%CO_2. Trypan blue was added to quench the fluorescence of extracellular bacteria/beads sticking on the neutrophil surface. Percentage of the cells which ingested beads and the cells which did not ingest beads were obtained by flow cytometry and analyzed by FACS Diva software. P2: non-phagocytosing neutrophils and P3: phagocytosing neutrophils. **(A)** Unstimulated neutrophils with beads, **(B)** stimulated neutrophils with beads.

2.2.11 Western blot analysis

Neutrophils (5x10^6 cells/1 ml NET medium) were unstimulated or stimulated with PMA or iICs for 15 min at 37˚C. In some cases, neutrophils were pre-incubated for 30 min with 3µM CP-673451 at 37˚C. For PDGFR- western blots, U87-MG cells (5x10^6/ml) were used. Whole cell lysates were prepared using TCA as described [118]. Briefly, after incubation, the cells were centrifuged 5 min at 400 x g. The pellets were then resuspended in 500 µl of ice cold 10 % TCA solution and incubated for 10 min on ice and subsequently centrifuged for 5 min at 14000 x g at 4°C. The pellets were washed two times with 500 µl 100 % acetone for 5 min at 14000 x g at 4 °C. The pellet was then re-suspended in 1x sample buffer and boiled for 7 min at 100°C in case of phospho-protein western blots and the pellet was heated at 98°C for 4 min for the PDGFRβ blots. Lysates were then centrifuged for 5 min at 14000 x g and supernatants were collected. Lysates were electrophoresed on 10 % SDS-PAGE gels and transferred to nitrocellulose membranes. Membranes were blocked for 30 min at room temperature with blocking buffer. Then membranes were incubated shaking overnight at 4 °C with primary antibodies against human phospho-Akt (Thr^{308}), phospho-p44/42 MAPK (ERK1/2,

Thr^{202}/Tyr^{204}), phospho p38 MAPK (Thr^{180}/Tyr^{182}), phospho-PKC alpha/beta II(Thr638/641), phospho-PKC-δ (Tyr^{311}), phospho-PI3K p85 (Tyr^{458})/p55 (Tyr^{199}), Phospho-Src Family(Tyr416), anti-PDGFR, Phospho-tyrosine pan, Phospho-threonine, Phospho-serine, beta-actin. The membranes were then treated with HRP-conjugated anti-rabbit or anti-mouse IgG for 2 h at room temperature. The chemiluminescence signals were obtained with the help of Immobilon Western Chemiluminescence HRP substrate and signals were measured at chemiluminescence reader. For quantification, the ratio of phospho-proteins signals to beta-actin signal was determined using Bio 1D software.

2.2.12 Phospho-enrichment of threonine phosphorylated proteins

Phospho enrichment of threonine phosphorylated proteins were achieved by Immunoprecipitation, a technique which permits the purification of specific proteins from the protein mixture was used to separate phospho-threonine proteins from the whole cell lysate. Anti-phospho-threonine Sepharose® Bead Conjugated antibody was used to enrich phospho-threonine proteins according to manufacturer's protocol.

Fresh human neutrophils were isolated from blood. 40x10^6 neutrophils/1 ml NET-medium were pre-incubated for 30 min with 3μM CP-673451, and control samples were treated with 0.1% dmso at 37˚C. The neutrophils were stimulated with PMA (20nM) for 20 min 37°C. The cells were then centrifuged at 300 x g for 5 min at RT and washed once with 1xPBS, followed by lysis with ice cold 1xRIPA buffer with a protease inhibitor for 10 min in ice. The lysed cells were then centrifuged at 14000 x g at 4°C. Anti-phospho threonine Sepharose bead conjugates were added at 1 mg/ml concentration to the lysates and incubated overnight at 4°C shaking. The lysates were then washed five times with lysis buffer and 20 μl 1x sample buffer was added to the pellet and heated for 4 min at 99°C. The lysates are then centrifuged and loaded into 10 % gel for SDS-PAGE with molecular weight markers. After the proteins have separated according to sizes in the gel, the gel was stained with 10 ml sterile Coomassie stain for 1 h and background stains were removed by washing with 100ml distilled water. Bands of the Control (Ctrl) lanes were compared to the CP-673451 treated (tr) lanes for finding missing bands. The missing lanes identified in phospho-threonine blots are compared with the same area in

the phospho-threonine lanes in the gel. The method was established to cut out the positive band control at the corresponding missing band from the coomassie stained gel and to send it for Mass spectrometry analysis and protein identification. Picture of the gel was taken with the help of a scanner.

2.2.13 Assessment of viability by Annexin V-PI staining

During apoptosis cells translocate phosphatidylserine (PS) to the external surface of the membrane. Annexin V has a high affinity for this externalized PS and exhibits calcium-dependent binding to PS. The measurement of Annexin V binding to the cell surface as indicative for apoptosis was performed in conjugation with a dye exclusion test using propidium iodide (PI). Apoptosis was determined by Annexin V-FITC and PI staining. $5x10^5$ cells/100 µl complete medium were added with inhibitors of different concentrations (10 µM, 3 µM, 1 µM, 0.3 µM, 0.1 µM) or with 0.1%dmso, or with medium and incubated for 1 h, 4 h, and 7 h and 22 h at 37˚C, 5 % CO_2 . After incubation, cells were stained by Annexin V-FITC (1 µl) and PI (1 µl) for 30 min in the dark at 4°C with 1 mM $CaCl_2$, washed and re-suspended in complete medium. The labeled neutrophil populations were then analyzed by FACS Canto II and FACS Diva software to differentiate as viable, apoptotic and necrotic populations. Intact/viable cells were both Annexin V and PI negative, apoptotic cells were Annexin V positive PI negative, and necrotic cells were Annexin V and PI positive **(Fig. 9)**.

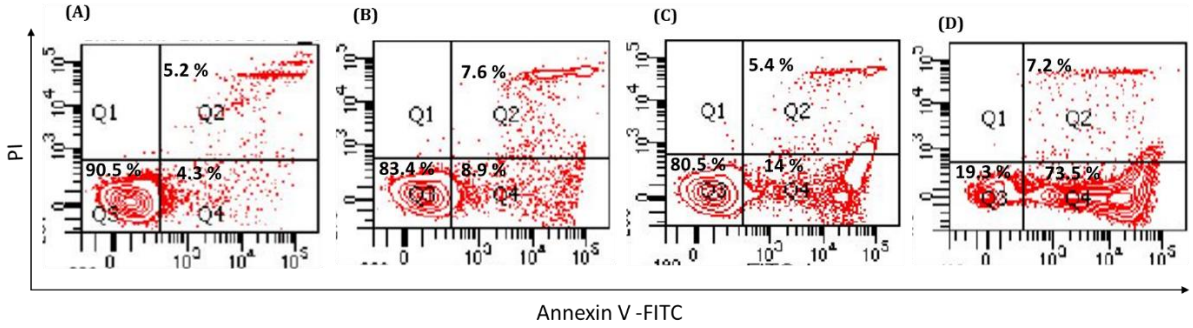

Figure. 9 Assessment of neutrophil viability at different time points using flow cytometry. Neutrophils were incubated for 1 h **(A)**, 4 h **(B)**, 7 h **(C)**, and 22 h **(D)** in complete medium at 37˚C with 5 % CO_2. The cells were then stained with Annexin V-FITC and PI and cell viability was assessed by flow cytometry and FACS Diva software. The percentage of cells in each quadrant was determined. Both Annexin V and PI double negative cells were defined as viable cells (Q3), Annexin V positive and PI negative cells were defined as apoptotic (Q4), and Annexin V and PI double positive cells were defined as necrotic (Q2).

2.2.14 LDH-Cytotoxicity assay

Cytotoxicity of cells was tested with LDH kit from Thermo Scientific™ Pierce™, to specifically check necrosis of the cells after treatment with inhibitors. Lactate dehydrogenase (LDH) is a cytosolic enzyme present in many different cell types. Plasma membrane damage releases LDH into the cell culture medium. Extracellular LDH in the culture supernatant can be quantified by a coupled enzymatic reaction in which LDH catalyzes the conversion of lactate to pyruvate via NAD+ reduction to NADH. Diaphorase then uses NADH to reduce a tetrazolium salt (INT) to a red formazan product that can be measured at 490nm. The level of formazan formation is directly proportional to the amount of LDH released into the medium, which is indicative of cytotoxicity **(Fig. 10).**

Neutrophils ($2x10^5$ cells/100 µl NET medium) were incubated for 1 h and 7 h at 37˚C with 0.1 µM-3 µM CP-673451 or with 0.1% dmso or NET-medium. The cells were centrifuged 300 x g and the supernatants were transferred to a new plate. Additionally, LDH_{max} (LDH maximum) samples, with completely lysed cells, and LDH_{spont} (LDH spontaneous) samples from untreated cells were also prepared from neutrophils. The supernatants of the differentially treated cells were mixed with Reaction Mixture (from the kit). After 30 min of incubation at RT the reaction was stopped by adding Stop Solution (from the kit). Absorbance at 490 nm and reference 680 nm is measured using a plate-reading spectrophotometer. LDH activity was determined from the OD values obtained. OD values obtained for inhibitor treated samples were compared with the 0.1% dmso controls.

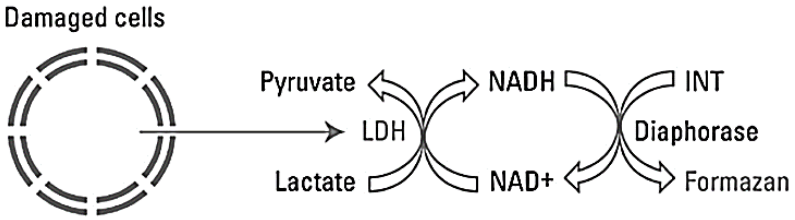

Figure 10. LDH detection principle. From www.thermofisher.com

2.2.15 RNA isolation from human neutrophils

To perform RNA-Sequencing and gene expression analysis RNA from neutrophils was isolated. $10x10^6$ cells in 1ml NET-medium were incubated with 3 µM CP-673451 or with 0.1% dmso or with medium for 30 min at 37˚C, followed by stimulation with PMA for 3 h 30 min at 37˚C. The cells were then washed with ice-cold 1x PBS and continued to isolate RNA by using Qiagen RNA Blood mini kit according to manufacturer's protocol. For DNase treatment, Qiagen RNase-Free DNase Set was used, according to manufacturer's protocol. The RNA was eluted in 35 µl of RNAase free water and frozen immediately for analysis with Nanodrop, Bioanalyzer and for RNA Sequencing procedures.

2.2.16 RNA quantification

RNA concentrations and purity were assessed with nanophotometer, the interpretation is by correlating absorbance with concentration. Nucleic acids absorb UV light at 260 nm due to nucleic acids and at 280 nm typically proteins and phenolic compounds have a strong absorbance. For pure RNA samples, A260/280 ratios should be around 2.1 and a lower ratio indicates protein contamination. In a pure sample, the A260/230 should be close to 2.0, higher values indicate the presence of organic contaminants, such as phenol, TRIzol etc. In addition, the concentration of the total RNA was determined by the nanophotometer [119]. The RNA measurements were performed according to the manufacturer's protocol.

The RNA integrity analysis with Bioanalyzer was performed by Ms. Miriam Freitag (LIED, University of Lübeck). The integrity of RNA is a major concern for gene expression studies and traditionally has been evaluated using the 28S to 18S rRNA ratio, as a method that has been shown to be inconsistent [120]. There are several subtypes of RNA; tRNA (transfer RNA), rRNA (ribosomal RNA), and mRNA (messenger RNA), all involved in the process of translation. The most prominent species is (~85%) rRNA and is the most immediately visible species when analyzed by electrophoresis and thus it's used for determining RNA quality [121, 122]. The Agilent 2100 Bioanalyzer helped to perform a quantification and quality control of RNA with the help of Agilent RNA 6000 Nano Kit according to the manufacturer's protocol. The provided RNA samples moved

through micro-channels and sample components were electrophoretically separated. The fluorescent dye molecules intercalated into RNA strands. They are then detected by their fluorescence and translated into images (showing bands) and electropherograms (peaks) for 28S rRNA and 18S [121]. The RNA Integrity Number (RIN) is automatically obtained. The samples with RIN number equal or above 3 are taken for RNA Seq.

2.2.17 RNA Seq

RNA Seq, an RNA profiling based on next-generation sequencing was used to study gene expression changes. RNA Sequencing was performed with the help of Illumina Sequencer and Illumina high through put kit by Dr. Sven Kuenzel (MPI, Plön, Germany) according to manufacturer's protocol. Briefly, the mRNA is fragmented and copied into cDNA. The cDNA is sequenced using high-throughput sequencing method. These reads were then computationally mapped to a reference genome to a transcriptional map, where the number of reads aligned to each gene gives a measure of its level of expression [123]. The RNA Seq data was used to examine the differentially expressed genes in different treatments.

2.2.18 RNA Seq data analyses

The RNA Seq data analyses were performed by Prof. Hauke Busch (LIED, University of Lübeck). A principal component analysis (PCA) was performed to evaluate the differences and relatedness of transcription profiles among different conditions. The PCA was calculated using the R/Bioconductor package labdsv and is based on the transcript per million (TPM) values of the 10000 most variable genes across samples according to their interquartile range (IQR).

2.2.19 Statistical analysis

If not stated differently, the presented data were generated from independent experiments with neutrophils isolated from different blood donors. Statistical analysis was performed with the GraphPad Prism software 6 using Student's t-test for using GraphPad Prism 6 software. A p-value ≤ 0.05 was considered statistically significant.

Chapter 3. Results

3.1 Identification of inhibitors which do not inhibit ROS release but inhibit NETosis

Ever since the process of Neutrophil Extracellular Trap (NET) formation was first described in 2014 [29], there is a growing interest to understand the signaling mechanisms involved in NET formation. NETosis induced by PMA and iIC is dependent on ROS production. Although several upstream signaling pathways of ROS production induced by PMA and iIC have been recently identified, the downstream mechanisms of ROS production which leads to NETosis are poorly understood [55, 78, 80, 81]. To specifically understand the downstream pathways of ROS production leading to NETosis, this study used a screening approach with an inhibitor library containing 141 different molecular target inhibitors **(List of the inhibitors - supplementary data-1)**.

In my experiment, human neutrophils were treated with inhibitors and induced ROS production and NETosis with PMA. NET and ROS release was measured by SytoxGreen and luminol, respectively, as described previously [55, 93]. Neutrophils pre-treated with DPI (20nM) and stimulated with PMA served as positive control for inhibition both ROS production and NETosis inhibition. The study revealed two inhibitors of PMA-induced NETosis, which do not inhibit the upstream ROS generation **(Fig. 11, 12)**. The two inhibitors were D14 and D83 among the D1-D141 inhibitors. The inhibitor D14 is called CP-673451 (an inhibitor of PDGFR) and D83 is called Doxorubicin (an inhibitor of Topoisomerase II).

Similarly, neutrophils were treated with inhibitors and induced ROS production and NETosis with iIC. NET and ROS release was measured by SytoxGreen and luminol, respectively, as described previously [55]. Neutrophils pre-treated with DPI (20nM) and stimulated with PMA served as positive control for inhibition both ROS production and NETosis inhibition. The study revealed two inhibitors of iIC-induced NETosis, which do not inhibit the upstream ROS generation **(Fig. 13, 14)**. The inhibitors were D14 or CP-673451 (an inhibitor of PDGFR) and D83 or Doxorubicin (an inhibitor of Topoisomerase II). Interestingly, the same two inhibitor candidates could inhibit both PMA- and iIC- induced NETosis **(Fig. 11, 13)**.

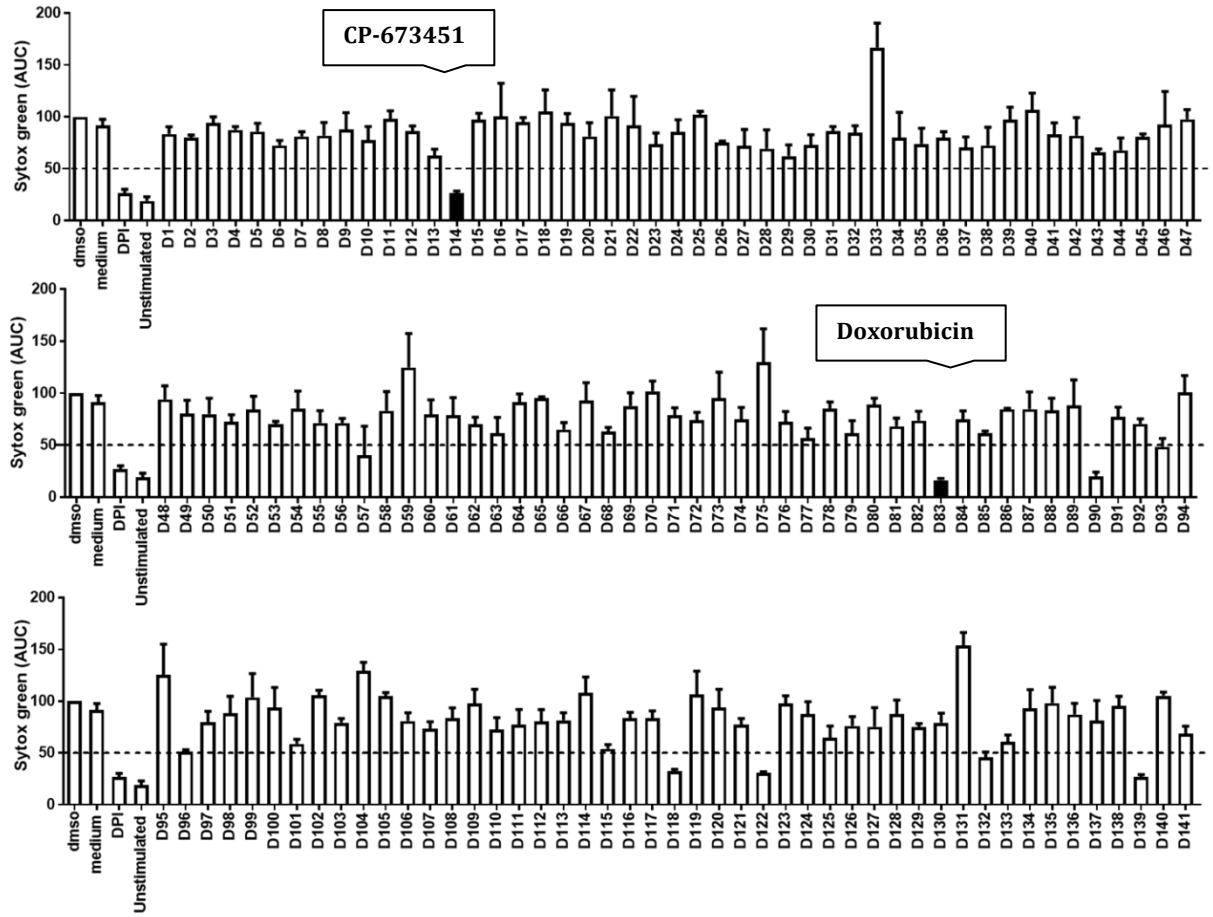

Figure 11. Screening for inhibitors of PMA-induced NETosis. Primary human neutrophils were treated with 141 inhibitors (at a concentration of 10μM) or controls (dmso and medium) and stimulated with PMA (20nM). PMA induced ROS-dependent NET formation was assessed by measuring extracellular DNA with the SytoxGreen assay. Real-time generation of NETs was monitored for 4 h at 37˚C from neutrophils. The normalized area under the curve (AUC) values of real-time kinetics are shown, where dmso treated-PMA stimulated neutrophils were normalized to 100 %. (mean ± SEM). Inhibition is defined as AUC values below 50 % threshold (shown with the dotted lines) of the dmso treated-PMA stimulated neutrophils. *n=3* independent experiments.

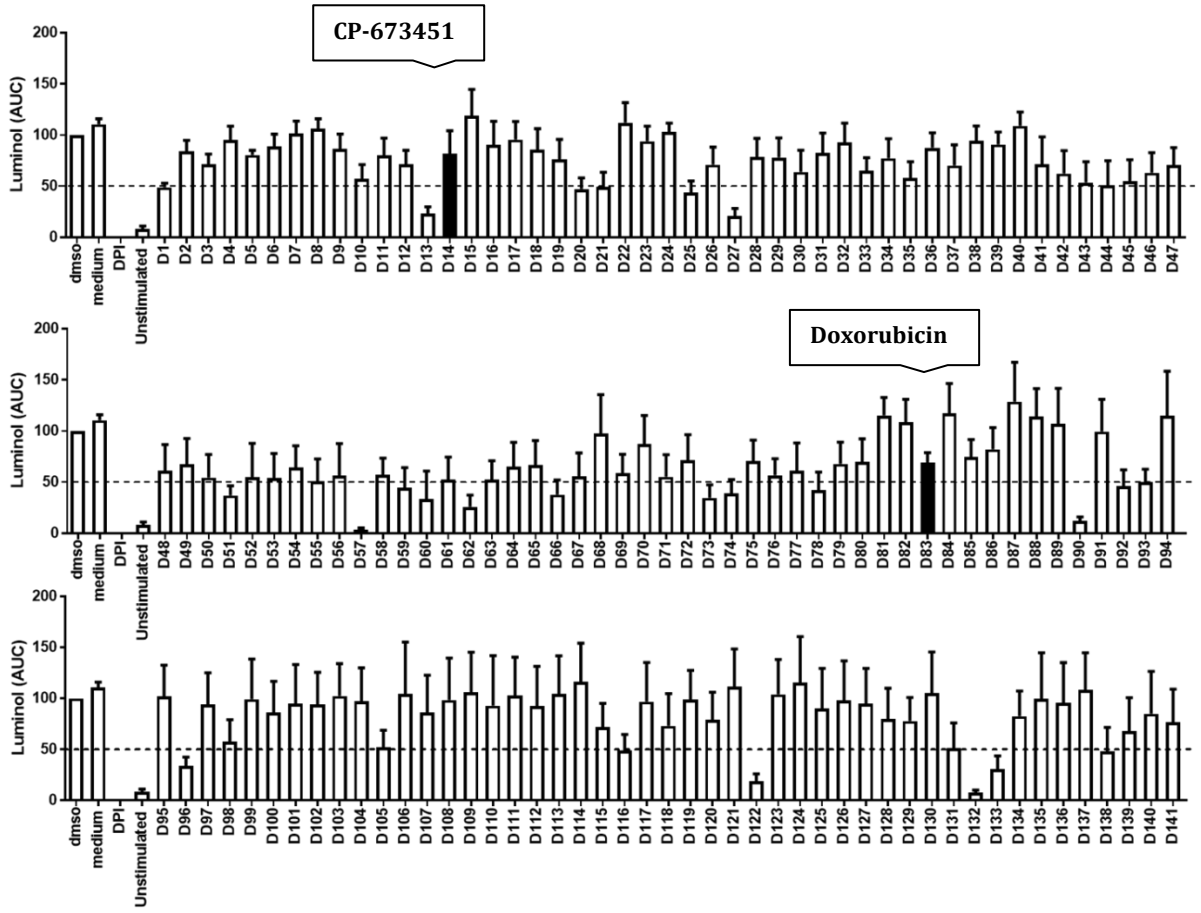

Figure 12. Screening for inhibitors of PMA-induced ROS production. Primary human neutrophils were treated with 141 inhibitors (at a concentration of 10μM) or controls (dmso and medium) and stimulated with PMA (20nM). PMA induced intra-/extracellular ROS production was measured by luminol-amplified chemiluminescence assay. Real-time generation of NETs was monitored for 1 h at 37˚C from neutrophils. The normalized area under the curve (AUC) values of real-time kinetics are shown, where dmso treated-PMA stimulated neutrophils were normalized to 100 %. (mean ± SEM). Inhibition is defined as AUC values below 50 % threshold (shown with the dotted lines) of the dmso treated-PMA stimulated neutrophils. *n=3* independent experiments.

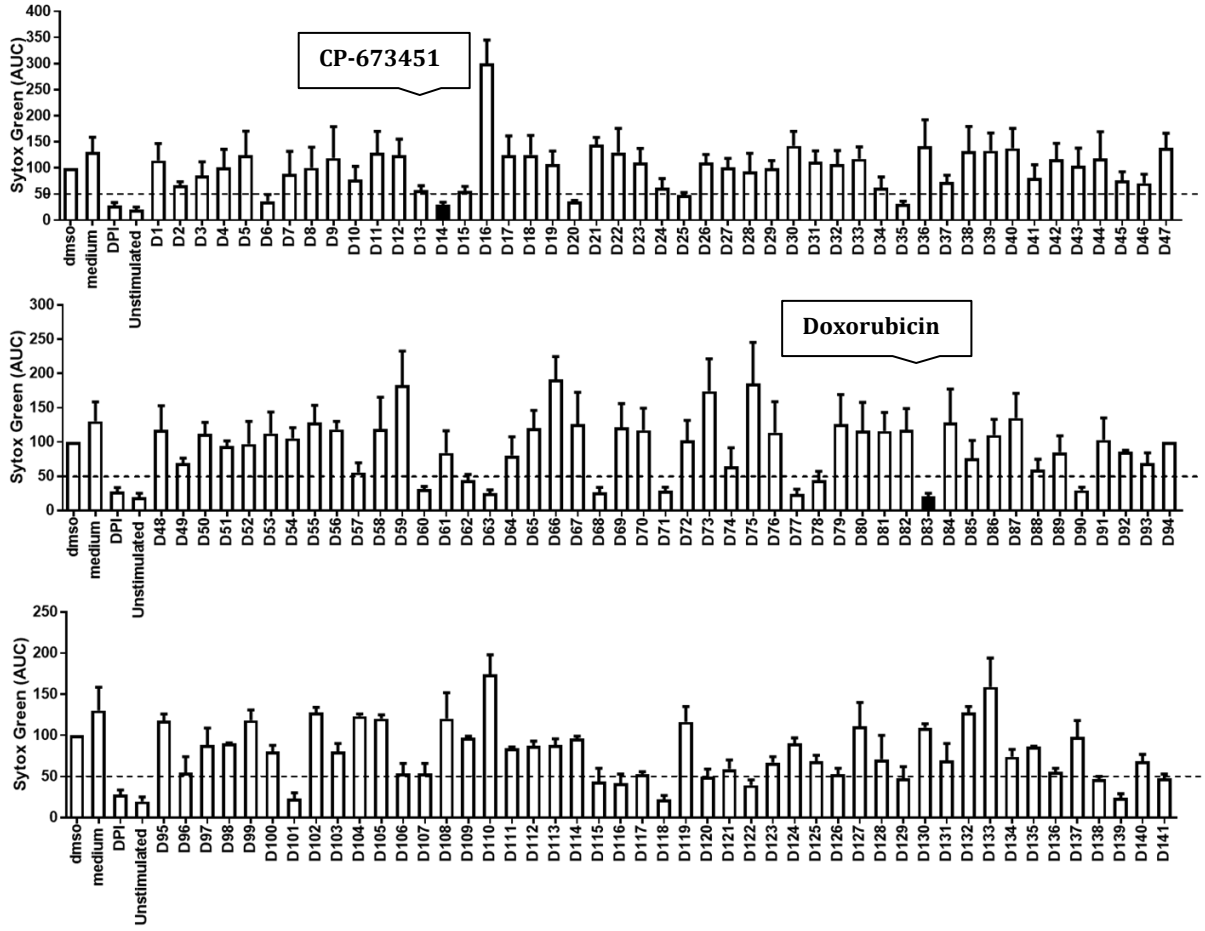

Figure 13. Screening for inhibitors of iIC-induced NETosis. Primary human neutrophils were treated with 141 inhibitors (at a concentration of 10μM) or controls (dmso and medium) and stimulated with immobilized immune complexes (iIC). iIC induced ROS-dependent NET formation was assessed by measuring extracellular DNA with the SytoxGreen assay. Real-time generation of NETs was monitored for 4 h at 37˚C from neutrophils. The normalized area under the curve (AUC) values of real-time kinetics are shown, where dmso treated- iIC stimulated neutrophils were normalized to 100 %. (mean ± SEM). Inhibition is defined as AUC values below 50 % threshold (shown with the dotted lines) of the dmso treated- iIC stimulated neutrophils. *n=3* independent experiments.

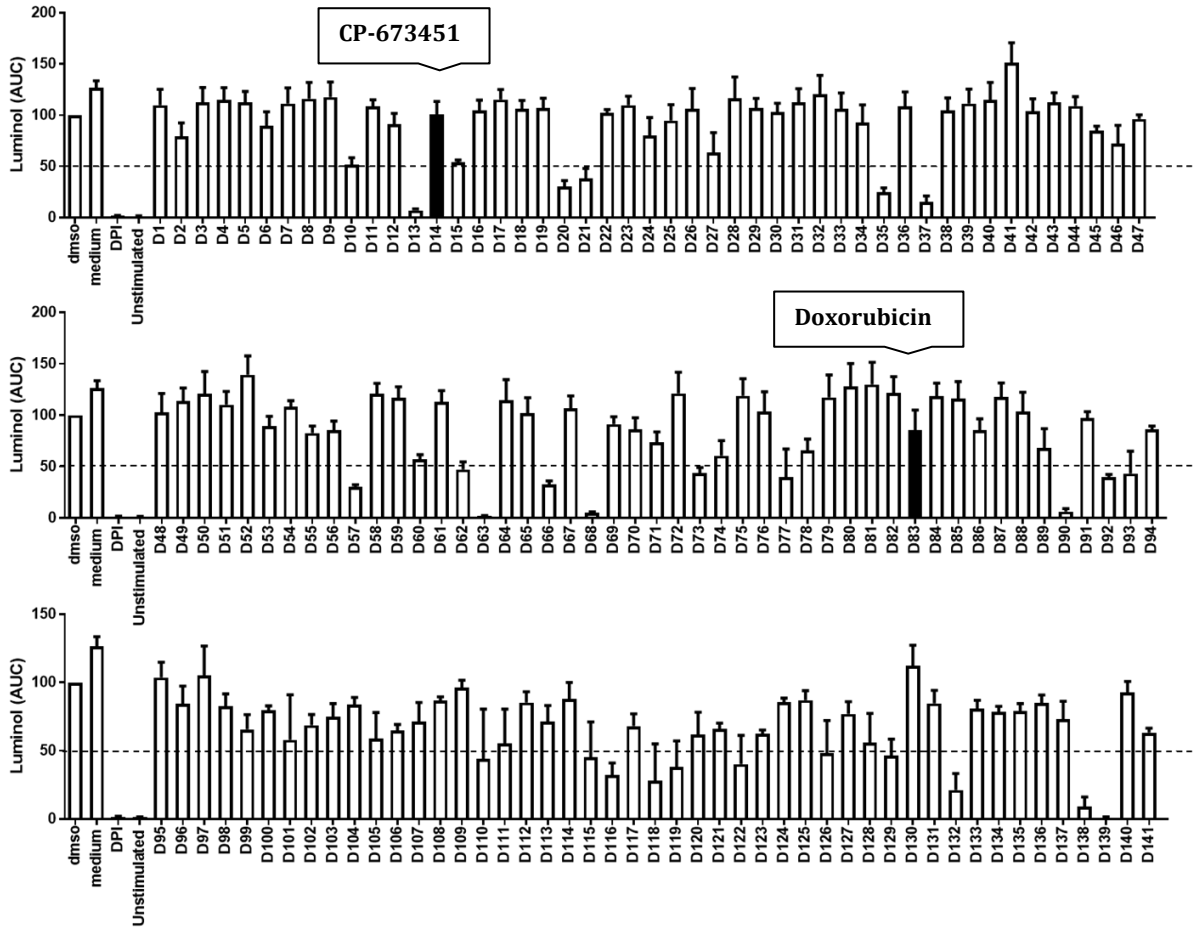

Figure 14. Screening for inhibitors of iIC-induced ROS production. Primary human neutrophils were treated with 141 inhibitors (at a concentration of 10μM) or controls (dmso and medium) and stimulated with immobilized immune complexes (iIC). iIC induced intra-/extracellular ROS production was measured by luminol-amplified chemiluminescence assay. Real-time generation of NETs was monitored for 1 h at 37˚C from neutrophils. The normalized area under the curve (AUC) values of real-time kinetics are shown, where dmso treated-iIC stimulated neutrophils were normalized to 100 %. (mean ± SEM). Inhibition is defined as AUC values below 50 % threshold (shown with the dotted lines) of the dmso treated-iIC stimulated neutrophils. *n=3* independent experiments.

3.2 Dose dependent inhibition of PMA- and iIC-induced NET formation by CP-673451

The screening **(Fig. 11-14)** identified D14 (CP-673451) as a substance which inhibits both PMA- and iIC-induced NETosis but not PMA- and iIC-induced ROS production. Next, I investigated the effect of CP-673451 at various concentrations to exclude potential off-target effects due to high concentrations and to determine the lowest potential dose needed for NETosis inhibition. PMA and iIC induced ROS production and NET formation were measured after exposure of neutrophils to different concentrations of CP-673451. Different concentrations of CP-673451 ranging from 0.1 μM to 3 μM were tested.

Results from the SytoxGreen and luminol kinetic assay re-confirmed the preliminary screening results that CP-673451 inhibits PMA-induced NETosis without affecting the PMA-induced ROS production **(Fig. 15)**. I found that CP-673451 could inhibit PMA-induced NETosis in a dose dependent manner. CP-673451 inhibited PMA-induced NET formation at a concentration of as low as 0.3 μM **(Fig. 15 (B, D))**. However, an inhibitory effect on ROS production was observed at a concentration of 3 μM but not in lower concentrations **(Fig. 15 (A, C)).**

In order to confirm the inhibition of NETosis with CP-673451, a morphological analysis by fluorescent microscopy (FM) was performed. SytoxGreen staining was used to view the NET-DNA and the control nuclear DNA with fluorescent microcopy as described previously [117]. Neutrophils pre-treated with DPI (a common inhibitor of ROS-dependent NETosis inhibitor) [55] was also included in the staining analyses.

FM analysis confirmed the NET formation with PMA **(Fig. 15-E)**. PMA induced a cloud like NET structure or sometimes a NETotic cell with decondensed DNA stained with SytoxGreen was observed **(Fig. 15-E)**. No visible effect of dmso was observed in PMA-induced NETosis **(Fig. 15-E)**. Moreover, DPI treated neutrophils failed to release NETs **(Fig. 15-E)**. FM analyses of CP-673451 treated neutrophils confirmed the results from the kinetic assay and showed a visible dose-dependent inhibition of PMA-induced NETosis with 1 μM-3 μM concentrations **(Fig. 15-E)**.

Similarly, the SytoxGreen and luminol kinetic assay also re-confirmed the preliminary screening results that CP-673451 inhibits iIC-induced NETosis without affecting the iIC-induced ROS production. CP-673451 could inhibit iIC-induced NETosis in a dose dependent manner. CP-673451 inhibited iIC-induced NET formation at a lower potential concentration of 3 μM **(Fig. 16 (B, D))**. CP-673451 showed no inhibitory effect on iIC-induced ROS production **(Fig. 16 (A, C)).**

FM analysis confirmed the NET formation induced by iIC **(Fig. 16-E)**. iIC induced NETs were more NET fiber like structures, stained with SytoxGreen **(Fig. 16-E)**. No visible effect of dmso was observed in iIC-induced NETosis **(Fig. 16-E)**. Moreover, DPI treated neutrophils failed to release iIC-induced NET formation **(Fig. 16-E)**. FM analyses of CP-673451 treated neutrophils confirmed the results from the kinetic assay and showed a visible dose-dependent inhibition of iIC-induced NETosis in the range of 0.3 μM-3 μM concentrations **(Fig. 16-E)**.

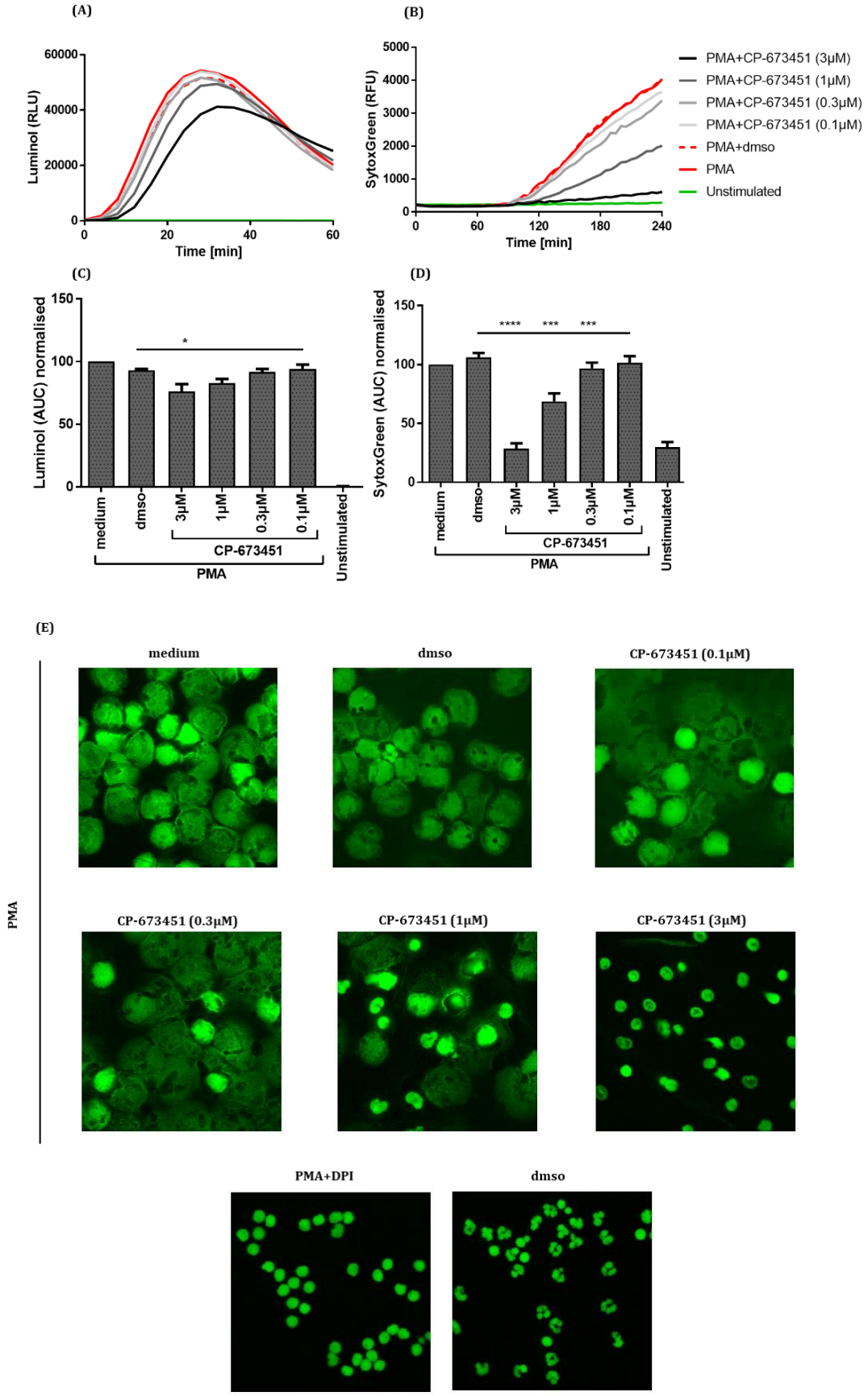

Figure 15. Dose dependent inhibition of PMA-induced NETosis by CP-673451 without inhibiting ROS production. Primary human neutrophils were treated with 0.1µM-

3μM of CP-673451 or controls (dmso and medium) and stimulated with PMA (20nM) or left unstimulated. PMA induced intra-/extracellular ROS production was measured by luminol-amplified chemiluminescence assay. Real-time generation of ROS was monitored for 1 h at 37˚C from neutrophils**.** PMA induced ROS-dependent NET formation was assessed by measuring extracellular DNA with the SytoxGreen assay. Real-time release of NETs was monitored for 4 h at 37˚C from neutrophils. Representative real-time kinetics of PMA-induced ROS production **(A)** and NET release **(B)** are shown. The normalized areas under the curve (AUC) values of real-time kinetics of ROS production (C) and NET release (D) are shown. (mean ± SEM). *n = 6* independent experiments. **p < 0.05, ***p < 0.001* as compared to dmso treated PMA controls. **(E)** Neutrophils were treated with 3μM-0.1 μM of CP-673451 or 0.1% dmso or medium for 30 min at 37˚C, then stimulated with PMA or left unstimulated. Cells were fixed after 4 h incubation. DNA was stained with SytoxGreen. Images were taken with Keyence BZ-9000E using a 340 Plan Fluor EL NA 0.60 Ph2 objective at 100x and BZ II analyzer software. *n = 2* independent experiments

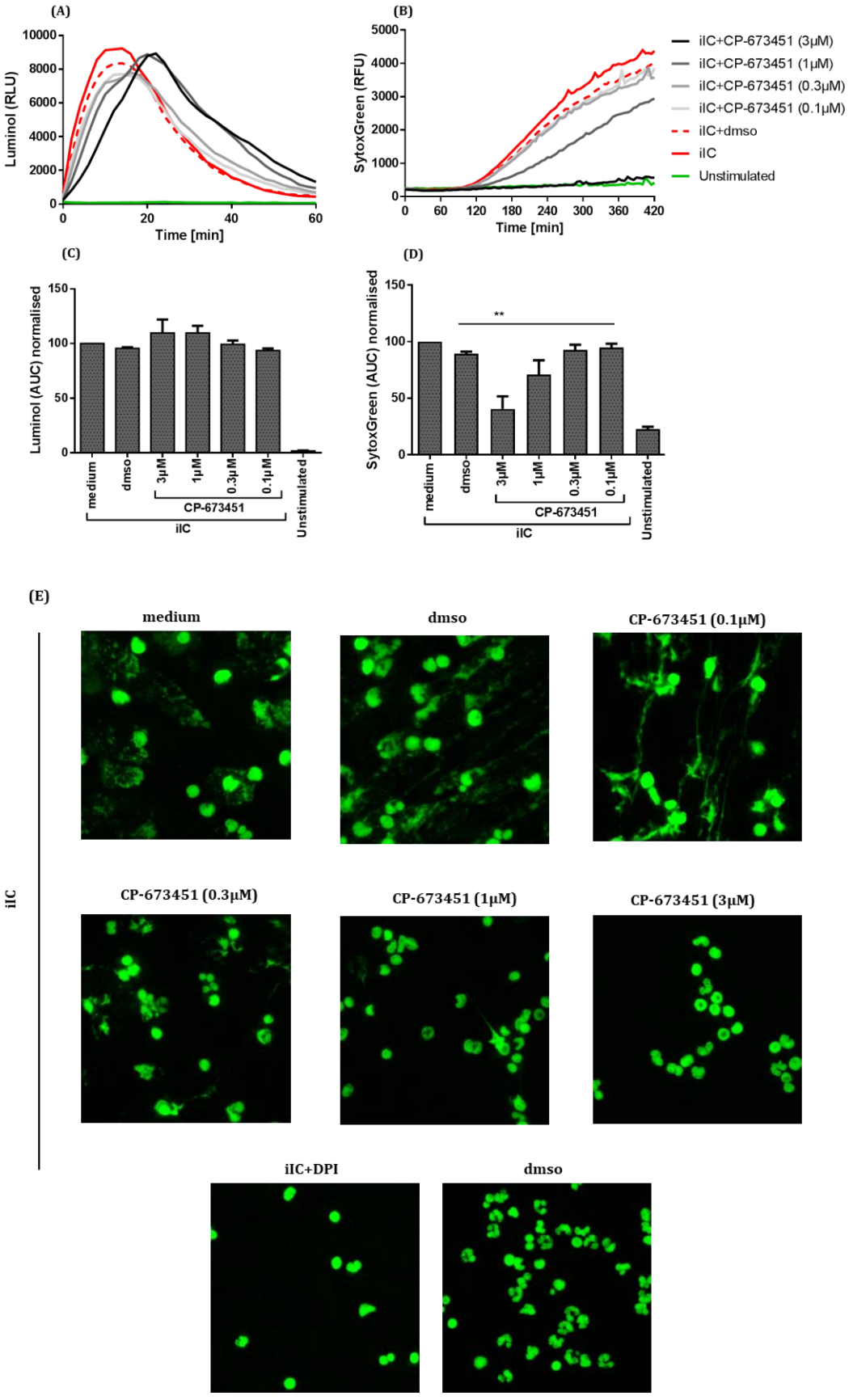

Figure 16. Dose dependent inhibition of iIC-induced NETs by CP-673451 without inhibiting ROS production. Primary human neutrophils were treated with 0.1µM-3µM of CP-

673451 or controls (dmso and medium) and stimulated with iIC or left unstimulated. iIC induced intra-/extracellular ROS production was measured by luminol-amplified chemiluminescence assay. Real-time generation of ROS was monitored for 1 h at 37˚C from neutrophils**.** iIC-induced ROS-dependent NET formation was assessed by measuring extracellular DNA with the SytoxGreen assay. Real-time release of NETs was monitored for 7 h at 37˚C from neutrophils. Representative real-time kinetics of iIC-induced ROS production **(A)** and NET release **(B)** are shown. The normalized area under the curve (AUC) values of real-time kinetics of ROS production (C) and NET release (D) are shown. (mean ± SEM). *n = 6* independent experiments. ***p < 0.01* as compared to dmso treated iIC controls. **(E)** Neutrophils were treated with 3μM-0.1 μM of CP-673451 or 0.1% dmso or medium for 30 min at 37˚C, then stimulated with iIC or left unstimulated. Cells were fixed after 7 h incubation. DNA was stained with SytoxGreen. Images were taken with Keyence BZ-9000E using a 340 Plan Fluor EL NA 0.60 Ph2 objective at 100x and BZ II analyzer software. *n = 2* independent experiments

3.3 Effect of Doxorubicin in PMA- and iIC-induced NETosis

The screening **(Fig. 11-14)** also identified D83 (Doxorubicin) as a substance which inhibits both PMA- and iIC-induced NETosis but not PMA- and iIC-induced ROS production. Therefore, I investigated the effect of Doxorubicin at various concentrations to exclude potential off-target effects due to high concentrations and to determine the lowest potential dose needed for NETosis inhibition. PMA and iIC induced ROS production and NET formation were measured after exposure of neutrophils to different concentrations of Doxorubicin (DOX). Different concentrations of Doxorubicin ranging from 0.1 μM to 3 μM were tested.

Results from the SytoxGreen and luminol kinetic assay re-confirmed the preliminary screening results that Doxorubicin inhibits PMA-induced NETosis. I found that Doxorubicin could inhibit PMA-induced NETosis in a dose dependent manner. Doxorubicin inhibited PMA-induced NET formation at a lower potential concentration of 0.1 μM **(Fig. 17 (B, D))**. However, an inhibitory effect on ROS production was observed at a concentration of 3 μM but not in lower concentrations **(Fig. 17 (A, C)).**

To confirm the inhibition of NETosis with Doxorubicin (DOX), a morphological analysis by fluorescent microscopy (FM) was performed with SytoxGreen. Neutrophils pre-treated with DPI (a common inhibitor of ROS-dependent NETosis inhibitor) were used as positive control for NETosis inhibition. PMA induced NET formation and no visible effect of dmso was observed in PMA-induced NETosis. Moreover, DPI treated neutrophils failed to release NETs. However, unexpectedly FM analyses of Doxorubicin

(DOX) treated neutrophils did not inhibited NET formation as observed in the kinetic assay **(Fig. 17-E)**.

Similarly, the SytoxGreen and luminol kinetic assay was performed to confirm the preliminary screening results that Doxorubicin (DOX) inhibits iIC-induced NETosis without affecting the iIC-induced ROS production **(Fig. 18 A-D)**. Doxorubicin could inhibit iIC-induced NETosis in a dose dependent manner in the kinetic assay **(Fig. 18 (B, D))**. Doxorubicin inhibited iIC-induced NET formation at a lower potential concentration of 0.1 µM in the kinetic assay **(Fig. 18 (B, D))**. Doxorubicin (DOX) showed inhibitory effect on iIC-induced ROS production at a concentration of 3 µM but not at lower concentrations **(Fig. 18 (A, C)).**

FM analysis showed NET formation induced by iIC with SytoxGreen staining **(Fig. 18-E)**. No visible effect of dmso was observed in iIC-induced NETosis **(Fig. 18-E)**. Moreover, DPI treated neutrophils failed to release iIC-induced NET formation **(Fig. 18-E)**. However, FM analyses failed to confirm the NETosis inhibition observed in the kinetic assay **(Fig. 18-E)**. As the FM analyses showed no inhibition of PMA- or iIC-induced NETosis in morphological analysis, Doxorubicin (DOX) was eliminated from further studies **(Fig. 17-E, 18-E)**.

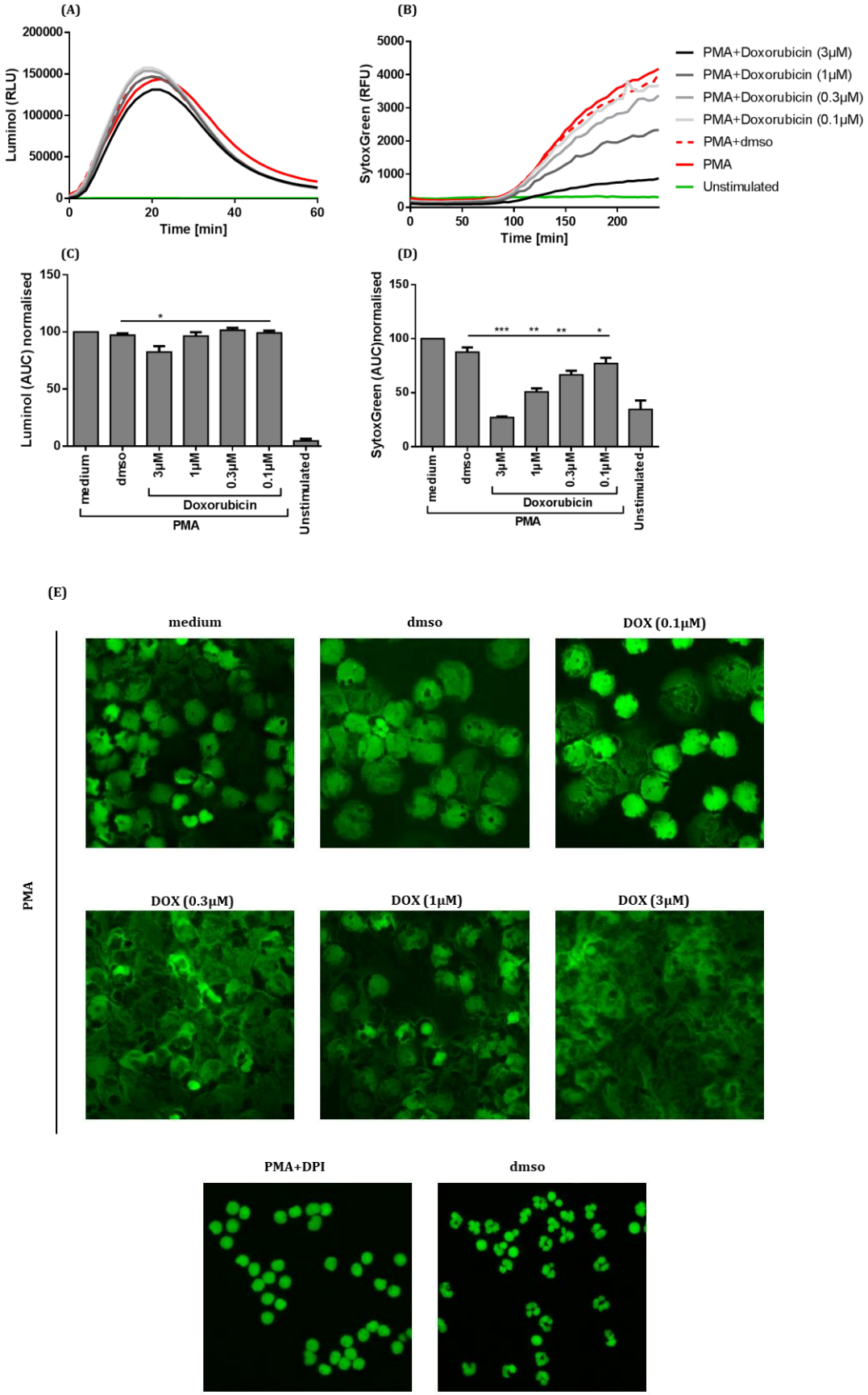

Figure 17. Effect of Doxorubicin in PMA-induced ROS production and NET formation. Primary human neutrophils were treated with 0.1µM-3µM of Doxorubicin (DOX) or controls

(dmso and medium) and stimulated with PMA (20nM) or left unstimulated. PMA induced intra-/extracellular ROS production was measured by luminol-amplified chemiluminescence assay. Real-time generation of ROS was monitored for 1 h at 37˚C from neutrophils**.** PMA induced ROS-dependent NET formation was assessed by measuring extracellular DNA with the SytoxGreen assay. Real-time release of NET was monitored for 4 h at 37˚C from neutrophils. Representative real-time kinetics of PMA-induced ROS production **(A)** and NET release **(B)** are shown. The normalized areas under the curve (AUC) values of real-time kinetics of ROS production **(C)** and NET release **(D)** are shown. (mean ± SEM). *n = 6* independent experiments**p < 0.05, **p < 0.01, ***p < 0.001* as compared to dmso treated PMA controls. **(E)** Neutrophils were treated with 3µM-0.1 µM of Doxorubicin (DOX) or 0.1% dmso or medium for 30 min at 37˚C, then stimulated with PMA or left unstimulated. Cells were fixed after 4 h incubation. DNA was stained with SytoxGreen. Images were taken with Keyence BZ-9000E using a 340 Plan Fluor EL NA 0.60 Ph2 objective at 100x and BZ II analyzer software. *n = 2* independent experiments.

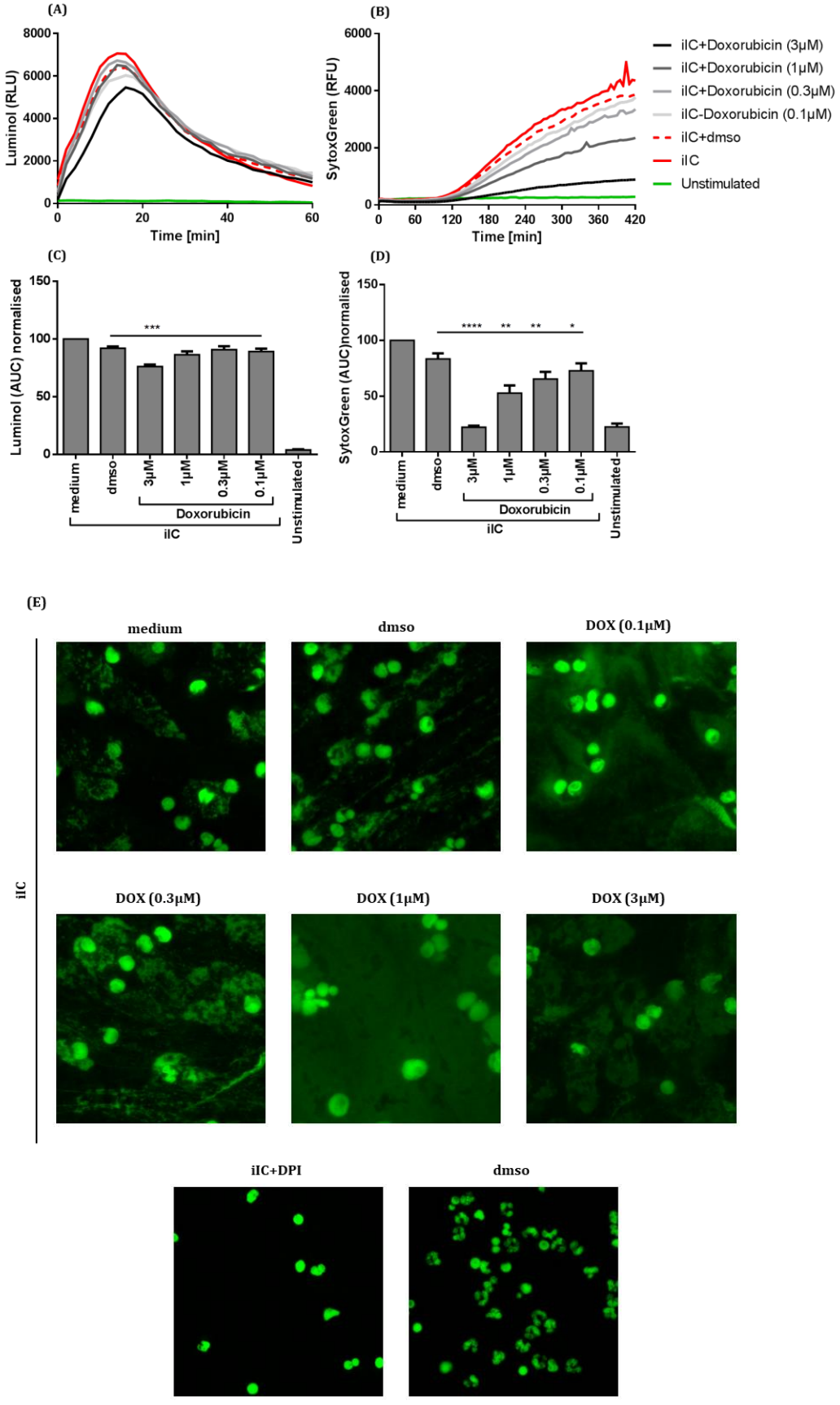

Figure 18. Effect of Doxorubicin in iIC-induced ROS production and NET formation. Primary human neutrophils were treated with 0.1µM-3µM of Doxorubicin (DOX) or controls

(dmso and media) and stimulated with iIC or left unstimulated. iIC-induced intra-/extracellular ROS production was measured by luminol-amplified chemiluminescence assay. Real-time generation of ROS was monitored for 1 h at 37˚C from neutrophils**.** iIC-induced ROS-dependent NET formation was assessed by measuring extracellular DNA with the SytoxGreen assay. Real-time release of NET was monitored for 7 h at 37˚C from neutrophils. Representative real-time kinetics of iIC-induced ROS production **(A)** and NET release **(B)** are shown. The normalized areas under the curve (AUC) values of real-time kinetics of iIC-induced ROS production **(C)** and NET release (D) are shown. (mean ± SEM). *n = 6* independent experiments. **p < 0.05, **p < 0.01, ***p < 0.001* as compared to dmso treated iIC controls. **(E)** Neutrophils were treated with 3µM-0.1 µM of Doxorubicin (DOX) or 0.1% dmso or medium for 30 min at 37˚C, then stimulated with iIC or left unstimulated. Cells were fixed after 7 h incubation. DNA was stained with SytoxGreen. Images were taken with Keyence BZ-9000E using a 340 Plan Fluor EL NA 0.60 Ph2 objective at 100x and BZ II analyzer software. *n = 2* independent experiments.

3.4 Screening for potential targets of CP-673451 involved in NETosis inhibition

The small molecule inhibitor CP-673451 has been shown to be target selective and has a >450-fold selectivity to PDGFRα/β over other angiogenic receptors such as VEGFR1/2/3 [106]. However, most of the CP-673451's inhibitory studies were performed in tumor cells at a dosage of 1 nM-100 nM. As the inhibition of NETosis needed a higher dosage than the previous studies, the potential off-target effects could not be excluded. Furthermore, since CP-673451 is known to target for a certain extent on VEGFR1/2/3, it was necessary to check whether VEGFR1/2/3 can be the target in NETosis inhibition. The report that neutrophils eventual do not express PDGFR [99] made a potential off target effect even more likely. Therefore, my first approach to identify the target was to address potential off-target effects.

To investigate if inhibition of VEGFR1/2/3 is involved in CP-673451-mediated NETosis inhibition, specific inhibitors of VEGFR 1/2/3 were tested in PMA/iIC induced NETosis in SytoxGreen-kinetic assay system. Neutrophils were treated with VEGFR1/2/3 inhibitors: AMG-706 (inhibitor of VEGFR 1/2/3) and ZD6474 (inhibitor of VEGFR 2/3) and, subsequently NET formation was induced with PMA/iIC. CP-673451 treated neutrophils served as positive control for NETosis inhibition **(Fig. 19)**. Inhibitors of VEGFR1/2/3 AMG-706 and ZD6474 did not inhibit PMA and iIC induced NETosis **(Fig. 19)**. CP-673451 as shown previously **(Fig. 11, 12)** inhibited NET formation **(Fig.19)**.

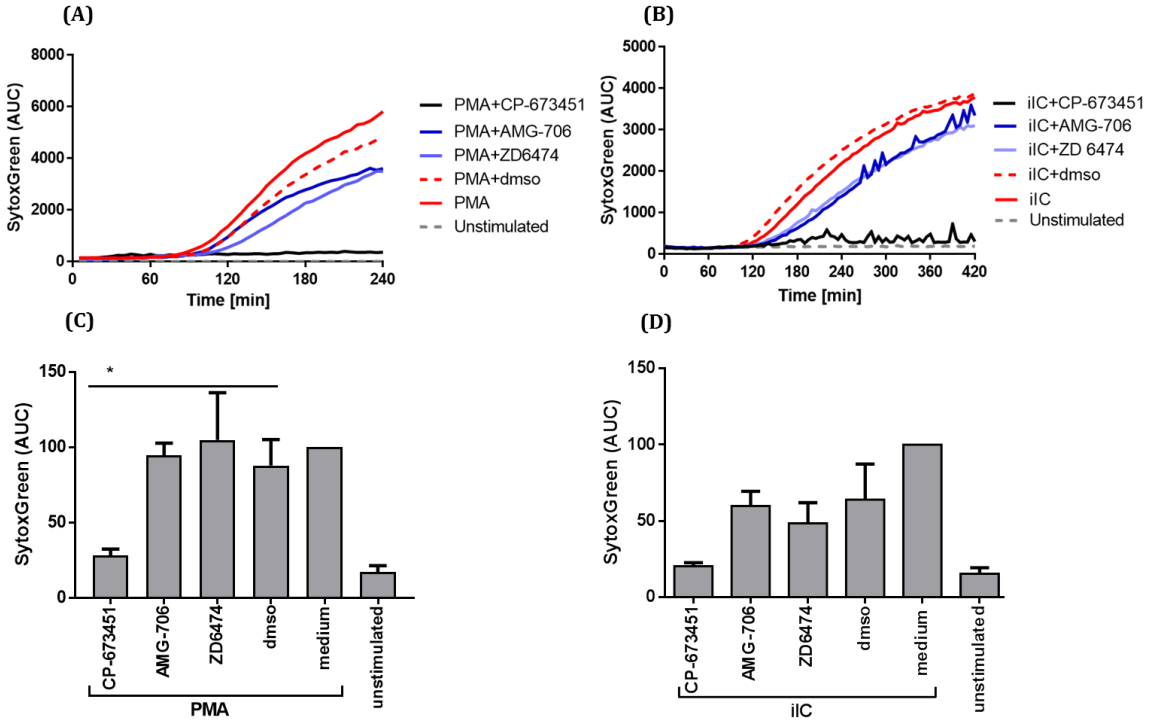

Figure 19. Inhibitors of VEGFR1/2/3 do not inhibit PMA/iIC-induced NETosis. Neutrophils were treated with 10µM of CP-673451, AMG-706, ZD6474 or dmso or medium and stimulated with PMA or added to iIC coated surfaces or left unstimulated. The release of neutrophil extracellular traps (NETs) was monitored at 37°C, for 4 h for PMA and 7 h for iIC stimulation. Representative real-time kinetics NET release for PMA **(A)** and iIC **(B)** was measured by SytoxGreen. Normalized area under the curve (AUC) values for PMA-induced NET formation **(C)** and iIC-induced NET formation **(D)** are plotted. (mean ± SEM). *n = 3, *p < 0.05* as compared to dmso treated PMA/iIC controls.

3.5 Effects of Sunitinib on PMA- and iIC-induced ROS and NETosis

The second approach to clarify the target selectivity of CP-673451 on the NETosis inhibition was by using another selective inhibitor of PDGFR called Sunitinib in the PMA- and iIC- induced ROS and NETosis assays. Neutrophils were treated with Sunitinib and stimulated with PMA and iIC for ROS production and NETosis. Unlike CP-673451, Sunitinib inhibited PMA and iIC induced ROS production **(Fig. 20 (A, C), 21 (A, C))**. In line with the strong inhibitory effect of Sunitinib on iIC-induced ROS production, the iIC-induced NET release was also markedly inhibited **(Fig. 21)**. However, only a tendency of inhibition of PMA induced NETosis was observed **(Fig. 20 (B, D)**. These results show that Sunitinib does not inhibit NETosis without affecting upstream ROS production and its inhibitory effect is not NETosis specific. Therefore, studying Sunitinib cannot clarify the effect of CP-673451 on NETosis.

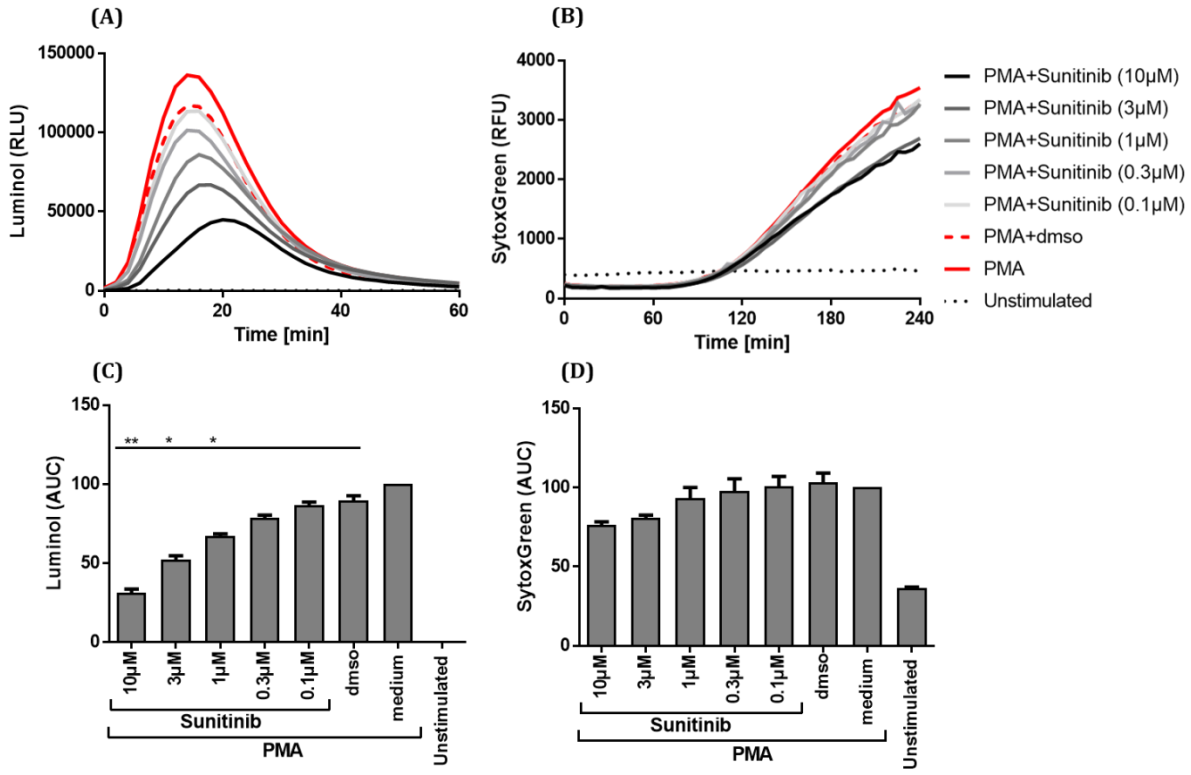

Figure 20. Sunitinib partially inhibits PMA induced ROS production but not PMA-induced NETosis. Neutrophils (1x10^6/ml in NET medium) were treated with 0.1μM-10μM of Sunitinib or dmso or medium and stimulated with PMA or left unstimulated. Production of intra- and extracellular ROS was monitored for 1 h and release of neutrophil extracellular traps (NETs) induced by PMA was monitored for 4 h at 37°C. Representative real-time kinetics of ROS production was measured by luminol **(A).** Representative real-time kinetics NET release was measured by SytoxGreen **(B)**. Normalized areas under the curve (AUC) values of ROS production **(C)** and NET release **(D)** were plotted. (mean ± SEM). *n = 3, *p < 0.05, **p < 0.01* as compared to dmso treated PMA controls.

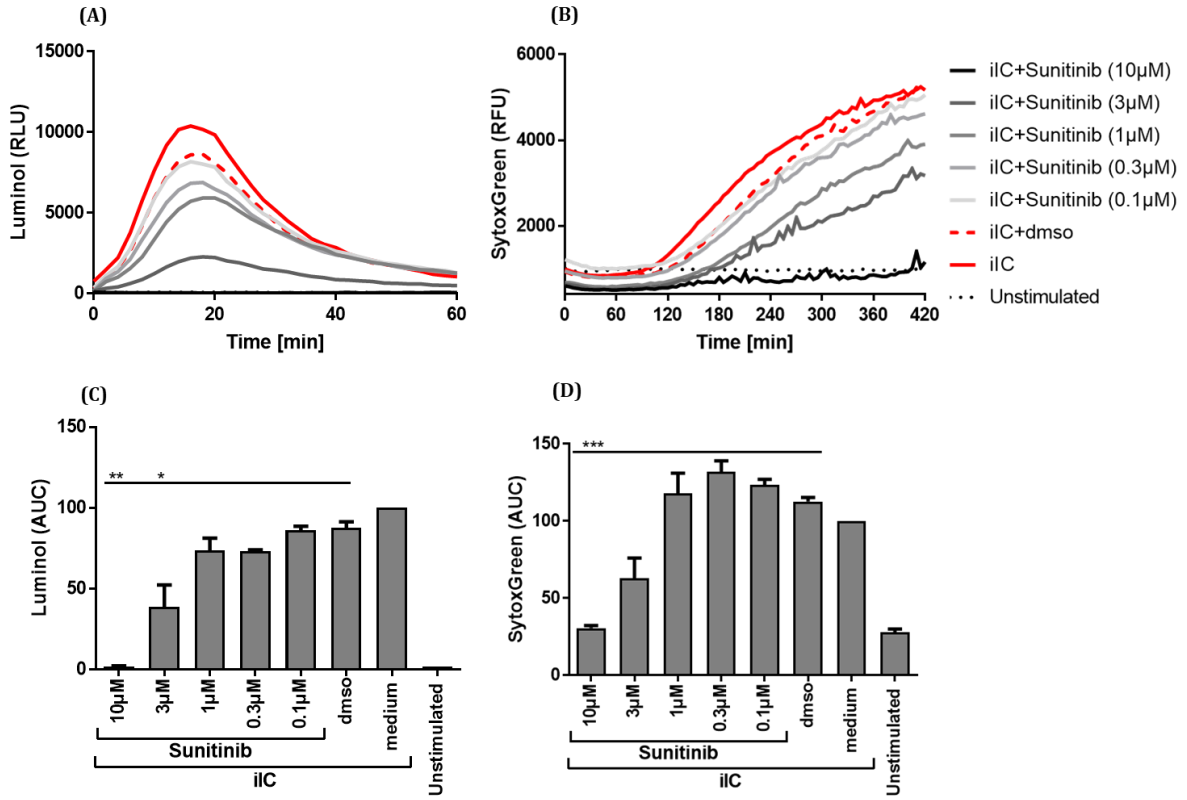

Figure 21. Sunitinib inhibits iIC-induced ROS production and NETosis in a dose dependent manner. Neutrophils (1x10^6/ml in NET medium) were treated with 0.1µM-10µM of Sunitinib or dmso or medium and incubated on iIC-coated surfaces or left unstimulated. Production of intra- and extracellular ROS was monitored for 1 h and release of neutrophil extracellular traps (NETs) induced by iIC was monitored for 7 h at 37°C. Representative real-time kinetics of ROS production was measured by luminol **(A)** and NET release was measured by SytoxGreen **(B)**. Normalized area under the curve (AUC) values of ROS production **(C)** and NET release **(D)** are plotted (mean ± SEM). *n = 3, *p < 0.05, **p < 0.01, ***p < 0.001* as compared to dmso treated iIC controls.

3.6 Neutrophils do not express PDGF-Receptor

Platelet-derived growth factor (PDGF) was shown to be chemotactic for neutrophils [98]. However, later studies showed that neutrophils lack detectable mRNA for and showed that human neutrophils do not possess functional PDGF receptor [99]. Therefore, the third approach to verify the target selectivity of CP-673451 was to directly check the protein expression of PDGFR in human neutrophils. Western blot analysis was performed with neutrophil lysates to check protein expression of PDGFR. The U-87MG, human glioblastoma cells served as positive control for PDGFR expression and T129 cell lysate was also used as positive control for PDGFR expression which was a ready-made lysate. Western blot analysis verified the absence of protein expression of PDGFR in human neutrophils **(Fig. 22).** The assay confirmed the expression of PDGFR in U-87MG and T129 cells **(Fig. 22).**

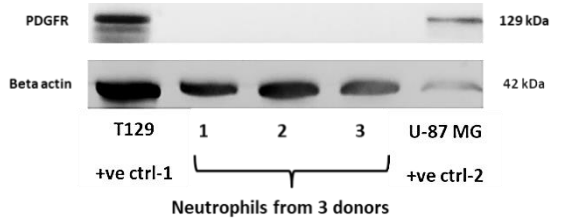

Figure 22. Neutrophils do not express PDGFR. Freshly isolated neutrophils form different donors and U-87 MG cell line were lysed and analyzed by western blot with an anti-PDGFR antibody. U-87 MG cells served as positive control for expressing PDGFR. T129 cell line lysates were available ready-made, which served as an additional positive control for the PDGFR expression. Equal loading was shown by reprobing the blots with anti-human β-actin antibody. Neutrophil lysates prepared from 3 donors were analyzed *(n = 3)*.

3.7 CP-673451 does not block upstream pathways of PMA-induced ROS production involved in NETosis

Many studies have shown the activation of PKC and phosphorylation of p38-MAPK, ERK1/2, PI3K, and Akt occur in response to various NETosis stimuli [55, 77, 80, 86]. PMA induced ROS-dependent NETosis mechanisms were followed by phosphorylation of PKC, p38-MAPK, ERK1/2, PI3K, Akt. Although these pathways were believed to be upstream to ROS, they are critical in NETosis [55, 80], therefore it was necessary to check if CP-673451 treatment inhibits the phosphorylation of these molecules.

Western blot analysis of PMA stimulated neutrophils with or without CP-673451 was analyzed for phosphorylation of PKC α/βII, p38-MAPK, ERK1/2, PI3K, and Akt. Phosphorylation of PKC α/βII was enhanced with stimulation of PMA and PKC δ was phosphorylated after PMA stimulation **(Fig. 23)**. Enhanced phosphorylation of PI3K and phosphorylation of Akt was seen after PMA stimulation **(Fig. 23)**. The p38 MAPK and ERK1/2 also phosphorylated after PMA stimulation **(Fig. 23)**. The immunoblotting results confirmed that the phosphorylation of PKC α/βII, PKC δ, p38-MAPK, ERK1/2, PI3K, and Akt were not inhibited by CP-673451 treatment **(Fig. 23)**. These findings indicate that upstream pathways of PMA-induced ROS production, which are involved in PMA-induced NET formation, are not affected by CP-673451. Interestingly, CP-673451 alone was tending to activate p38-MAPK, ERK1/2, and Akt pathways **(Fig. 23)**.

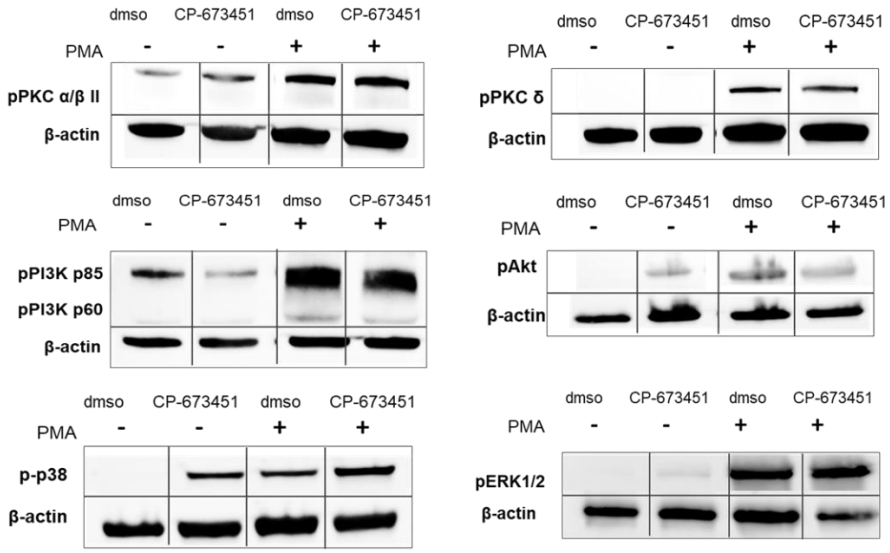

Figure 23. Signaling events activated after PMA-stimulation in neutrophils are not inhibited by CP-673451. Neutrophils were incubated with medium or dmso or 3μM CP-673451 for 30 min at 37˚C and cells were stimulated with PMA (20nM) for 20 min at 37˚C and whole-cell lysates was prepared and separated by SDS-PAGE. Phosphorylation of PKC α/β, PKC δ, PI3K, Akt, ERK1/2, and p38 MAPK was analyzed by using phospho PKC α/β, Thr638/641) (D40G4), phospho-PKC δ, phospho-PI3K p85 (Tyr458)/p55 (Tyr199), phospho-p44/42 MAPK (ERK1/2, Thr202/Tyr204), phospho-Akt (Thr308), and phospho-p38 MAPK (Thr180/Tyr182) antibodies. Equal loading was shown by reprobing the blots with anti-human β-actin antibody. Blots shown are representative for 2-3 independent experiments. *(n=2-3).*

3.8 CP-673451 does not block upstream pathways of iIC-induced ROS production involved in NETosis

In the case of iIC-induced ROS dependent NETosis, phosphorylation of p38-MAPK, ERK1/2, Akt, and PI3K are critical events. Published report showed that the activation of PI3K, Akt, ERK1/2, or p38 MAPK results directly from Src family kinases/receptor activation and is not ROS mediated, as ROS inhibition did not affect their phosphorylation [55]. Since phosphorylation events found to be critical for NETosis I investigated whether CP-673451 has influence of these events. Western blot analysis of the neutrophils exposed to CP-673451 and stimulated with iIC was carried out to analyze the phosphorylation of p38-MAPK, ERK1/2, PI3K, Akt, and Src. W estern blot analysis revealed that CP-673451 does not inhibit iIC-induced phosphorylation of p38-MAPK, ERK1/2, PI3K, Akt, and Src **(Fig. 24)**. These western blot studies verified that CP-673451 does not target or inhibit any of these known pathways of iIC-induced NETosis. Similar to the previous result **(Fig. 24)**, CP-673451 alone was tending to activate p38-MAPK, ERK1/2, and Akt pathways, which lead to cause enhanced phosphorylation in iIC stimulated neutrophils **(Fig. 24)**.

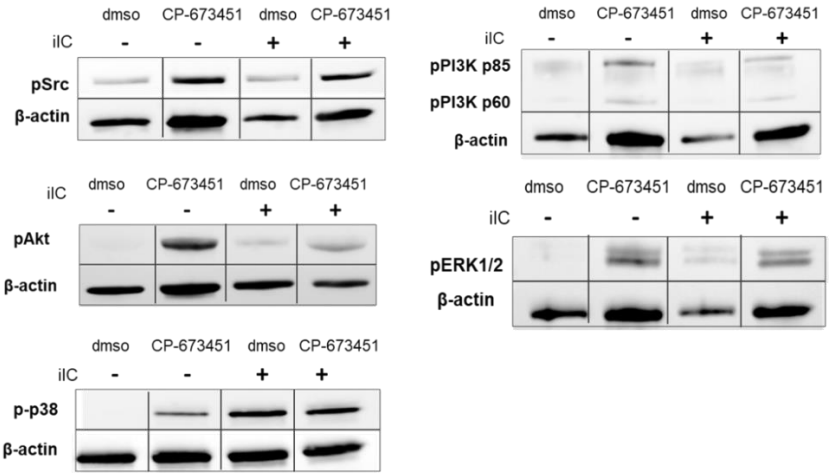

Figure 24. Signaling molecules activated during iIC-induced NETosis are not inhibited by CP-673451. Neutrophils were pre-treated with medium or dmso, or 3μM CP-673451 for 30 min at 37˚C and stimulated by incubating the cells on iIC-coated surfaces at 37˚C for 20 min. Whole-cell lysates were prepared and separated by SDS-PAGE. Phosphorylation of Src, PI3K, Akt, ERK1/2, and p38 MAPK was analyzed by using phospho-Src (Tyr416), phospho-PI3K p85 (Tyr458)/p55 (Tyr199), phospho-p44/42 MAPK (ERK1/2, Thr202/Tyr204), phospho-Akt (Thr308), and phospho-p38 MAPK (Thr180/Tyr182) antibodies. Equal loading was shown by reprobing the blots with anti-human β-actin antibody. Blots shown are representative for 2 independent experiments. *(n=2)*.

3.9 CP-673451 treatment leads to phosphorylation of Akt, ERK1/2, and P38 MAPK

The activation of p38 MAPK, ERK1/2 pathways are involved in oxidative burst in human neutrophils [81, 124]. In addition, phosphorylation of p38 MAPK, ERK1/2, Akt are important in ROS-dependent PMA- and iIC-induced NETosis [55, 80, 86]. Interestingly, the western blot studies for phospho-proteins after PMA- and iIC- stimulation revealed an enhanced phosphorylation of p38 MAPK and Akt by CP-673451 alone without any additional stimulation compared to the dmso treated neutrophils **(Fig. 25 (A, B))**. In addition, ERK1/2 also tends to be phosphorylated upon CP-673451treatment **(Fig. 25 (C))** compared to the dmso treated neutrophils.

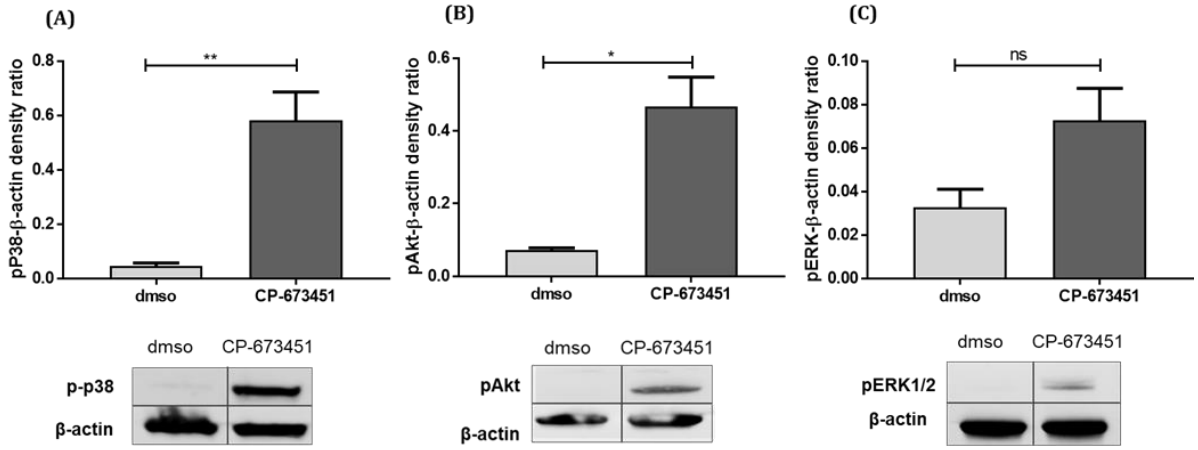

Figure 25. CP-673451 treatment leads to phosphorylation of p38 MAPK, ERK1/2, and Akt in neutrophils. Neutrophils were incubated with dmso or 3μM CP-673451 for 50 min at 37˚C and whole-cell lysates was prepared. dmso treated neutrophils served as solvent control. Whole-cell lysates were separated by SDS-PAGE. Phosphorylation of Akt, ERK1/2, and p38 MAPK was analyzed by using phospho-44/42 ERK1/2 (Thr202/Tyr204), phospho-Akt (Thr308), and phospho-p38 MAPK (Thr180/Tyr182) antibodies. Equal loading was shown by reprobing with anti-human β-actin antibody **(A-C)**. Blots shown are representative of 4-5 independent experiments. For quantification the signals, ratio of pAkt, pERK, and pp38 to β-actin signal were determined using Bo 1D software. Mean ± SEM values of the ratios are plotted in bar graph **(A-C)**. *(n=4-5). *p <0.05, **p <0.01, ns=non-significant* as compared with solvent control (0.1% dmso).

3.10 Screening for changes in tyrosine, serine, and threonine phosphorylated proteins upon CP-673451 treatment

The eukaryotic protein kinases that directly phosphorylate proteins are divided into two major classes: those that phosphorylate tyrosine and those that phosphorylate serine and threonine [125]. Phosphorylation of several proteins are involved in PMA induced NETosis [80]. To assess if the phosphorylation events induced by PMA is affected by CP-673451, the tyrosine, threonine, and serine phospho proteins were screened by immunoblotting.

The phosphorylated tyrosine and serine proteins present in PMA stimulated (Ctrl) and PMA stimulated and CP-673451 treated (tr) samples had showed similar pattern of the phospho-protein bands. However, threonine phosphorylated proteins had two clear bands missing in the CP-673451 treated (tr) neutrophil lysates compared to the control (Ctrl) **(Fig. 26-A)**. This indicated an inhibitory action by CP-673451 in phosphorylation of two, so far unknown proteins. According to the molecular weight marker, the bands were of sizes between 30 kDa and 20 kDa **(Fig. 26-B)**.

To identify the proteins corresponding to the missing bands, all the proteins other than phospho-threonine proteins needed to be removed so that the purified protein bands corresponding to missing bands can be analyzed and identified. Therefore, phospho-protein-enrichment was performed, which purified phospho threonine proteins by using an anti-phospho threonine antibody immobilized to Sepharose beads. Neutrophils were treated or untreated with CP-673451 and stimulated with PMA for 20 min. The lysates were prepared using 1xRIPA buffer containing protease inhibitors. The lysates were then incubated overnight with the anti-phospho threonine antibody immobilized to Sepharose beads and washed with the lysis buffer. The proteins were denaturated in presence of SDS and β-mercapto ethanol and centrifuged to separate the proteins and beads. The proteins electrophoresed on 10 % SDS-PAGE gels and the gels were then stained with Coomassie stain to detect proteins. The phospho-threonine bands of sizes between 30 kDa and 20 kDa were observed. Unfortunately, the bands were not visible after Coomassie staining. Therefore, I was not able to cut them out for further protein identification **(Fig. 26 (B)).**

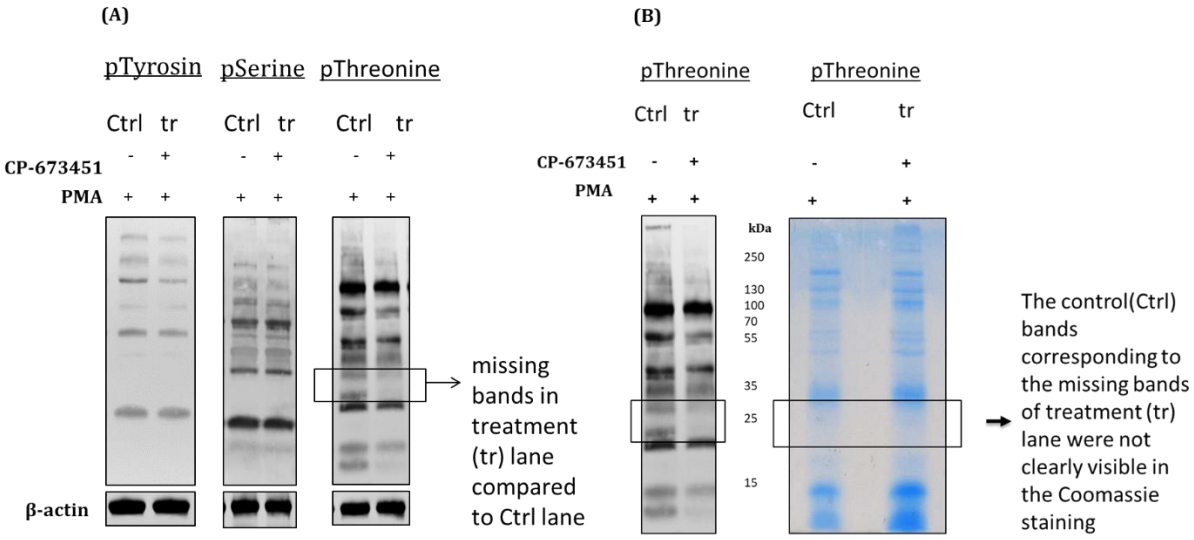

Figure 26. Immunoblotting and Coomassie staining for phospho-threonine proteins from neutrophils treated with CP-673451. **(A)** Neutrophils were incubated with dmso, or 3μM CP-673451 for 30 min at 37˚C and then stimulated with PMA for 20 min at 37˚C and whole-cell lysates were prepared with TCA mediated lysis. Whole-cell lysates were separated in 10% SDS-PAGE. Phosphorylation Tyrosine, Serine, and Threonine proteins were analyzed by using phospho-tyrosine, phospho-serine, and phospho-threonine Abs. Equal loading was shown by reprobing with anti-human β-actin Abs. Bands of the Control (Ctrl) lanes were compared to the CP-673451 treated (tr) lanes for finding missing bands. Blots shown are from single preliminary screening experiment. **(B)** Neutrophils (40 x 10^6 cells/ml) were incubated with 0.1% dmso, or 3μM CP-673451 for 30 min at 37˚C and then stimulated with PMA for 20 min at 37˚C. Whole-cell lysates were prepared with 1xRIPA buffer followed by immune purification of phospho-threonine proteins by anti-phospho threonine Sepharose bead conjugates. Whole-cell lysates were separated in 10% SDS-PAGE and the gel was stained with Coomassie for 1 h and destained with distilled water. Bands of the Control (Ctrl) lanes were compared to the CP-673451 treated (tr) lanes for finding missing bands. Gel shown is from a single preliminary experiment. The missing lanes identified in phospho-threonine blots are compared with the same area in the phospho-threonine lanes in the gel.

3.11 CP-673451 does not inhibit Ionomycin induced-NETosis

NETosis can be induced by various stimuli and based on the type of stimulus there are different pathways described [55, 70, 74, 78, 80, 86, 88, 126]. PMA and iIC induce NETosis in a ROS-dependent manner, where NADPH-oxidase generated ROS plays a major role in inducing NETosis [55, 80, 127]. However, there is ROS-independent NETosis such as the NETosis induced by Ionomycin, where inhibition of NADPH oxidase does not interrupt NETosis [88]. The signaling mechanisms involved in Ionomycin induced NET formation have been shown to differ from the ones induced by PMA and iIC [41, 88].

My present study has shown that CP-673451 treatment does not inhibit ROS or activation of the signaling pathways upstream to ROS is involved in downstream inhibition of NETosis. In a preliminary experiment, different concentrations (2.57 μM-7 μM) of Ionomycin were tested for inducing NETosis **(Fig. 27 (A, C))**. An optimal concentration of 5 μM of Ionomycin found to induce NETosis was decided to use in further assays. The effect of CP-673451 (0.1 μM -10 μM) on Ionomycin induced NETosis was tested **(Fig. 27 (E-F))**, to check if CP-673451 can serve as a general inhibitor of NETosis. The study showed that, CP-673451 did not inhibit the Ionomycin induced NET formation even at 10 μM concentrations **(Fig. 27 (E, F))**. In addition, DPI, an inhibitor of NADPH-oxidase also did not inhibit Ionomycin-induced NETosis, as it is a NADPH-oxidase-independent type of NETosis **(Fig. 27 (B, D))**.

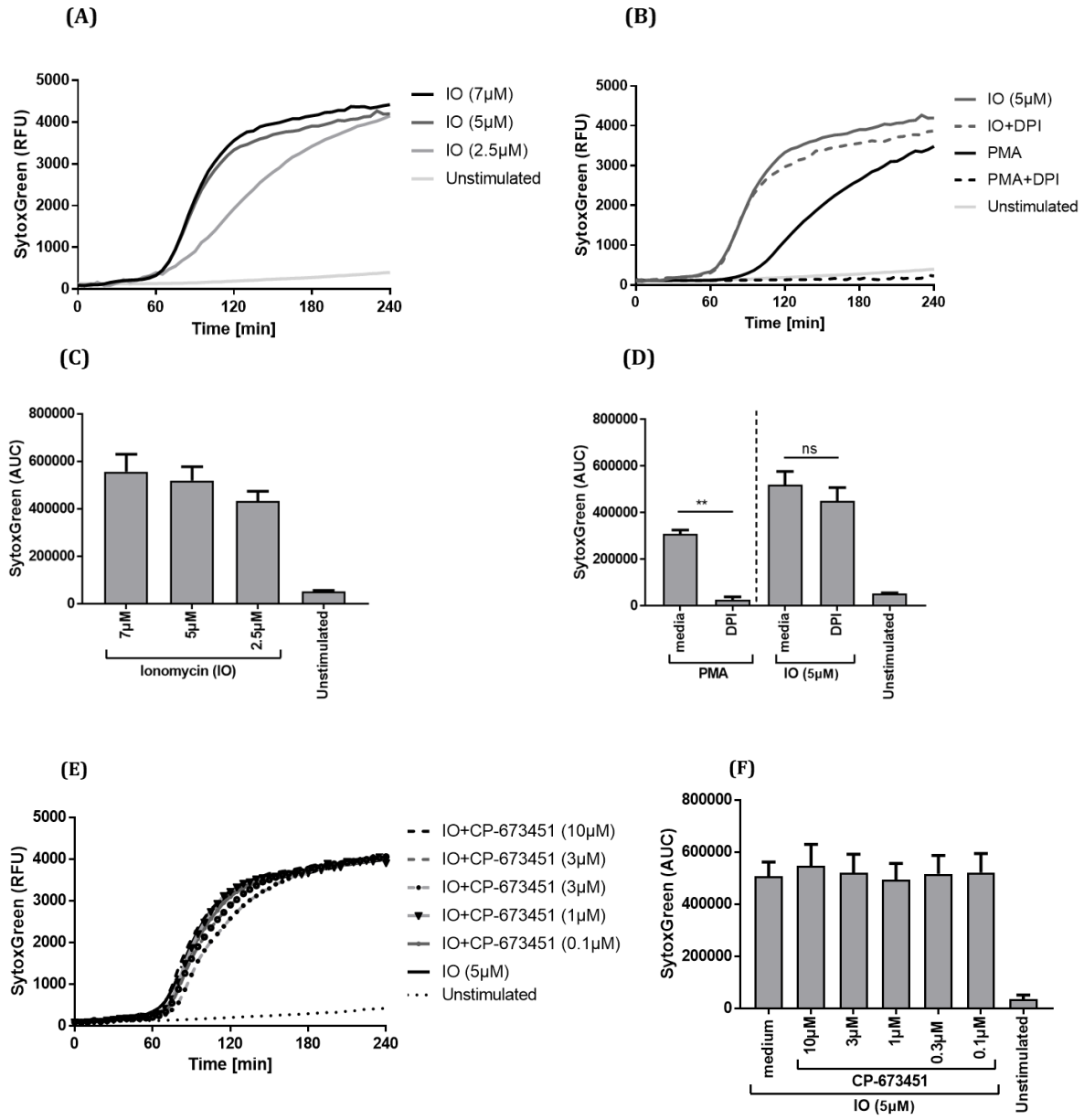

Figure 27. CP-673451 does not inhibit Ionomycin- induced NETosis. **(A)** Neutrophils were stimulated with Ionomycin (IO) (2.5 μM, 5 μM, and 7 μM) or left unstimulated and the release of neutrophil extracellular traps (NETs) was monitored for 4 h at 37°C, measured by SytoxGreen. **(B)** Neutrophils ($1x10^6$/ml) were treated with medium or DPI (20 nM) and then stimulated with IO (5 μM) or PMA (20nM) or left unstimulated. The release of neutrophil extracellular traps (NETs) was monitored for 4 h at 37°C, measured by SytoxGreen. **(C, D)** Areas under the curve (AUC) values (mean ± SEM) of fluorescence intensities (RFUs) were plotted. **(E)** Neutrophils ($1x10^6$/ml) were treated with 0.1 μM-10 μM of CP-673451 or dmso and stimulated with IO (5 μM) or left unstimulated. The release of neutrophil extracellular traps (NETs) was monitored for 4 h at 37°C, measured by SytoxGreen. **(F)** Area under the curve (AUC) values (mean ± SEM) of fluorescence intensities (RFUs) was plotted. *n = 3, **p <0.01, ns=non-significant* as compared with the respective positive controls.

3.12 CP-673451 does not induce apoptosis or necrosis in neutrophils

Many of the pharmacological inhibitors have a drawback of causing cytotoxicity [128]. CP-673451 has been used in different cells at a concentration between 1 nM-200 nM ranges [106, 109], but in this study 0.1 µM-3 µM concentrations of CP-673451 have been used in neutrophils. The possibility of CP-673451 inducing apoptosis or necrosis in neutrophils at these concentrations was investigated. To exclude the possibility of induction of apoptosis by CP-673451, the neutrophils were treated with CP-673451 for 4h and 7h and 22 h at 37°C. After the treatment, the neutrophils were stained with Annexin V-FITC stain and propidium iodide (PI) for staining apoptotic and necrotic cells. The viability test by FACS analysis **(Fig. 9)** revealed that CP-673451 does not induce apoptosis or necrosis in human neutrophils **(Fig. 28 A-C)**. In addition, the results of staining after 22 h of CP-673451 showed that, CP-673451 did not inhibit the natural neutrophil apoptosis occurring overnight **(Fig.28-C)**.

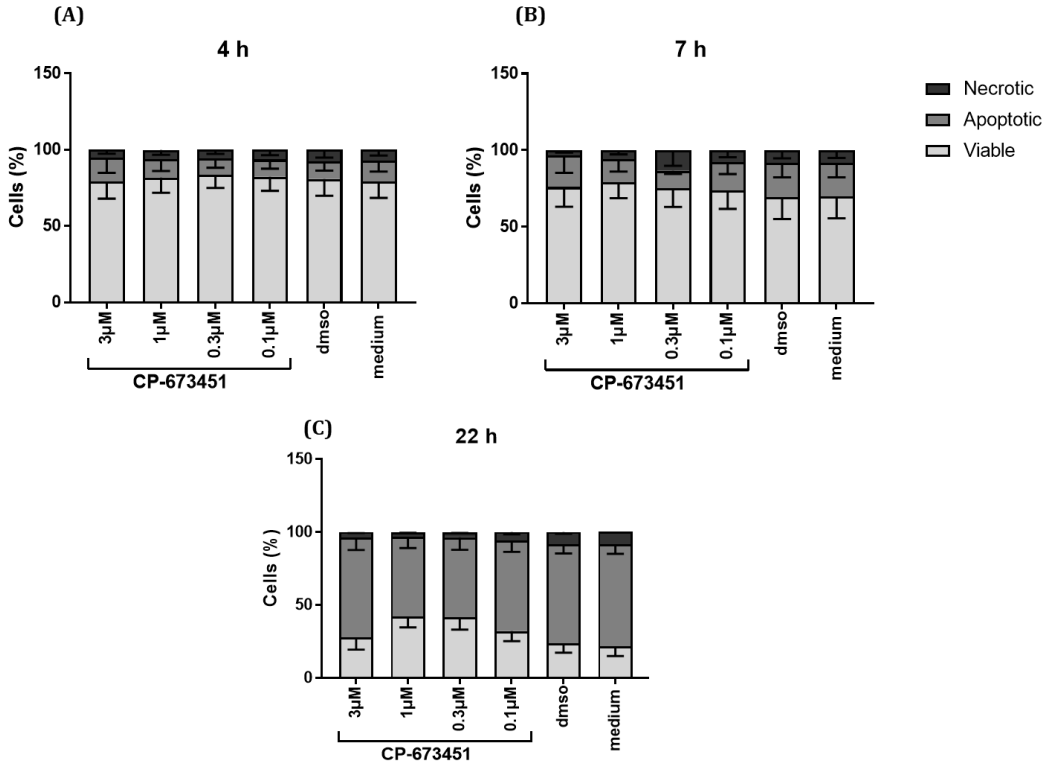

Figure 28. CP-673451 does not induce apoptosis or necrosis of neutrophils. Neutrophils were incubated with 0.1 µM-3 µM CP-673451 for 4 h, 7 h, and 22 h at 37°C. dmso and medium are used as controls. Neutrophil viability was determined by Annexing V and PI staining and analyzed by flow cytometry. Considering Annexin V and PI negative neutrophils as viable, Annexin V positive alone as apoptotic, and Annexin V and PI double positive as necrotic. Percentages of differentially stained cells are shown in (mean ± SEM) of three independent experiments, (*n=3),* compared with solvent control (0.1% dmso).

As necrotic cells disintegrate rapidly, these cells would not be counted by FACS. Therefore, an LDH release assay was performed after treating neutrophils with CP-673451 for 4h and 7h at 37°C to confirm its non-toxicity. The amounts of LDH released after each time points were correlated to the necrosis rate. The LDH assay results were in agreement with the FACS results, confirming no induction of necrosis due to CP-673451 treatment **(Fig. 29)**.

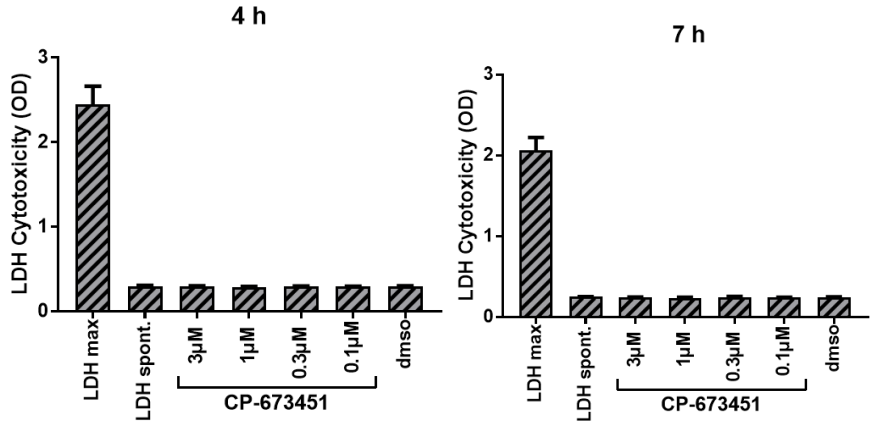

Figure 29. CP-673451 does not induce cytotoxicity in neutrophils. Neutrophils were incubated for 1 h and 7 h at 37˚C with 0.1 µM-3 µM CP-673451 or with dmso or NET-medium. The LDH released into the medium was transferred to a new plate. Additionally, LDH_{max} (LDH maximum) samples, with completely lysed cells, and LDH_{spont} (LDH spontaneous) samples from untreated cells were also prepared. The supernatants of the differentially treated cells were mixed with Reaction Mixture (from the kit) and incubated for 30 min at RT Reactions were stopped by adding Stop Solution (from the kit). LDH_{max} (LDH maximum) samples served as positive control for lysis/cytotoxicity and LDH_{spont} (LDH spontaneous) served as negative control for lysis/cytotoxicity. Absorbance at 490 nm and reference 680 nm was measured using a spectrophotometer. LDH activity was determined from the OD values obtained whose (mean ± SEM) are shown in of three independent experiments, (n=3), compared with solvent control (dmso).

3.13 CP-673451 does not affect neutrophil effector functions other than NETosis

To use CP-673451 as NETosis inhibitor in future therapeutic options, it is important to check whether CP-673451 is affecting or inhibiting neutrophil functions other than NETosis. At the same time, studying CP-673451 in other functions might provide hint to

the pathway it is targeting. Therefore, basic neutrophil functions including; activation, migration and phagocytosis were assessed after treatment with CP-673451.

3.13.1 CP-673451 does not affect neutrophil phagocytic ability

Phagocytosis is a major anti-microbial function of neutrophils [13, 14]. Inhibiting NETosis and phagocytosis at the same time could lead to reduced anti-microbial defense against pathogens. Neutrophils pre-treated with CP-673451 was stimulated with LPS and IFN$_\gamma$ and allowed to phagocytose fluorescent latex beads or *S. aureus* bioparticles. The phagocytosis of beads and bioparticles was analyzed by FACS **(Fig. 8)**.

The phagocytosis rate of beads and *S. aureus* by neutrophils pre-treated with CP-673451 was not different from the control dmso treated neutrophils after stimulation **(Fig. 30)**. Hence, no inhibition of the phagocytic function was observed due to CP-673451 treatment in neutrophils **(Fig. 30)**.

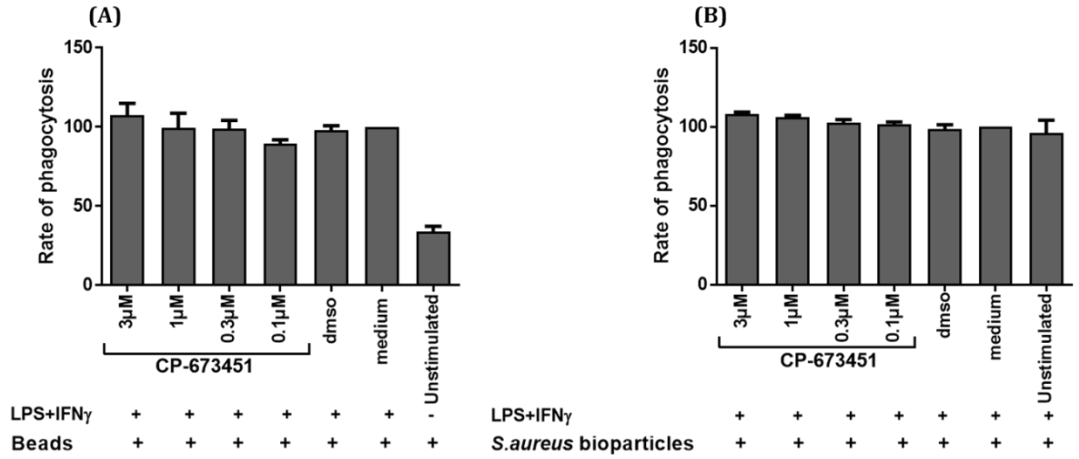

Figure 30. CP-673451 does not inhibit phagocytic function of neutrophils. Neutrophils were incubated with 0.1 μM-3 μM CP-673451 or dmso or medium for 30 min at 37°C. The cells were then co-incubated with FluoSphere carboxylate-modified latex beads added in 1 to 10 ratios to neutrophils **(A)** or Alexa-Fluor 488 conjugated non-viable *Staphylococcus aureus* bioparticles in 2:1 ratio; *S. aureus* to neutrophils **(B)**. Cells were then stimulated with LPS (100ng/ml) and IFN$_\gamma$ (200 U/ml) for 30 min at 37°C. Trypan blue was added to quench the fluorescence of extracellular bacteria/beads sticking on the neutrophil surface. Phagocytosis was assessed by flow cytometry and analyzed by FACS Diva software. Percentage of the cells with ingested beads or bioparticles were measured and values were normalized to medium control. Values ± SEM are shown*, (n=4)* as compared with solvent control (0.1% dmso).

3.13.2 The effect of CP-673451 on neutrophil migration

It is important for neutrophils to be able to migrate to the site of infection, mostly by chemotaxis. Therefore, I tested whether CP-673451 has an influence on the migration of neutrophils *in vitro*. CP-673451 treated neutrophils were tested, for chemotaxis, where the migration is directional towards stimulants like IL-8 [129] and for chemokinesis, where there is a random migration in response to stimulants like TNF-α [130]. Neutrophils were pre-treated with CP-673451 and allowed to migrate on a trans well plate with the stimulants IL-8 for chemotaxis and TNF-α for chemokinesis. The migrated cells were lysed and quantified with the help of β-glucuronidase assay and migration index values were calculated. Chemotaxis of neutrophils towards IL-8 was not affected by CP-673451 treatment **(Fig. 31)**. However, TNF-α mediated random migration was inhibited by 3μM concentrations of CP-673451 **(Fig. 31)**.

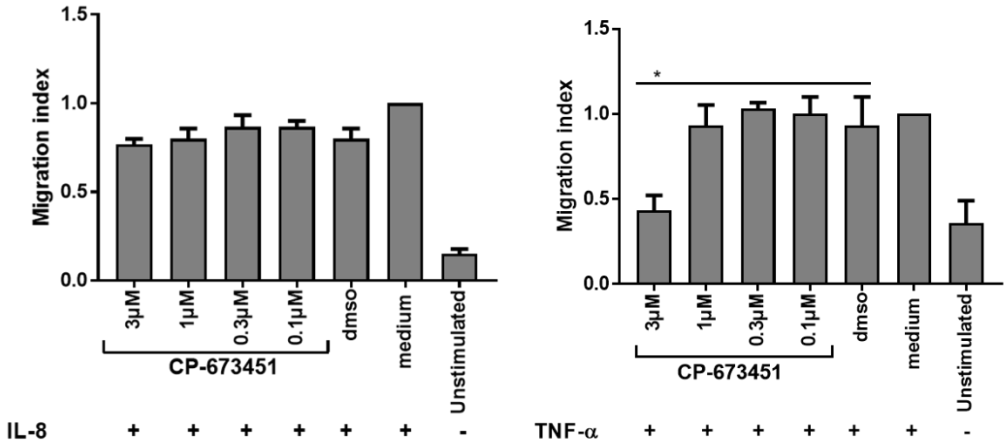

Figure 31. CP-673451 does not inhibit neutrophil chemotaxis but affects chemokinesis at higher concentrations. Neutrophils were preincubated with 0.1 μM-3 μM CP-673451 or dmso, or medium for 30 min at 37°C. The neutrophil suspension was transferred to trans well filter in 24 well plate which in its lower well contained chemotactic stimulus, IL-8 (25 ng/ml), or the chemokinesis stimulant, TNF-α (50 ng/ml) or medium. The cells were allowed to migrate for 1h at 37°C. The migrated cells were then lysed with of 1% Triton X-100. parallelly, untreated fresh neutrophil lysates were transferred to a 96 well plate and serially diluted. β-glucuronidase assay was carried out in acetate buffer, containing 4-Nitrophenyl β-D-glucuronide and incubated overnight at 37°C. The reaction was stopped by glycine buffer and the absorbance of the lysates was then measured at 405 nM and reference 620 nM. A standard curve was obtained with serially diluted known concentrations of the cells and OD values were used to determine migration index. The migration index values were normalized to stimulant control. (± SEM). *(n=3), *p < 0.05* as compared with solvent control (0.1 % dmso).

3.13.3 CP-673451 does not inhibit neutrophil activation

Neutrophil activation plays an important role in the inflammatory response to bacterial infections. Many stimuli like LPS have been shown to be a major mediator of neutrophil activation which is accompanied by an early down-regulation of L-selectin (CD62L) and up-regulation of CD11b on the neutrophil surface [131]. To investigate whether CP-673451 affects the activation of the neutrophils, neutrophils were pre-treated with CP-673451 and stimulated with LPS and IFN_{γ}, TNF-α, and fMLP. The shedding of CD62L and upregulation of CD11b was assessed by staining and FACS analysis **(Fig. 7)**. CP-673451 treatment did not inhibit neutrophil activation in response to any of the stimuli tested **(Fig. 32)**. Interestingly, with CP-673451 treatment appeared to have a tendency to enhance the activation phenotype induced by LPS and IFN_{γ}, TNF-α, and fMLP **(Fig. 32)**.

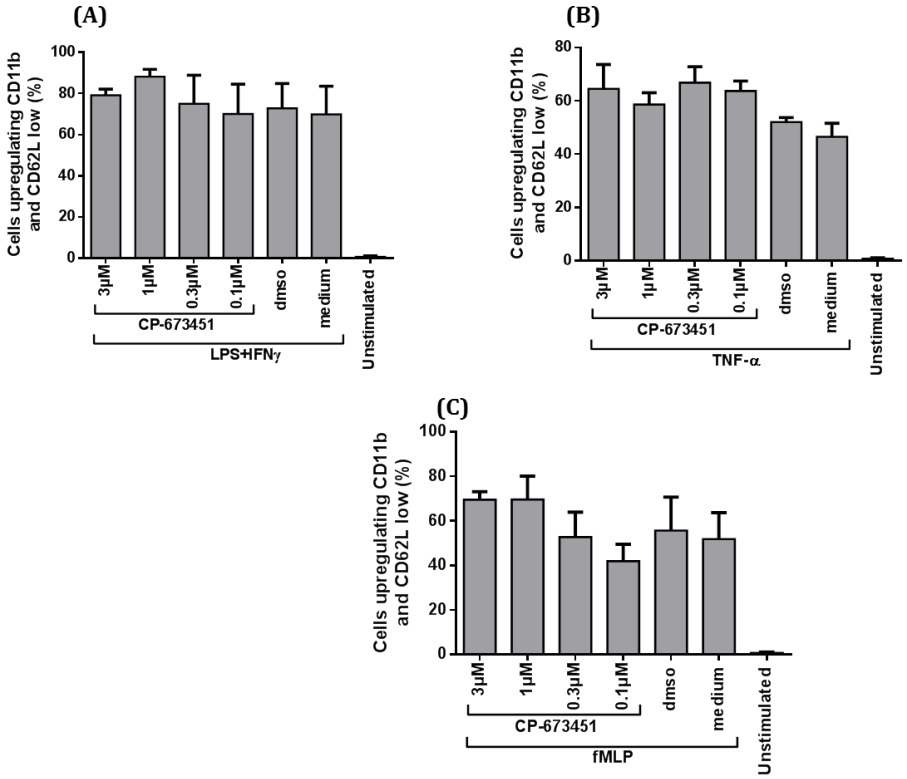

Figure 32. CP-673451 does not inhibit LPS+IFN$_{\gamma}$-, TNF-α-, and fMLP-mediated neutrophil activation. Neutrophils were incubated with 0.1 μM-3 μM CP-673451 or 0.1% dmso or medium for 30 min at 37°C. The cells were then stimulated with LPS (100ng/ml) together with IFN_{γ} (200 U/ml), TNF-α (100ng/ml), and fMLP (1μM) for 4 h at 37°C. The cells were then stained with fluorescent-conjugated antibodies against CD11b and CD62L for 30 min at 4°C. Percentage of the cells upregulating CD11b and shedding CD62L was assessed by flow cytometry and analyzed by FACS Diva software. Percentage mean values of neutrophils upregulating CD11b and shedded CD62L are shown, (± SEM), *(n=3)* as compared with solvent control (dmso).

3.14 CP-673451 activates neutrophils

As neutrophils treated with CP-673451 showed a tendency of enhanced activation in response to stimulants, neutrophils treated with CP-673451 alone were tested for the activation phenotype by measuring upregulation of CD11b and shedding of CD62L **(Fig. 7)**. Interestingly, CP-673451 could activate neutrophils in a dose dependent manner which was assessed by upregulation of CD11b and shedding of CD62L by FACS analysis **(Fig. 33)**. The neutrophil activation by CP-673451 was comparable to LPS-mediated neutrophil activation **(Fig. 33)**.

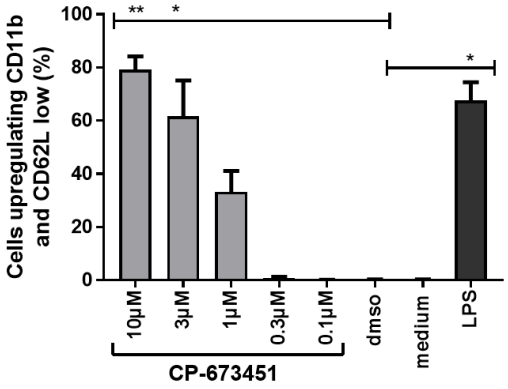

Figure 33. CP-673451 activates neutrophils in a dose dependent manner. Neutrophils were incubated for 30 min at 37°C. The cells were then co-incubated with 0.1 µM-10 µM CP-673451 or 0.1% dmso or medium or with LPS (100ng/ml) for 4 h at 37°C. The cells were then stained with fluorescent-conjugated antibodies against CD11b and CD62L for 30 min at 4°C. Percentage of the cells upregulating CD11b and shedding CD62L was assessed by flow cytometry and analyzed by FACS Diva software. Percentage mean values of neutrophils upregulating CD11b and shedded CD62L are shown, (± SEM), *(n=3), *p <0.05, **p <0.01,* as compared with solvent control (dmso).

3.15 The neutrophil-activating property of CP-673451 is not due to endotoxin-contamination

Dose dependent activation of neutrophils by CP-673451 was an unexpected result and the inhibitor molecule has not been reported to exert such property. I therefore suspected that endotoxin contamination could be responsible for the neutrophil activating activity of CP-673451. To exclude this possibility, neutrophils were treated with Polymyxin-B (PMB) and stimulated by CP-673451 or LPS. Polymyxin B (PMB) is able to neutralize the effect of endotoxin [132]. Activation phenotype was assessed by

measuring upregulation of CD11b and shedding of CD62L FACS staining **(Fig. 7)**. PMB treatment neutralized LPS mediated neutrophil activation, hence no upregulation of CD11b and shedding of CD62L were observed **(Fig. 34)**. However, CP-673451 mediated dose-dependent neutrophil activation was not blocked by polymyxin-B, indicating that the activating property of CP-673451 is not due to LPS contamination **(Fig. 34)**.

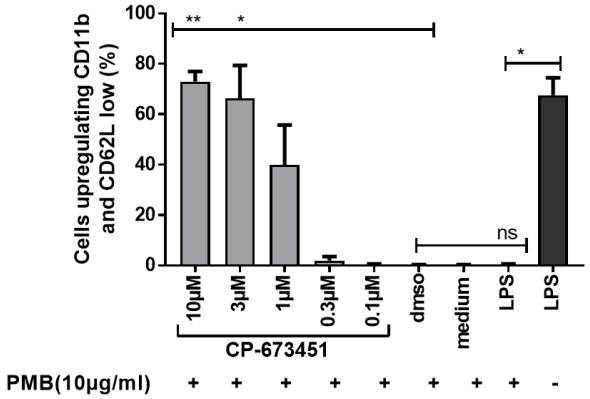

Figure 34. Activation property of CP-673451 in neutrophils is not due to endotoxin contamination. Neutrophils were incubated with Polymyxin-B (PMB) (10 µg/ml) or with medium for 30 min at 37°C. The cells were then stimulated with 0.1 µM-10 µM CP-673451 or 0.1% dmso or medium or with LPS (100 ng/ml) for 4 h at 37°C. The cells were then stained with fluorescent-conjugated antibodies against CD11b and CD62L for 30 min at 4°C. Percentage of the cells upregulating CD11b and shedding CD62L was assessed by flow cytometry and analyzed by FACS Diva software. Percentage mean values of neutrophils upregulating CD11b and shedded CD62L are shown, (± SEM)*, (n=3), *p <0.05, **p <0.01,* as compared with solvent control (dmso).

3.16 CP-673451 induces differential gene expression changes in human neutrophils

The relevance of transcription and translation in NETosis remains unclear. A previous study argues that PMA-induced NETosis is transcription and translation independent and neutrophils contain all the factors required for NET formation when they emerge from the bone marrow as differentiated cells [76]. However, a recent study suggested that kinases including Erk1/2, cSrc, p38, and Akt activate transcription during PMA-induced NETosis and inhibition of transcription inhibits PMA-induced NETosis without affecting the ROS production [133]. As the relevance of transcriptional responses in CP-673451-mediated signaling in neutrophils were not known and as CP-673451 itself

activates Erk1/2, p38, and Akt pathways, its role in modulating gene expression in PMA-induced NETosis was needed to be clarified. In addition, inhibition of transcription could inhibit PMA-induced NETosis without inhibiting ROS production. Therefore, the ability of CP-673451 to suppress transcription was also needed to be analyzed.

Neutrophils were pre-treated with 3μM CP-673451 or dmso and stimulated with PMA or left unstimulated. Total RNA was extracted and a high throughput RNA Seq was performed and differential expression of genes was assessed in three independent experiments. A principal component analysis (PCA) was performed to evaluate the differences and relatedness of transcription profiles among different conditions. PCA clustered the multidimensional data into assigned sets of variables and showed transcription profile patterns in each condition. These analyses showed that transcriptomes of unstimulated, CP-673451 -treated, PMA-stimulated (NET-forming) and CP-673451 -treated-PMA-stimulated (NET-inhibiting) neutrophils form distinct clusters **(Fig. 35)**.

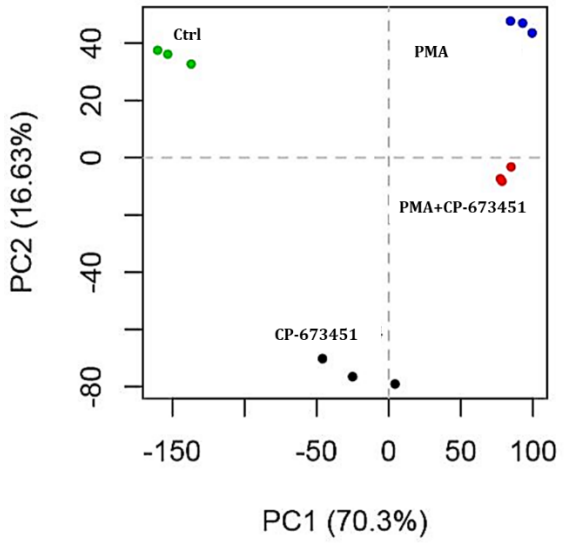

Figure 35. Principle component analysis (PCA) showing differences in transcription profiles among differently treated neutrophils. Neutrophils ($10x10^6$ in 1 ml NET-medium) were pre-treated with 3μM CP-673451 or dmso for 30 min at 37°C and stimulated with PMA or left unstimulated 3 h 30 min at 37°C. The total RNA was extracted and a high throughput RNA Seq was performed. The differential transcriptional patterns under each condition were assessed by principle component analysis. The PCA was calculated using the R/Bioconductor package labdsv and based on the transcript per million (TPM) values of the 10000 most variable genes across samples according to their interquartile range (IQR). The three different colors represent different treatments. The green dots; neutrophils treated with diluent control (dmso), black dots; neutrophils treated with CP-673451, red dots; CP-673451 treated neutrophils stimulated with PMA, blue dots; neutrophils stimulated with PMA. *(n=3).*

The principle component analysis (PCA) **(Fig. 35)** clearly shows the related transcriptional patterns clustering together with three different donors (showed as three dots of same color) of same treatment. The data also shows a separated cluster for unstimulated-dmso treated control (Ctrl) samples from all the other conditions. There was a clear separation of the samples along the PCA axis **(Fig. 35)**. The CP-673451 treated neutrophil samples also stand out **(Fig. 35)**. Interestingly, there were also differences between PMA stimulated samples compared to CP-673451 pre-treated-PMA stimulated samples **(Fig. 35)**. This indicates CP-673451's involvement in changing PMA-induced transcriptional pattern.

Comparing the up and down regulated genes of untreated and CP-673451-treated neutrophils might further provide the involvement of CP-673451 in modulation neutrophil gene expressions. Furthermore, involvement of CP-673451 in inhibiting NETosis can be analyzed by comparing the differentially up and down regulated genes of PMA stimulated neutrophils and CP-673451 treated- PMA stimulated neutrophils. These data have not been analyzed in detail due to lack of time, but the preliminary analysis data are provided **(in the supplementary CD attached)**.

Chapter 4. Discussion

4.1 CP-673451 induces neutrophil activation and inhibits an unknown pathway of NETosis, downstream of ROS production

Neutrophils, the first cells to arrive at an infection site exert several potent antimicrobial mechanisms. NET formation is one of these mechanisms. NETs can capture and kill the invading pathogen [1, 2]. On the other hand, recent studies show that many diseases are associated with NETosis including autoimmune diseases [38, 60, 65, 134]. Since NETs expose potential autoantigens such as histones, dsDNA, and granule enzymes they have been suspected to mediate autoimmune responses due to immune complexes (ICs) formation [55, 62, 135-137]. However, the molecular mechanism behind NET formation is still not clear.

There are two main NETosis mechanisms described; the classical, reactive oxygen species (ROS)-dependent and the early/rapid ROS-independent pathway [32, 33]. Most of the stimuli described to induce NETosis are dependent on ROS production by the NADPH- oxidase complex [34]. The importance of ROS production in NETosis has been shown with the help of several enzymatic inhibitor of NADPH-complex, showing inhibition of ROS production affects NETosis [30, 70, 87, 127]. Moreover, neutrophils from CGD patients, who lack a functional NADPH also failed to release NETs [38, 93]. However, it is not yet clear which pathways are involved in NET formation downstream of ROS production.

In this study, I studied two stimuli; PMA and immobilized immune complex (iIC), both inducing ROS-dependent NETosis. PMA is a synthetic stimulus. The PMA induced ROS-dependent NETosis has been studied extensively [138]. Immune complex (iIC) is a physiological stimulus which has been recently shown to induce NETosis [55]. In this study, I identified two inhibitors; CP-673451 (targeting PDGFR) and Doxorubicin (targeting Topoisomerase II) inhibiting PMA and iIC-induced NETosis without affecting PMA and iIC induced ROS production **(Fig. 11-14)**. Because the inhibitors were specifically inhibiting NETosis but not the upstream ROS production, the inhibitors were believed to be targeting downstream of ROS production pathways and upstream of NETosis.

Although Doxorubicin was seen to inhibit PMA- and iIC-induced NETosis in a dose dependent manner in SytoxGreen kinetic assays, Doxorubicin did not show NETosis inhibition in morphological analysis **(Fig. 17, 18)**. Moreover, other inhibitors targeting Topoisomerase II did not inhibit NETosis **(data not shown)**. In addition, Doxorubicin was not toxic to neutrophils **(data not shown).** As morphological analysis could not confirm the kinetic assay results, Doxorubicin was eliminated from the later studies. The study couldn't reveal why Doxorubicin showed inhibitory effect on SytoxGreen signal in the kinetic assay. It was suspected that Doxorubicin might be interfering with the SytoxGreen signal detection. It has been in discussion in studies that small molecule libraries used for screening are themselves fluorescent, leading to potential false positive results through interference [139]. Interestingly, Doxorubicin itself was fluorescent, which could have led to the false positive inhibitory readout through interference. Fortunately, a morphological confirmation was applied in this research which revealed the artifact. A test experiment with DNA together with Doxorubicin by using the SytoxGreen detection assay could clarify the hypothesis of signal interference caused by Doxorubicin. As there are several studies based on small molecule libraries carried out in drug discovery research, it is vital to cut out assay artifacts as early as possible to avoid spending time and resources pursuing compounds that are not actually impacting the desired biology but rather are false positives [139].

The small molecule inhibitor, CP-673451 was found inhibiting PMA- and iIC-induced NETosis in a dose dependent manner in the SytoxGreen-kinetic assay and the results were in line with the morphological analysis **(Fig. 15)**. In the morphological analyses, PMA induced NETosis was seen as a cloud like structures or with a very densely packed DNA in a large NETotic cell stained with SytoxGreen, this phenotype was consistent with the previous studies [140].

The lowest effective dose of CP-673451 to inhibit PMA-induced NETosis was found to be 0.3 μM in the SytoxGreen kinetic assay **(Fig. 15)**. To confirm the kinetic assay results, morphological observations of the neutrophils were performed with SytoxGreen staining. However, in the morphological observation 1 μM concentration of CP-673451 was needed to inhibit PMA-induced NETosis. The nuclear morphology of neutrophils was not very clear to examine with the SytoxGreen staining. The CP-673451-treated-PMA stimulated neutrophils were a slightly larger than the untreated cells and the

nuclear lobes were not as clearly seen as in untreated cells **(Fig. 15-E)**. 3µM CP-673451-treated-PMA stimulated neutrophil's inhibitory morphology was comparable with DPI-treated PMA stimulated neutrophils. Similarly, CP-673451 also inhibited iIC-induced NETosis at a lowest dose of 1µM **(Fig. 16)**. The iIC-induced NETs were thin fiber-like structures. SytoxGreen staining could clearly show the inhibition of the NET formation with CP-673451 **(Fig. 16-E)**. However, to visualize the NET-fiber structures properly, electron microscopic pictures need to be taken.

The most widely used method of NETosis detection is a nuclear staining using a non-cell permeable dye, SytoxGreen, which is the same technique used in this study. Since necrotic cells can be stained with SytoxGreen, an assay for neutrophil viability was conducted. The possibility of CP-673451 inducing apoptosis in neutrophils was investigated. I found that CP-673451 does not induce neutrophil apoptosis or necrosis **(Fig. 28 (A-C))** and it does not delay or inhibits neutrophil apoptosis **(Fig. 28-C)**. This indicates that the neutrophil apoptosis pathway has been not affected or inhibited by CP-673451. The study also excluded that CP-673451 induces necrosis **(Fig. 28, 29).** The results of FACS staining with the cell permeable dye propidium iodide and the LDH release assay excluded the possibility of CP-673451 to cause cytotoxicity **(Fig. 28, 29)**. These results collectively indicate the specificity of the inhibitor towards specific cell death, the NETosis. CP-673451 did not induce cytotoxicity **(Fig. 29)**, which makes it suitable for studies in future therapeutic options for NET-related diseases.

Even though, the study identified CP-673451 as an inhibitor of NETosis, the target of this inhibitor was needed to be confirmed. However, the pharmacological inhibitors often show off-target effects which complicate the interpretation of the results and the understanding of the precise role of the involved receptors and mode of action of the inhibitors [106]. CP-673451 is a known inhibitor of platelet growth factor receptor (PDGFR). CP-673451 has shown to be effective against PDGFR at concentrations ranging from 1 nM-100 nM in several tumor cells. CP-673451 is known to exhibit >450-fold selectivity toward PDGFR over other angiogenic receptors including vascular endothelial growth factor receptor- 1, -2, and -3 (VEGFR1/2/3) [106]. In this study, I have used higher concentrations (up to 3 µM) of CP-673451 for NETosis inhibition **(Fig. 15-16)**, which could lead to off-target effects. Thus, other known targets of CP-673451 such as VEGFR1/2/3 were investigated for playing a role in NETosis. Inhibitors of

VEGFR1/2/3 were tested in PMA and iIC-induced NETosis assay, but these inhibitors could not inhibit NETosis even at a concentration of 10μM **(Fig. 19)**. This showed that VEGFR1/2/3 were not the target of CP-673451 which is involved in NETosis. However, this finding does not confirm PDGFR as the target of CP-673451 in neutrophils.

To check if PDGFR is the target involved in NETosis inhibition, another widely available PDGFR inhibitor, Sunitinib [141] was tested in PMA- and iIC-induced NET assays. However, Sunitinib did not inhibit PMA-induced NETosis but inhibited iIC-induced NETosis. However, Sunitinib inhibited also iIC-induced ROS and partially affected PMA-induced ROS, which indicates that Sunitinib seems to be affecting some other off target pathways in neutrophils which affect ROS production **(Fig. 20, 21)**. Collectively, Sunitinib did not act on neutrophils at a similar way as CP-673451, indicating that inhibition of PDGFR might not be leading to ROS-independent-NETosis-inhibition.

Although in 1988 platelet derived growth factor (PDGF) was shown to be chemotactic for neutrophils, in 1995 it was showed that human neutrophils lack functional PDGFRs [98, 99]. As PDGFR is the major target of CP-673451 and the presence of PDGFR in neutrophils were unclear, I assessed protein expression of PDGFR in human neutrophils by immunoblotting. I detected no protein expression of PDGFR in neutrophils. This result was in agreement with another study in 1995 which also showed that neutrophils lack detectable mRNA for PDGF-receptors [99] **(Fig. 22)**, implying that PDGFR is apparently not the target of CP-673451 regarding inhibition of NETosis.

PMA is the most frequently used compound to induce ROS-dependent NETosis, signaling mechanisms involved have been studied broadly [55, 68, 80]. PMA stimulation leads to direct activation of protein kinase-c (PKC) in neutrophils. NETosis induced by PMA is PKC and NADPH oxidase (NOX) dependent. PMA stimulates conventional (α, βI, βII, γ) and novel (δ, ε, η, θ) PKC isoforms [77]. Conventional PKCs have a prominent role in NET formation. PKCβ is the major isoform crucial in NET formation [78]. PKC downstream phosphorylates p38-MAPK, ERK1/2, Akt and activates NADPH oxidase [55, 77, 78, 80, 81]. Activation of p38-MAPK and ERK1/2 has been identified to be involved in ROS generation [78, 80]. However, some studies also found that these pathways are downstream of ROS production and inhibiting the ROS will also inhibit p38-MAPK, ERK1/2 activation [81]. PMA-induced NETosis also depends on Akt activation and Akt activation is downstream of ROS production [86].

As it was confirmed from my present study that CP-673451 does not inhibit ROS, it was also necessary to check if CP-673451 does not inhibit the activation of known signaling molecules upstream of NETosis. I found that PMA tends to enhance the induced phosphorylation of conventional isoform, PKC α/β and PMA-induced phosphorylation of novel PKC isoform, PKC δ **(Fig. 23).** This results was in agreement with the activation studies of PKC isoforms induced by PMA [78]. In addition, PMA induced phosphorylation of p38-MAPK, ERK1/2, and Akt was observed in this study **(Fig. 23)**. This was in line with the previous results indicating the significance of these pathways in PMA-induced NETosis [55, 78, 80, 86]. My present study showed that activation of PKC α/β, PKC δ, p38-MAPK, ERK1/2, and Akt through phosphorylation was not inhibited by CP-673451 **(Fig. 23)**. This showed that CP-673451 does not inhibit PMA-induced NETosis by inhibiting any of these molecular targets and indicates that the target of CP-673451 is probably downstream of PKC, p38-MAPK, ERK1/2, Akt, and oxidative burst pathways.

Unlike PMA, iIC stimulation in neutrophils requires surface molecule mediated activation. iIC has been shown to induce ROS production and NET formation in neutrophils involving activation of Fc_{γ}RIIIB and Mac-1, and further downstream activating Syk/Src signaling, which further activates ERK1/2, PI3K/Akt, and p38 MAPK pathways [55]. However, activation of ERK1/2, PI3K/Akt or p38 MAPK results directly from Src family kinases/receptor activation and is not ROS mediated, as the ROS inhibition did not affect their phosphorylation [55]. I found that the CP-673451 does not inhibit phosphorylation of ERK1/2, PI3K/ Akt, and p38 MAPK, indicating that neither ERK1/2, PI3K/Akt pathways nor the upstream activation of Fc_{γ}RIIIB, Mac-1, Syk/Src were inhibited by CP-673451 treatment **(Fig. 24)**. This also suggests that the target of CP-673451 is further downstream of these pathways and ROS production induced by iIC.

Interestingly, I found that CP-673451 itself activates p38 MAPK, ERK1/2, and Akt pathways **(Fig. 25)**. Other than in ROS-dependent NETosis, the two major MAPK pathways extracellular signal-regulated kinases 1 and 2 (ERK 1/ 2) and p38 MAPK are involved in several cellular functions [142-144]. Similarly, Akt is involved in modulating neutrophil activation, chemotaxis, and survival other than in ROS-dependent NETosis [145-148]. As these three signaling molecules are phosphorylated during NETosis, it can

also be said that CP-673451 activates the same pathways involved in PMA- and iIC-induced NETosis **(Fig. 25)**. The significance of CP-673451-mediated activation of p38 MAPK, ERK1/2, and Akt in inhibiting NETosis remains to be clarified. This study suggests that the target of CP-673451 involved in NETosis inhibition could possibly downstream of p38 MAPK, ERK1/2, and Akt pathways.

As CP-673451 inhibited both PMA and iIC induced NETosis without affecting the upstream pathways and ROS production, it was assumed that CP-673451 may affect a common NETosis pathway-independent of ROS pathway. This hypothesis was investigated by testing CP-673451 in a ROS-independent-NETosis system, with Ionomycin. Ionomycin is known to act as a motile Ca^{2+} carrier which enhances Ca^{2+} influx and activates PAD4 which induces NETosis in an NADPH-oxidase (NOX)-independent manner [38, 88, 90, 92]. PAD4, a calcium-dependent enzyme, is shown to be critical in Ionomycin-induced NETosis. Inhibition of PAD4 nearly abolishes Ionomycin induced NETs [40]. PAD4 mediates citrullination of histones. Citrullination is the conversion of positively charged arginine side chains into polar but uncharged citrulline side chains, by deimination [93]. Ionomycin induced NETosis was not inhibited by DPI (NOX-inhibitor), which is in line with the results of previous studies [88, 90]. CP-673451 also did not inhibit Ionomycin-induced NET formation **(Fig. 27)**. This would mean that Ionomycin-induced NETosis pathway including calcium influx, PAD4 activation and in turn citrullination of histones is not affected by CP-673451. This showed that CP-673451 does not inhibit a general NETosis pathway, but might be exclusively inhibiting NOX-dependent NETosis pathways, downstream of NOX activation.

As phosphorylation of proteins is a crucial post-translational modification observed in many described NETosis pathways [55, 80, 86], a preliminary screening for phosphorylation of all tyrosine, serine, and threonine proteins was conducted to examine the phosphorylation pattern changes due to CP-673451. I found that CP-673451 did not inhibit any of the phospho tyrosine or phospho serine proteins, but inhibited threonine phosphorylation of two proteins **(Fig. 26-A)**. However, when phospho threonine enriched proteins were examined with coomassie staining to see the same inhibitory phenotype, the two phospho-proteins were not stained, probably due to their low abundance **(Fig. 26-B)**. The experiment was not conclusive as it was a

single screening. Improvement of phospho threonine enrichment protocol with higher number of cells might reveal the inhibitory phenotype (the missing bands), which can be compared with the control samples and the proteins could be cut out and identified by mass spectrometry.

Most proteins required for neutrophil antimicrobial activity are synthesized during the granulopoiesis and packed in specialized granules [76]. NETosis, however was not shown to depend on translation. Nevertheless, there is a bias regarding the relevance of transcription in Nox-dependent- and Nox-independent-NETosis [76, 133]. PMA- and *C. albicans*-induced NETosis were shown to occur independently of *de novo* gene expression [76, 149]. As MAPK signaling is involved in NETosis and in activation of a transcriptional program of neutrophils, two MAPK-mediated pathways were described in previous studies. One pathway, that relies on transcription to produce chemokines and to amplify the inflammatory response. The second pathway is transcription-independent and results in the induction of NET formation and other antimicrobial effects [76]. A recent study has reported that in PMA-mediated Nox-dependent NETosis, activation of different transcription factors are driven by various kinase cascades including Erk, Akt, p38 and cSrc [133].

In this study, I investigated the relevance of gene expression changes in PMA-induced NETosis inhibition by CP-673451. In the preliminary analysis of the data **(Fig. 35)**, I found that PMA stimulation induced differential gene expression in 4 h compared to the unstimulated neutrophils. This finding is in agreement with the recent study showing the transcriptional firing occurring due to PMA-stimulation [133]. Interestingly, I also found that there is differential regulation between PMA stimulated and CP-673451-treated- PMA stimulated neutrophils. This shows that indeed there exist gene expression changes between the NETosis and CP-673451-mediated NETosis-inhibitory processes in neutrophils. This indicated that CP-673451 might be inhibiting NETosis by changes in gene expressions. Besides, CP-673451 itself results in differential gene expression compared to untreated neutrophils **(Fig. 35)**. This is possibly related to the previous results of activation of p38 MAPK, ERK, and Akt **(Fig. 25)** which collectively showed the cellular responses by CP-673451 alone. Even though, activation of p38 MAPK, ERK, and Akt occurs in PMA stimulated neutrophils, the transcriptional responses between the two responses are distinct **(Fig. 35)**. This indicates the

differences in downstream signaling of PMA and CP-673451 after activation of p38 MAPK, ERK, and Akt. A closer look at the up and down regulated genes might reveal the genes involved in CP-673451-mediated neutrophil activation and CP-673451-mediated NETosis inhibition. Unfortunately, due to lack of time the analyses of the up and down regulated gene were not included in this thesis **(data available in the supplementary CD)**.

CP-673451 has been used in several xenograft models and is suggested as an anti-tumor drug [106]. NETosis has been shown harmful in several diseases including cancer and several autoimmune diseases [9, 38, 43, 61-64, 66]. Blocking or controlling NETosis without affecting other anti-microbial neutrophil functions would be a future treatment option. In this study, I examined if CP-673451 treatment on neutrophils affect any of the neutrophil basic anti-microbial functions. I found that CP-673451 does not inhibit neutrophil activation mediated by pro-inflammatory stimuli; TNF-α, fMLP, LPS and IFN_{γ} **(Fig. 32)**, indicating that CP-673451 does not affect neutrophil activation ability in response to different stimuli.

Interestingly, CP-673451 itself could activate neutrophils in a dose dependent manner **(Fig. 33)**. I also confirmed that this activation property of CP-673451 was not due to endotoxin contamination **(Fig. 34)**. CP-673451 tends to show an additive effect on activation in the presence of other stimulants. This is in line with the phosphorylation results of p38 MAPK, ERK1/2, and Akt observed after treatment of neutrophils with CP-673451 **(Fig. 25)**. These results collectively confirmed the neutrophil activation by CP-673451. However, the role of the neutrophil activation in the inhibitory effect of CP-673451 on NETosis remains to be clarified.

Neutrophils migrate towards the sites of infection or inflammation. Chemotaxis or the directional migration towards the site of infection is triggered by chemokines such as IL-8. TNF-alpha induces migration of neutrophils is a chemokinetic or random migration rather than chemotactic response [130]. In this study, I investigated the effect of CP-673451 on chemotaxis and chemokinesis migrations in trans well assay system. I showed that chemotaxis mediated by IL-8 was not affected/inhibited by CP-673451 **(Fig. 31-A)**. However, chemokinesis mediated by TNF-α was reduced at a higher dose of CP-673451 (3μM) **(Fig. 31-B)**. This study couldn't explain the inhibition of TNF-alpha mediated migration inhibition with higher concentrations of CP-673451. However, the

TNF-alpha mediated neutrophil activation was not affected by CP-673451 **(Fig. 32-B)**. CP-673451 affected only chemokinesis mediated by TNF-alpha but not chemotaxis mediated by IL-8 **(Fig. 31)**. However, TNF-alpha mediated migration inhibition by CP-673451 was not affected by 1μM which is the lowest NETosis inhibitory concentration **(Fig. 31-B)**.

One of the major anti-microbial neutrophil functions is the phagocytosis [9]. Inhibiting the phagocytic ability of neutrophils would lead to insufficient anti-microbial defense. In this study, I investigated the effect of CP-673451 in neutrophil phagocytic ability. The phagocytic ability of the neutrophils was not inhibited by CP-673451 **(Fig. 30)**. This study also showed that ROS production was not affected by CP-673451. Together, these results suggest that the efficient phagocytosis and probably the killing the pathogen are not affected by CP-673451. It could be said that even though NETosis is inhibited by CP-673451 the other important antimicrobial defense functions are unaffected. These results also indicate that the pathways involved in PMA and iIC-induced NETosis downstream of ROS generation is unique and different from the pathways involved in other neutrophil anti-microbial functions and CP-673451 is selectively inhibit the NETosis pathway. This selectivity of CP-673451 in inhibiting NETosis makes it considerable for studies on future treatment options for NET-associated diseases.

This study successfully identified an inhibitor of NETosis, CP-673451. CP-673451 could inhibit PMA- and iIC-induced NETosis without inhibiting PMA- and iIC-induced ROS production **(Fig. 36)**. Interestingly, it was found that CP-673451 activates neutrophils by upregulating the surface marker CD11b and by phosphorylating p38 MAPK, Akt and ERK1/2 **(Fig. 36)**. In addition, the study also found that CP-673451 induces gene expression changes in neutrophils. Although the study could not identify the target of CP-673451 involved in NETosis inhibition, further studies on the identified activation pathways and the gene expression analyses might help in revealing the target of CP-673451 involved in NETosis inhibition.

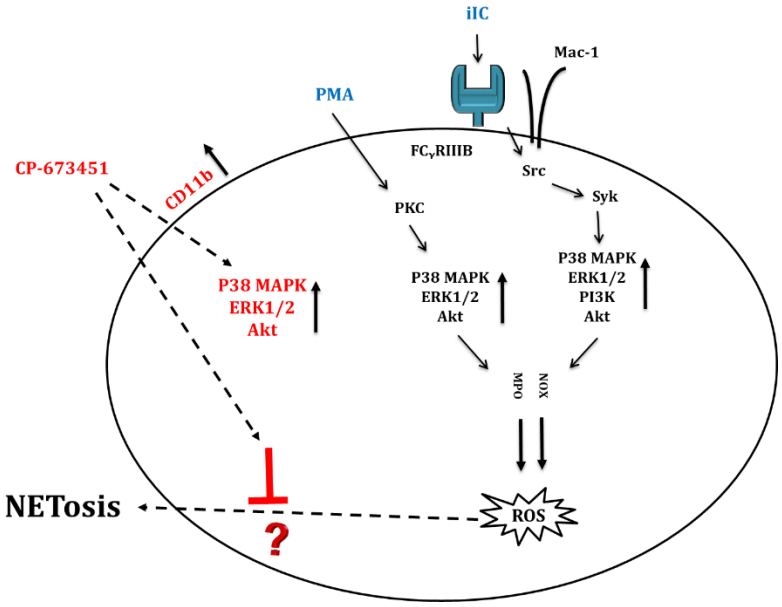

Figure 36. Hypothesis for CP-673451-mediated potential mechanism in the inhibition of NETosis. PMA activates neutrophils by directly stimulating protein kinase-c (PKC) which in turn activates p38 MAPK, ERK, and Akt pathway, leading to NADPH oxidase (NOX) and myeloperoxidase (MPO) mediated ROS production which downstream leads to NETosis by undergoing an unknown mechanism. iIC stimulates neutrophils via $FC_{\gamma}RIIIB$ and Mac-1 resulting downstream activation of Syk/Src, p38 MAPK, ERK, and Akt pathways and induces NOX and MPO mediated ROS. Downstream to ROS generation, NETosis is induced by an unknown mechanism. CP-673451 induces CD11b upregulation and leading to neutrophil activation and in turn activates p38 MAPK, ERK, and Akt pathways. CP-673451 inhibits NETosis by targeting an unknown NETosis pathway downstream of ROS production.

Bibliography

1. Ermert, D., et al., *Candida albicans escapes from mouse neutrophils.* J Leukoc Biol, 2013. **94**(2): p. 223-36.
2. da Silva, F.M., A.M. Massart-Leën, and C. Burvenich, *Development and maturation of neutrophils.* VET QUART., 1994. **16**(4): p. 220-225.
3. Borregaard, N., *Neutrophils, from marrow to microbes.* Immunity, 2010. **33**(5): p. 657-70.
4. Amulic, B., et al., *Neutrophil function: from mechanisms to disease.* Annu Rev Immunol, 2012. **30**: p. 459-89.
5. Kolaczkowska, E. and P. Kubes, *Neutrophil recruitment and function in health and inflammation.* Nat Rev Immunol, 2013. **13**(3): p. 159-75.
6. McEver, R.P. and R.D. Cummings, *Role of PSGL-1 binding to selectins in leukocyte recruitment.* J Clin Invest, 1997. **100**(11 Suppl): p. S97-103.
7. Kansas, G.S., *Selectins and their ligands: current concepts and controversies.* Blood, 1996. **88**(9): p. 3259-87.
8. Constantin, G., et al., *Chemokines trigger immediate beta2 integrin affinity and mobility changes: differential regulation and roles in lymphocyte arrest under flow.* Immunity, 2000. **13**(6): p. 759-69.
9. Mayadas, T.N., X. Cullere, and C.A. Lowell, *The multifaceted functions of neutrophils.* Annu Rev Pathol, 2014. **9**: p. 181-218.
10. Borregaard, N. and J.B. Cowland, *Granules of the human neutrophilic polymorphonuclear leukocyte.* Blood, 1997. **89**(10): p. 3503-21.
11. Lacy, P., *Mechanisms of Degranulation in Neutrophils.* Allergy, Asthma & Clinical Immunology, 2006. **2**(3): p. 98.
12. Choi, K.Y., L.N. Chow, and N. Mookherjee, *Cationic host defence peptides: multifaceted role in immune modulation and inflammation.* J Innate Immun, 2012. **4**(4): p. 361-70.
13. van Kessel, K.P.M., J. Bestebroer, and J.A.G. van Strijp, *Neutrophil-Mediated Phagocytosis of Staphylococcus aureus.* Front Immunol, 2014. **5**(467).
14. Haas, A., *The phagosome: compartment with a license to kill.* Traffic, 2007. **8**(4): p. 311-30.
15. Wright, H.L., R.J. Moots, and S.W. Edwards, *The multifactorial role of neutrophils in rheumatoid arthritis.* Nat Rev Rheumatol, 2014. **10**(10): p. 593-601.
16. Scapini, P., et al., *The neutrophil as a cellular source of chemokines.* Immunol Rev, 2000. **177**: p. 195-203.
17. Tecchio, C., A. Micheletti, and M.A. Cassatella, *Neutrophil-Derived Cytokines: Facts Beyond Expression.* Front Immunol, 2014. **5**(508).
18. Kasama, T., et al., *Neutrophil-derived cytokines: potential therapeutic targets in inflammation.* Curr Drug Targets Inflamm Allergy, 2005. **4**(3): p. 273-9.
19. Kuwabara, W.M., et al., *NADPH oxidase-dependent production of reactive oxygen species induces endoplasmatic reticulum stress in neutrophil-like HL60 cells.* PLoS One, 2015. **10**(2): p. e0116410.
20. Babior, B.M., J.T. Curnutte, and R.S. Kipnes, *Biological defense mechanisms. Evidence for the participation of superoxide in bacterial killing by xanthine oxidase.* J Lab Clin Med, 1975. **85**(2): p. 235-44.

21. Parkos, C.A., et al., *Purified cytochrome b from human granulocyte plasma membrane is comprised of two polypeptides with relative molecular weights of 91,000 and 22,000.* J Clin Invest, 1987. **80**(3): p. 732-42.
22. Nisimoto, Y., et al., *The p67(phox) activation domain regulates electron flow from NADPH to flavin in flavocytochrome b(558).* J Biol Chem, 1999. **274**(33): p. 22999-3005.
23. Han, C.H., et al., *Regulation of the neutrophil respiratory burst oxidase. Identification of an activation domain in p67(phox).* J Biol Chem, 1998. **273**(27): p. 16663-8.
24. Kettle, A.J. and C.C. Winterbourn, *Myeloperoxidase: a key regulator of neutrophil oxidant production.* Redox Rep, 1997. **3**(1): p. 3-15.
25. Segal, B.H., et al., *Genetic, biochemical, and clinical features of chronic granulomatous disease.* Medicine (Baltimore), 2000. **79**(3): p. 170-200.
26. Li, Y. and M.A. Trush, *Diphenyleneiodonium, an NAD(P)H oxidase inhibitor, also potently inhibits mitochondrial reactive oxygen species production.* Biochem Biophys Res Commun, 1998. **253**(2): p. 295-9.
27. Williams, H.C. and K.K. Griendling, *NADPH oxidase inhibitors: new antihypertensive agents?* J Cardiovasc Pharmacol, 2007. **50**(1): p. 9-16.
28. O'Donnell, B.V., et al., *Studies on the inhibitory mechanism of iodonium compounds with special reference to neutrophil NADPH oxidase.* Biochem J, 1993. **290**(Pt 1): p. 41-9.
29. Brinkmann, V., et al., *Neutrophil extracellular traps kill bacteria.* Science, 2004. **303**(5663): p. 1532-5.
30. Fuchs, T.A., et al., *Novel cell death program leads to neutrophil extracellular traps.* J Cell Biol, 2007. **176**(2): p. 231-41.
31. Matoszka, N., et al., *[NET and NETosis--new phenomenon in immunology].* Postepy Hig Med Dosw (Online), 2012. **66**: p. 437-45.
32. Pilsczek, F.H., et al., *A novel mechanism of rapid nuclear neutrophil extracellular trap formation in response to Staphylococcus aureus.* J Immunol, 2010. **185**(12): p. 7413-25.
33. Yipp, B.G. and P. Kubes, *NETosis: how vital is it?* Blood, 2013. **122**(16): p. 2784-94.
34. Rochael, N.C., et al., *Classical ROS-dependent and early/rapid ROS-independent release of Neutrophil Extracellular Traps triggered by Leishmania parasites.* Sci. Rep. 2015. **5**: p. 18302.
35. Metzler, K.D., et al., *Myeloperoxidase is required for neutrophil extracellular trap formation: implications for innate immunity.* Blood, 2011. **117**(3): p. 953-9.
36. Metzler, K.D., et al., *A myeloperoxidase-containing complex regulates neutrophil elastase release and actin dynamics during NETosis.* Cell Rep, 2014. **8**(3): p. 883-96.
37. Papayannopoulos, V., et al., *Neutrophil elastase and myeloperoxidase regulate the formation of neutrophil extracellular traps.* J Cell Biol, 2010. **191**(3): p. 677-91.
38. Kaplan, M.J. and M. Radic, *Neutrophil Extracellular Traps: Double-Edged Swords of Innate Immunity.* J Immunol, 2012. **189**(6): p. 2689-2695.
39. Neeli, I., S.N. Khan, and M. Radic, *Histone deimination as a response to inflammatory stimuli in neutrophils.* J Immunol, 2008. **180**(3): p. 1895-902.
40. Wang, Y., et al., *Histone hypercitrullination mediates chromatin decondensation and neutrophil extracellular trap formation.* J Cell Biol, 2009. **184**(2): p. 205-13.

41. Hemmers, S., et al., *PAD4-Mediated Neutrophil Extracellular Trap Formation Is Not Required for Immunity against Influenza Infection.* PLOS ONE, 2011. **6**(7): p. e22043.
42. Almyroudis, N.G., et al., *NETosis and NADPH oxidase: at the intersection of host defense, inflammation, and injury.* Front Immunol, 2013. **4**: p. 45.
43. Gupta, S. and M.J. Kaplan, *The role of neutrophils and NETosis in autoimmune and renal diseases.* Nat Rev Nephrol, 2016. **12**(7): p. 402-13.
44. Steinberg, B.E. and S. Grinstein, *Unconventional roles of the NADPH oxidase: signaling, ion homeostasis, and cell death.* Sci STKE, 2007. **2007**(379): p. pe11.
45. Wartha, F. and B. Henriques-Normark, *ETosis: a novel cell death pathway.* Sci Signal, 2008. **1**(21): p. pe25.
46. Remijsen, Q., et al., *Neutrophil extracellular trap cell death requires both autophagy and superoxide generation.* Cell Res, 2011. **21**(2): p. 290-304.
47. Itakura, A. and O.J. McCarty, *Pivotal role for the mTOR pathway in the formation of neutrophil extracellular traps via regulation of autophagy.* Am J Physiol Cell Physiol, 2013. **305**(3): p. C348-54.
48. Khan, M.A., et al., *JNK Activation Turns on LPS- and Gram-Negative Bacteria-Induced NADPH Oxidase-Dependent Suicidal NETosis.* Sci Rep, 2017. **7**(1): p. 3409.
49. Yipp, B.G., et al., *Infection-induced NETosis is a dynamic process involving neutrophil multitasking in vivo.* Nat Med, 2012. **18**(9): p. 1386-1393.
50. Halverson, T.W.R., et al., *DNA Is an Antimicrobial Component of Neutrophil Extracellular Traps.* PLoS Pathog, 2015. **11**(1).
51. Lee, M.J., et al., *The Fungal Exopolysaccharide Galactosaminogalactan Mediates Virulence by Enhancing Resistance to Neutrophil Extracellular Traps.* PLOS Pathogens, 2015. **11**(10): p. e1005187.
52. Urban, C.F., et al., *Neutrophil extracellular traps capture and kill Candida albicans yeast and hyphal forms.* Cellular Microbiology, 2006. **8**(4): p. 668-676.
53. Clark, S.R., et al., *Platelet TLR4 activates neutrophil extracellular traps to ensnare bacteria in septic blood.* Nat Med, 2007. **13**(4): p. 463-9.
54. Chen, K., et al., *Endocytosis of soluble immune complexes leads to their clearance by FcγRIIIB but induces neutrophil extracellular traps via FcγRIIA in vivo.* Blood, 2012. **120**(22): p. 4421-31.
55. Behnen, M., et al., *Immobilized Immune Complexes Induce Neutrophil Extracellular Trap Release by Human Neutrophil Granulocytes via FcγRIIIB and Mac-1.* The Journal of Immunology, 2014. **193**(4): p. 1954-1965.
56. Richards, R.C., et al., *Histone H1: an antimicrobial protein of Atlantic salmon (Salmo salar).* Biochem Biophys Res Commun, 2001. **284**(3): p. 549-55.
57. Papayannopoulos, V. and A. Zychlinsky, *NETs: a new strategy for using old weapons.* Trends Immunol, 2009. **30**(11): p. 513-21.
58. Parker, H., et al., *Myeloperoxidase associated with neutrophil extracellular traps is active and mediates bacterial killing in the presence of hydrogen peroxide.* J Leukoc Biol, 2012. **91**(3): p. 369-76.
59. Urban, C.F., et al., *Neutrophil extracellular traps contain calprotectin, a cytosolic protein complex involved in host defense against Candida albicans.* PLoS Pathog, 2009. **5**(10): p. e1000639.
60. Sur Chowdhury, C., et al., *Enhanced neutrophil extracellular trap generation in rheumatoid arthritis: analysis of underlying signal transduction pathways and potential diagnostic utility.* Arthritis Res Ther, 2014. **16**(3): p. R122.

61. Garcia-Romo, G.S., et al., *Netting neutrophils are major inducers of type I IFN production in pediatric systemic lupus erythematosus.* Sci Transl Med, 2011. **3**(73): p. 73ra20.
62. Kessenbrock, K., et al., *Netting neutrophils in autoimmune small-vessel vasculitis.* Nat Med, 2009. **15**(6): p. 623-625.
63. Berthelot, J.M., et al., *NETosis: At the crossroads of rheumatoid arthritis, lupus, and vasculitis.* Joint Bone Spine, 2017. **84**(3): p. 255-262.
64. Corsiero, E., et al., *NETosis as Source of Autoantigens in Rheumatoid Arthritis.* Front Immunol, 2016. **7**: p. 485.
65. Dwivedi, N. and M. Radic, *Citrullination of autoantigens implicates NETosis in the induction of autoimmunity.* Ann Rheum Dis, 2014. **73**(3): p. 483-91.
66. Lande, R., et al., *Neutrophils activate plasmacytoid dendritic cells by releasing self-DNA-peptide complexes in systemic lupus erythematosus.* Sci Transl Med, 2011. **3**(73): p. 73ra19.
67. Lin, A.M., et al., *Mast cells and neutrophils release IL-17 through extracellular trap formation in psoriasis.* J Immunol, 2011. **187**(1): p. 490-500.
68. Parker, H., et al., *Requirements for NADPH oxidase and myeloperoxidase in neutrophil extracellular trap formation differ depending on the stimulus.* J Leukoc Biol, 2012. **92**(4): p. 841-9.
69. Stephan, A. and M. Fabri, *The NET, the trap and the pathogen: neutrophil extracellular traps in cutaneous immunity.* Exp Dermatol, 2015. **24**(3): p. 161-6.
70. Lim, M.B., et al., *Rac2 is required for the formation of neutrophil extracellular traps.* J Leukoc Biol, 2011. **90**(4): p. 771-6.
71. Yost, C.C., et al., *Impaired neutrophil extracellular trap (NET) formation: a novel innate immune deficiency of human neonates.* Blood, 2009. **113**(25): p. 6419-6427.
72. Brinkmann, V. and A. Zychlinsky, *Beneficial suicide: why neutrophils die to make NETs.* Nat Rev Microbiol, 2007. **5**(8): p. 577-82.
73. Ermert, D., et al., *Mouse neutrophil extracellular traps in microbial infections.* J Innate Immun, 2009. **1**(3): p. 181-93.
74. Robinson, J.J., et al., *Activation of neutrophils by soluble and insoluble immunoglobulin aggregates from synovial fluid of patients with rheumatoid arthritis.* Ann Rheum Dis, 1993. **52**(5): p. 347-53.
75. Fossati, G., R.C. Bucknall, and S.W. Edwards, *Insoluble and soluble immune complexes activate neutrophils by distinct activation mechanisms: changes in functional responses induced by priming with cytokines.* Ann Rheum Dis, 2002. **61**(1): p. 13-9.
76. Sollberger, G., B. Amulic, and A. Zychlinsky, *Neutrophil Extracellular Trap Formation Is Independent of De Novo Gene Expression.* PLoS One, 2016. **11**(6): p. e0157454.
77. Way, K.J., E. Chou, and G.L. King, *Identification of PKC-isoform-specific biological actions using pharmacological approaches.* Trends Pharmacol Sci, 2000. **21**(5): p. 181-7.
78. Gray, R.D., et al., *Activation of conventional protein kinase C (PKC) is critical in the generation of human neutrophil extracellular traps.* J Inflamm (Lond), 2013. **10**: p. 12.
79. Babior, B.M., J.D. Lambeth, and W. Nauseef, *The neutrophil NADPH oxidase.* Arch Biochem Biophys, 2002. **397**(2): p. 342-4.

80. Hakkim, A., et al., *Activation of the Raf-MEK-ERK pathway is required for neutrophil extracellular trap formation.* Nat Chem Biol, 2011. **7**(2): p. 75-77.
81. Keshari, R.S., et al., *Reactive oxygen species-induced activation of ERK and p38 MAPK mediates PMA-induced NETs release from human neutrophils.* J Cell Biochem, 2013. **114**(3): p. 532-40.
82. Kramer, I.M., et al., *Purified protein kinase C phosphorylates a 47-kDa protein in control neutrophil cytoplasts but not in neutrophil cytoplasts from patients with the autosomal form of chronic granulomatous disease.* J Biol Chem, 1988. **263**(5): p. 2352-7.
83. Bouin, A.P., et al., *p40(phox) is phosphorylated on threonine 154 and serine 315 during activation of the phagocyte NADPH oxidase. Implication of a protein kinase c-type kinase in the phosphorylation process.* J Biol Chem, 1998. **273**(46): p. 30097-103.
84. Chessa, T.A., et al., *Phosphorylation of threonine 154 in p40phox is an important physiological signal for activation of the neutrophil NADPH oxidase.* Blood, 2010. **116**(26): p. 6027-36.
85. Konig, M.F. and F. Andrade, *A Critical Reappraisal of Neutrophil Extracellular Traps and NETosis Mimics Based on Differential Requirements for Protein Citrullination.* Front Immunol, 2016. **7**.
86. Douda, D.N., et al., *Akt is essential to induce NADPH-dependent NETosis and to switch the neutrophil death to apoptosis.* Blood, 2014. **123**(4): p. 597-600.
87. Yost, C.C., et al., *Impaired neutrophil extracellular trap (NET) formation: a novel innate immune deficiency of human neonates.* Blood, 2009. **113**(25): p. 6419-27.
88. Douda, D.N., et al., *SK3 channel and mitochondrial ROS mediate NADPH oxidase-independent NETosis induced by calcium influx.* Proc Natl Acad Sci U S A, 2015. **112**(9): p. 2817-22.
89. Pilsczek, F.H., et al., *A Novel Mechanism of Rapid Nuclear Neutrophil Extracellular Trap Formation in Response to Staphylococcus aureus.* The Journal of Immunology, 2010. **185**(12): p. 7413-7425.
90. Kauffman, R.F., R.W. Taylor, and D.R. Pfeiffer, *Cation transport and specificity of ionomycin. Comparison with ionophore A23187 in rat liver mitochondria.* J Biol Chem, 1980. **255**(7): p. 2735-9.
91. Liu, C. and T.E. Hermann, *Characterization of ionomycin as a calcium ionophore.* J Biol Chem, 1978. **253**(17): p. 5892-4.
92. Morgan, A.J. and R. Jacob, *Ionomycin enhances Ca2+ influx by stimulating store-regulated cation entry and not by a direct action at the plasma membrane.* Biochem J, 1994. **300 (Pt 3)**: p. 665-72.
93. Remijsen, Q., et al., *Dying for a cause: NETosis, mechanisms behind an antimicrobial cell death modality.* Cell Death Differ, 2011. **18**(4): p. 581-8.
94. Williams, L.T., *Signal transduction by the platelet-derived growth factor receptor.* Science, 1989. **243**(4898): p. 1564-70.
95. Heldin, C.H. and B. Westermark, *Mechanism of action and in vivo role of platelet-derived growth factor.* Physiol Rev, 1999. **79**(4): p. 1283-316.
96. Heldin, C.H. and J. Lennartsson, *Structural and Functional Properties of Platelet-Derived Growth Factor and Stem Cell Factor Receptors.* Cold Spring Harb Perspect Biol, 2013. **5**(8).
97. Andrae, J., R. Gallini, and C. Betsholtz, *Role of platelet-derived growth factors in physiology and medicine.* Genes Dev, 2008. **22**(10): p. 1276-312.

98. Deuel, T.F., et al., *Chemotaxis of monocytes and neutrophils to platelet-derived growth factor.* J Clin Invest, 1982. **69**(4): p. 1046-9.
99. Qu, J., et al., *Lack of effect of recombinant platelet-derived growth factor on human neutrophil function.* J Immunol, 1995. **154**(8): p. 4133-41.
100. Kelly, J.D., et al., *Platelet-derived growth factor (PDGF) stimulates PDGF receptor subunit dimerization and intersubunit trans-phosphorylation.* J Biol Chem, 1991. **266**(14): p. 8987-92.
101. Kazlauskas, A. and J.A. Cooper, *Autophosphorylation of the PDGF receptor in the kinase insert region regulates interactions with cell proteins.* Cell, 1989. **58**(6): p. 1121-33.
102. Bar-Sagi, D. and J.R. Feramisco, *Induction of membrane ruffling and fluid-phase pinocytosis in quiescent fibroblasts by ras proteins.* Science, 1986. **233**(4768): p. 1061-8.
103. Seger, R. and E.G. Krebs, *The MAPK signaling cascade.* Faseb j, 1995. **9**(9): p. 726-35.
104. Hanahan, D. and R.A. Weinberg, *The hallmarks of cancer.* Cell, 2000. **100**(1): p. 57-70.
105. Demetri, G.D., *Differential properties of current tyrosine kinase inhibitors in gastrointestinal stromal tumors.* Semin Oncol, 2011. **38 Suppl 1**: p. S10-9.
106. Roberts, W.G., et al., *Antiangiogenic and antitumor activity of a selective PDGFR tyrosine kinase inhibitor, CP-673,451.* Cancer Res, 2005. **65**(3): p. 957-66.
107. Carroll, M., et al., *CGP 57148, a tyrosine kinase inhibitor, inhibits the growth of cells expressing BCR-ABL, TEL-ABL, and TEL-PDGFR fusion proteins.* Blood, 1997. **90**(12): p. 4947-52.
108. Hojjat-Farsangi, M., *Small-molecule inhibitors of the receptor tyrosine kinases: promising tools for targeted cancer therapies.* Int J Mol Sci, 2014. **15**(8): p. 13768-801.
109. Yu, J.-C., et al., *Efficacy of the Novel Selective Platelet-Derived Growth Factor Receptor Antagonist CT52923 on Cellular Proliferation, Migration, and Suppression of Neointima following Vascular Injury.* Journal of Pharmacology and Experimental Therapeutics, 2001. **298**(3): p. 1172-1178.
110. Zaman, G.J., et al., *Tyrosine kinase activity of purified recombinant cytoplasmic domain of platelet-derived growth factor beta-receptor (beta-PDGFR) and discovery of a novel inhibitor of receptor tyrosine kinases.* Biochem Pharmacol, 1999. **57**(1): p. 57-64.
111. Jakus, Z., et al., *Critical but overlapping role of FcgammaRIII and FcgammaRIV in activation of murine neutrophils by immobilized immune complexes.* J Immunol, 2008. **180**(1): p. 618-29.
112. Briheim, G., O. Stendahl, and C. Dahlgren, *Intra- and extracellular events in luminol-dependent chemiluminescence of polymorphonuclear leukocytes.* Infect Immun, 1984. **45**(1): p. 1-5.
113. Stevens, P. and D. Hong, *The role of myeloperoxidase and superoxide anion in the luminol- and lucigenin-dependent chemiluminescence of human neutrophils.* Microchemical Journal, 1984. **30**(2): p. 135-146.
114. Bianchi, M., et al., *Restoration of NET formation by gene therapy in CGD controls aspergillosis.* Blood, 2009. **114**(13): p. 2619-2622.
115. Brinkmann, V., et al., *Neutrophil Extracellular Traps Kill Bacteria.* Science, 2004. **303**(5663): p. 1532-1535.

116. Behnen, M., et al., *Extracellular Acidification Inhibits the ROS-Dependent Formation of Neutrophil Extracellular Traps.* Front Immunol, 2017. **8**: p. 184.
117. Behnen, M., et al., *Extracellular Acidification Inhibits the ROS-Dependent Formation of Neutrophil Extracellular Traps.* Front Immunol, 2017. **8**(184).
118. Sarkar, A., et al., *Infection with Anaplasma phagocytophilum activates the phosphatidylinositol 3-Kinase/Akt and NF-kappaB survival pathways in neutrophil granulocytes.* Infect Immun, 2012. **80**(4): p. 1615-23.
119. Wilfinger, W.W., K. Mackey, and P. Chomczynski, *Effect of pH and ionic strength on the spectrophotometric assessment of nucleic acid purity.* Biotechniques, 1997. **22**(3): p. 474-6, 478-81.
120. Schroeder, A., et al., *The RIN: an RNA integrity number for assigning integrity values to RNA measurements.* BMC Molecular Biology, 2006. **7**: p. 3-3.
121. Khatter, H., et al., *Structure of the human 80S ribosome.* Nature, 2015. **520**(7549): p. 640-645.
122. Imbeaud, S., et al., *Towards standardization of RNA quality assessment using user-independent classifiers of microcapillary electrophoresis traces.* Nucleic Acids Research, 2005. **33**(6): p. e56-e56.
123. Wang, Z., M. Gerstein, and M. Snyder, *RNA-Seq: a revolutionary tool for transcriptomics.* Nature reviews. Genetics, 2009. **10**(1): p. 57-63.
124. Sim, S., et al., *NADPH oxidase-derived reactive oxygen species-mediated activation of ERK1/2 is required for apoptosis of human neutrophils induced by Entamoeba histolytica.* J Immunol, 2005. **174**(7): p. 4279-88.
125. Taylor, S.S., E. Radzio-Andzelm, and T. Hunter, *How do protein kinases discriminate between serine/threonine and tyrosine? Structural insights from the insulin receptor protein-tyrosine kinase.* Faseb j, 1995. **9**(13): p. 1255-66.
126. Kenny, E.F., et al., *Diverse stimuli engage different neutrophil extracellular trap pathways.* eLife, 2017. **6**: p. e24437.
127. *The Impact of Various Reactive Oxygen Species on the Formation of Neutrophil Extracellular Traps.* Mediators of Inflammation, 2012. **2012**.
128. McKim, J.M., *Building a Tiered Approach to In Vitro Predictive Toxicity Screening: A Focus on Assays with In Vivo Relevance.* Combinatorial Chemistry & High Throughput Screening, 2010. **13**(2): p. 188-206.
129. Henkels, K.M., et al., *IL-8-INDUCED NEUTROPHIL CHEMOTAXIS IS MEDIATED BY JANUS KINASE 3 (JAK3).* FEBS letters, 2011. **585**(1): p. 159-166.
130. Smart, S.J. and T.B. Casale, *TNF-alpha-induced transendothelial neutrophil migration is IL-8 dependent.* Am J Physiol, 1994. **266**(3 Pt 1): p. L238-45.
131. Soler-Rodriguez, A.M., et al., *Neutrophil activation by bacterial lipoprotein versus lipopolysaccharide: differential requirements for serum and CD14.* J Immunol, 2000. **164**(5): p. 2674-83.
132. Cardoso, L.S., et al., *Polymyxin B as inhibitor of LPS contamination of Schistosoma mansoni recombinant proteins in human cytokine analysis.* Microbial Cell Factories, 2007. **6**(1): p. 1.
133. Khan, M.A. and N. Palaniyar, *Transcriptional firing helps to drive NETosis.* Scientific Reports, 2017. **7**: p. 41749.
134. Perez-Sanchez, C., et al., *Diagnostic potential of NETosis-derived products for disease activity, atherosclerosis and therapeutic effectiveness in Rheumatoid Arthritis patients.* J Autoimmun, 2017.

135. Hakkim, A., et al., *Impairment of neutrophil extracellular trap degradation is associated with lupus nephritis.* Proc Natl Acad Sci U S A, 2010. **107**(21): p. 9813-8.
136. Radic, M. and T.N. Marion, *Neutrophil extracellular chromatin traps connect innate immune response to autoimmunity.* Seminars in Immunopathology, 2013. **35**(4): p. 465-480.
137. Dwivedi, N., et al., *Felty's Syndrome Autoantibodies Bind to Deiminated Histones and Neutrophil Extracellular Chromatin Traps.* Arthritis and rheumatism, 2012. **64**(4): p. 982-992.
138. Kamoshida, G., et al., *Spontaneous formation of neutrophil extracellular traps in serum-free culture conditions.* FEBS Open Bio, 2017. **7**(6): p. 877-886.
139. in *Assay Guidance Manual*, G.S. Sittampalam, et al., Editors. 2004, Eli Lilly & Company and the National Center for Advancing Translational Sciences: Bethesda (MD).
140. Kawakami, T., et al., *Rab27a Is Essential for the Formation of Neutrophil Extracellular Traps (NETs) in Neutrophil-Like Differentiated HL60 Cells.* PLoS ONE, 2014. **9**(1): p. e84704.
141. Roskoski, R., Jr., *Sunitinib: a VEGF and PDGF receptor protein kinase and angiogenesis inhibitor.* Biochem Biophys Res Commun, 2007. **356**(2): p. 323-8.
142. Cobb, M.H. and E.J. Goldsmith, *How MAP kinases are regulated.* J Biol Chem, 1995. **270**(25): p. 14843-6.
143. Nick, J.A., et al., *Selective activation and functional significance of p38alpha mitogen-activated protein kinase in lipopolysaccharide-stimulated neutrophils.* J Clin Invest, 1999. **103**(6): p. 851-8.
144. Bonner, S., et al., *Activation of extracellular signal-related protein kinases 1 and 2 of the mitogen-activated protein kinase family by lipopolysaccharide requires plasma in neutrophils from adults and newborns.* Infect Immun, 2001. **69**(5): p. 3143-9.
145. Chen, J., et al., *Akt isoforms differentially regulate neutrophil functions.* Blood, 2010. **115**(21): p. 4237.
146. Souza, L.R., et al., *G-CSF activation of AKT is not sufficient to prolong neutrophil survival.* Journal of Leukocyte Biology, 2013. **93**(6): p. 883-893.
147. Zhu, D., et al., *Deactivation of phosphatidylinositol 3,4,5-trisphosphate/Akt signaling mediates neutrophil spontaneous death.* Proc Natl Acad Sci U S A, 2006. **103**(40): p. 14836-41.
148. Zhang, Y., et al., *Kinase AKT controls innate immune cell development and function.* Immunology, 2013. **140**(2): p. 143-152.
149. Borregaard, N., O.E. Sorensen, and K. Theilgaard-Monch, *Neutrophil granules: a library of innate immunity proteins.* Trends Immunol, 2007. **28**(8): p. 340-5.

Supplementary data

I. Target-selective inhibitor library from Selleckchem (Houston, USA)

No.	Name of the Inhibitor	Target	No.	Name of the Inhibitor	Target
D1	AZD6244 (Selumetinib)	MEK1	D72	TAME	APC
D2	MK-2206 2HCl	Akt	D73	PHA-665752	c-Met
D3	17-AAG (Tanespimycin)	HSP 90	D74	MLN8237 (Alisertib)	Aurora A
D4	PFI-1	BRD4	D75	Dutasteride	5-alpha Reductase
D5	Rigosertib (ON-01910)	PLK-1	D76	Doxazosin mesylate	α1
D6	BIX 02189	MEK5	D77	MK-1775	Wee1
D7	Candesartan (Atacand)	angiotensin II receptor	D78	BIRB 796 (Doramapimod)	p38α MAPK
D8	Rosuvastatin calcium (Crestor)	HMG-CoA reductase	D79	GSK1292263	GPR119
D9	Bortezomib (Velcade)	20S proteasome	D80	Ketanserin (Vulketan Gel)	HTR2
D10	PD153035 HCl	EGFR	D81	SB 216763	GSK-3α
D11	Barasertib (AZD1152-HQPA)	Aurora B	D82	ADL5859 HCl	δ-opioid receptor
D12	Topotecan HCl	Topo I	D83	Doxorubicin (Adriamycin)	Topo II
D13	AS-605240	p110γ	D84	Etomidate	GABAA receptor
D14	CP 673451	PDGFR	D85	Quizartinib (AC220)	FLT3
D15	H 89 2HCl	PKA	D86	Tie2 kinase inhibitor	Tie-2
D16	SB 743921	kinesin spindle protein	D87	PF-4708671	S6K1
D17	Lenalidomide (Revlimid)	TNF-α	D88	Clozapine (Clozaril)	HTR1
D18	Vismodegib (GDC-0449)	hedgehog	D89	Donepezil HCl (Aricept)	AChE
D19	MK-8245	SCD	D90	CHIR-124	Chk1
D20	2-Methoxyestradiol	HIF-1α	D91	CI994 (Tacedinaline)	HDAC1
D21	Tipifarnib (Zarnestra)	FTase	D92	Entacapone	COMT
D22	EX 527	SIRT1	D93	10058-F4	c-Myc
D23	Allopurinol (Zyloprim)	xanthine oxidase	D94	Pancuronium (Pavulon)	nAChR
D24	BGJ398 (NVP-BGJ398)	FGFR	D95	ADX-47273	mGlu5

D25	Nilotinib (AMN-107)	Bcr-Abl	D96	Tideglusib	GSK-3β
D26	Iniparib (BSI-201)	PARP1	D97	Sitagliptin phosphate monohydrate	DPP-4
D27	ABT-751	β-tubulin	D98	SMI-4a	Pim1
D28	Letrozole	Aromatase	D99	Salbutamol sulfate (Albuterol)	β2
D29	Zibotentan (ZD4054)	ETA	D100	KX2-391	Src
D30	AM-1241	CB2	D101	TPCA-1	IKK2
D31	Enalaprilat dihydrate	ACE	D102	Mirabegron (YM178)	β3
D32	Aliskiren hemifumarate	renin	D103	RGD (Arg-Gly-Asp) Peptides	Integrin
D33	Rapamycin (Sirolimus)	mTOR	D104	Xylazine HCl	α2
D34	Linsitinib (OSI-906)	IGF-1R	D105	ZM 336372	c-Raf
D35	TGX-221	p110β	D106	Dizocilpine (MK 801)	NMDA
D36	MDV3100 (Enzalutamide)	AR	D107	Sodium 4-Aminosalicylate	NF-κB
D37	SP600125	JNK	D108	Tariquidar	P-gp
D38	Dapagliflozin	hSGLT2	D109	Tolterodine tartrate (Detrol LA)	mAChR
D39	Ranitidine (Zantac)	Histamine H2-receptor	D110	JTC-801	ORL1
D40	DAPT (GSI-IX)	γ-secretase	D111	ML130	NOD1
D41	Vandetanib (Zactima)	VEGFR2	D112	PTC124 (Ataluren)	CFTR
D42	Varespladib (LY315920)	PLA	D113	NSC 23766	Rac
D43	XAV-939	Wnt/β-catenin	D114	Tolvaptan (OPC-41061)	vasopressin receptor 2
D44	Ramelteon (TAK-375)	MT Receptor	D115	AZ 3146	Mps1
D45	SB 525334	ALK5	D116	GW441756	TrkA
D46	Nebivolol (Bystolic)	β1	D117	Birinapant (TL32711)	cIAP1
D47	Clemastine Fumarate	Histamine H1-receptor	D118	PRT062607 (P505-15, PRT2607, BIIB057) HCl	Syk
D48	Mubritinib (TAK 165)	Her2	D119	URB597	FAAH
D49	Y-27632 2HCl	ROCK1	D120	PAC-1	Caspase-3
D50	Odanacatib (MK 0822)	Cathepsin K	D121	WZ 811	CXCR4
D51	BIBR 1532	Telomerase	D122	Stattic	STAT3
D52	Celecoxib	COX-2	D123	UPF 1069	PARP2
D53	Fludarabine (Fludara)	STAT1	D124	BMS-806 (BMS 378806)	gp120
D54	Pimobendan (Vetmedin)	PDE3	D125	CH5424802	ALK
D55	PCI-34051	HDAC8	D126	GW9662	PPARγ
D56	SB590885	b-Raf	D127	SANT-1	Smoothened

D57	Enzastaurin (LY317615)	PKCβ	D128	GW2580	CSF-1R
D58	Abiraterone (CB-7598)	CYP17	D129	A66	p110α
D59	Fulvestrant (Faslodex)	ER	D130	Tofacitinib (CP-690550, Tasocitinib)	JAK3
D60	IC-87114	p110δ	D131	Evacetrapib (LY2484595)	CETP
D61	NVP-BEP800	HSP90β	D132	IPA-3	Pak1
D62	KU-60019	ATM	D133	ABT-199 (GDC-0199)	Bcl-2
D63	PF 573228	FAK	D134	TAK-875	GPR40
D64	PF 3716556	P-CAB	D135	APO866 (FK866)	NMPRTase
D65	Nutlin-3	MDM2	D136	Pifithrin-α	p53
D66	YM155	Survivin	D137	NLG919	IDO
D67	Decitabine	DNA Methyltransferase	D138	NU7441 (KU-57788)	DNA-PK
D68	BX-795	PDK-1	D139	CEP33779	JAK2
D69	Tadalafil (Cialis)	PDE5	D140	Rimonabant (SR141716)	CB1
D70	BS-181 HCl	CDK5	D141	TCID	DUB
D71	Roflumilast (Daxas)	PDE4			

Acknowledgements

First and foremost, I would like to express my sincere gratitude to my supervisor Prof. Dr. Tamás Laskay for his support in my research. He consistently steered me in the right the direction whenever I needed help.

I would like to thank Prof. Dr. med. Werner Solbach and Prof. Dr. Jan Rupp, the former and current directors of Department of Infectious Diseases and Microbiology for giving me the opportunity to perform my experiments in their department.

I would like to thank Prof. Dr. med Ralf Ludwig from Department of Dermatology, for being my first mentor and for sharing the chemical library of inhibitors with me. I also thank him for his positive attitude and vivid discussions.

I would like to thank my second mentor, PD Dr. Norbert Reiling from Research center Borstel, who took part in extensive discussions regarding my research.

I would like to express my gratitude to Prof. Hauke Busch for analyzing the RNA Seq data in a very short time and for agreeing to review my PhD thesis.

I would like to thank Prof. Rainer Duden for agreeing to be the Chairman for my PhD thesis.

I also thank PD Dr. Christina Zechel from Department of Neurosurgery, for providing me U87-MG cell line along with reagents and protocols for its culture and the lysate of T129 cell line.

I would like to thank Ms. Miriam Freitag (from LIED), for performing the RNA-quality analysis with Bioanalyzer.

I would also like to thank Prof. Dr. med. Detlef Zillikens and the research training group of Modulation of Autoimmunity (GRK1727), for making me a part of their research group and giving me opportunities to present my work in various meetings and for funding my project.

I would like to thank the former and current lab members Natallia Salei, Stephanie Lachmann, Tabea Walther, Martina Behnen-Haerer, and Sonja Möller for their feedback, cooperation and for the friendship during the last three years.

Last but not the least, I would like to thank my parents, my brother and Vadakkumcherry family for supporting me spiritually and always standing by my side throughout the PhD period and in my life in general.

Curriculum Vitae

Name: Gigy Varghese

Address: Paul-Ehrlich str. 4a

Date and place of birth: 23.05.1990 in Mahe, India

PROFESSIONAL EXPERIENCE

Research Assistant 10/2014 – 10/2017

University Clinic of Schleswig-Holstein

Department of Infectious Diseases and Microbiology (KIM)

Research group of Prof. T. Laskay, PhD

Student Research Assistant 05/2013 – 05/2014

Botanical Institute, Biocentre, University of Cologne

Research group of Prof. Dr. U.I. Flügge

EDUCATION

Research Scholar 10/2014 - present

Research Training Group GRK 1727

University of Lübeck, Germany

Masters in Biological Sciences 04/2012 – 05/2014

Biocentre, University of Cologne, Germany

Department of Plant physiology and biochemistry,

Ecology, Phycology, and Developmental biology

Bachelors in Biotechnology 08/2007 – 05/2010

Administrative Management College, Bangalore, India

Department of Biotechnology, Zoology and Chemistry